

# **Facets of non-Relativistic Effective Field Theories**

Dolors Eiras

**Universitat de Barcelona**

Departament d'Estructura i Constituents de la Matèria

11th July 2002



---

# Facets of non-Relativistic Effective Field Theories

---

Memoria de la tesis presentada por  
Dolors Eiras para optar al grado de  
Doctor en Ciencias Físicas

**Director de tesis: Dr. Joan Soto Riera**

Programa de doctorado del Departament  
d'Estructura i Constituents de la Matèria,  
"Partícules, Camps i Fenòmens Quàntics Col·lectius"

Bienio 97/99  
Universitat de Barcelona

Firmado: Joan Soto



*“Me producía un sentimiento de fatiga y de miedo percibir que todo aquel tiempo tan largo no sólo había sido vivido, pensado, segregado por mí sin una sola interrupción, sentir que era mi vida, que era yo mismo, sinó también que tenía que mantenerlo cada minuto amarrado a mí, que me sostenía, encaramado yo en su cima vertiginosa, que no podía moverme sin moverlo.”*

**El tiempo recobrado**

M. Proust



# Contents

<b>Introduction</b>	<b>1</b>
<b>1 Pionium's lifetime: last stage in a EFT's chain</b>	<b>5</b>
1.1 Motivation . . . . .	5
1.2 Scales intertwined in the non-relativistic approach . . . . .	6
1.3 Lagrangian for non-relativistic pions near threshold . . . . .	10
1.3.1 Local field redefinitions . . . . .	13
1.3.2 Zero charge sector . . . . .	15
1.4 Integrating neutral pions . . . . .	16
1.5 Integrating potential photons . . . . .	17
1.6 Quantum mechanical calculation . . . . .	18
1.6.1 Coulomb propagator in D space dimensions . . . . .	20
1.7 Results and numerics . . . . .	22
1.8 Remarks and conclusions . . . . .	25
<b>2 Light Fermion Finite Mass Effects in Non-relativistic Bound States</b>	<b>28</b>
2.1 Motivation . . . . .	28
2.2 Energy Shift . . . . .	31
2.3 Wave Function at the Origin . . . . .	32
2.4 Applications . . . . .	34
2.4.1 Exotic Atoms . . . . .	35
2.4.2 $\Upsilon(1S)$ and $\bar{t}t$ . . . . .	35

2.5	Related works . . . . .	36
<b>3</b>	<b>Renormalization issues in Nucleon-Nucleon EFT</b>	<b>44</b>
3.1	Motivation . . . . .	44
3.1.1	Reporting on previous work . . . . .	46
3.2	A convenient decomposition . . . . .	66
3.3	The isovector-singlet channel . . . . .	68
3.4	The isosinglet-vector channel . . . . .	70
3.4.1	Non-perturbative treatment of the SSB term . . . . .	71
3.4.2	Treating the SSB term perturbatively . . . . .	74
3.5	Isvector-vector channel . . . . .	76
3.6	Discussion . . . . .	77
<b>4</b>	<b>New predictions for inclusive heavy-quarkonium P-wave decays</b>	<b>81</b>
4.1	Motivation . . . . .	81
4.2	Computation . . . . .	85
4.3	Applications . . . . .	90
	<b>Conclusion</b>	<b>93</b>
	<b>Resumen</b>	<b>95</b>
	Sistemas no relativistas . . . . .	95
	Aspectos tratados . . . . .	98
<b>A</b>	<b>The DIRAC experiment</b>	<b>102</b>
A.1	Experimental method . . . . .	102
A.2	Experimental setup . . . . .	104
A.3	First experimental results . . . . .	105
<b>B</b>	<b>Reparametrization invariance</b>	<b>109</b>
<b>C</b>	<b><math>F_2</math> and <math>F_3</math></b>	<b>112</b>



<b>D</b>	<b>Energy Shift and Wave Function correction</b>	<b>114</b>
<b>E</b>	<b>The case <math>\alpha = -1</math></b>	<b>116</b>
<b>F</b>	<b>Proof of (3.4.1.9)</b>	<b>117</b>
<b>G</b>	<b>On <math>c_1</math> tuning</b>	<b>120</b>
<b>H</b>	<b>No continuous solutions of (3.1.1.37) when <math>R \rightarrow 0</math></b>	<b>124</b>
	<b>Acknowledgments</b>	<b>127</b>



# Introduction

Effective Field Theories (EFT) furnish us with the technical and conceptual background that enables the description of the low-energy physics degrees of freedom[1] of a given, interacting system. They aim at performing a systematic expansion, truncable with a controlled accuracy error, of non-renormalizable interactions among light modes, that is, those characterized by  $E(|\mathbf{p}|, m) \ll \Lambda$ , where  $\Lambda$  is some scale that fixes the frontier for excluded energies (momenta). Information on the heavier degrees has been integrated out and resides in the couplings of the EFT Lagrangian. That would seem to indicate that we need, in order to build the Effective Field Theory, the original one as a starting point. That this is not so becomes one of the main virtues of our framework. An EFT Lagrangian is constructed, as we will see in the first Chapter, in a general fashion, containing all terms allowed by the assumed global and local symmetries of our low-energy system, after stating a regularization procedure and renormalization scheme and having identified a set of small expansion parameters that will allow us to define a power counting in calculations. This produces the most general S-matrix elements consistent with analyticity, perturbative unitarity, cluster decomposition and the aforementioned symmetries. So couplings, those which trace back to the existence of non-included high virtuality states, can be left as free parameters to be fixed eventually by some convenient set of experiments. If matching cannot be performed due to its complexity or to our ignorance of the fundamental theory, we still are able to provide a realistic, sensible and consistently improbable approach to our problem.

Among the variety of fauna that populates the EFT world ( $\chi$ PT, Electroweak EFT, HQET, Landau-Ginzburg theory of superconductivity, ... ), our attention will be devoted to the non-relativistic species (NREFTs, specially worth the accounts in [2]), which was originally proposed by Caswell and Lepage as the most convenient means of mimetizing particle bound states[3]. In those, the common and

defining feature is that their relative velocity  $v$  comes to be a small parameter. Then  $m$ , the mass of at least one of the particles, belongs to the high-energy domain we do not wish to describe. The explicit appearance of growing powers of its inverse in the EFT Lagrangian's coefficients establishes a clear dimensional ordering for their associated operators. Those theories pervade nature: electromagnetically interacting systems (as positronium  $e^+e^-$  or muonium  $\mu^+e^-$ ), those bound by strong interaction (heavy quarkonia as  $\bar{t}t$ ,  $\bar{b}b$ ,  $\bar{b}c$  or  $\bar{c}c$ ) or formed and decaying by combined mechanisms (hydrogenoid atoms, pionium  $\pi^+\pi^-$ ), all of them benefit from the common feature of presenting related and well-separated energy (momenta) scales whose disentangling can be profited in order to ease the calculation. Even more, what is an advantage for the non-relativistic EFT formulation, appears as a cumbersome difficulty that the old approach of a Bette-Salpeter equation with its non-relativistic reduction does not solve satisfactorily: lack of systematicity, ambiguities and presumptions blur the physical picture.

The calculation of the bound state wave function and its energy levels presents, as a particularity and main difference with respect to scattering calculations, off-shell initial and final states. The implicit dependence of these on the interaction coupling constants ( $\{\alpha\}$ ) results in a non-trivial choice of order-by-order in  $\{\alpha\}$  contributions from different sorts of Feynman graphs. To be more specific, the leading order in  $\{\alpha\}$  does not follow from the number of vertices in the diagrams and it becomes completely unavoidable to resum an infinite series of them (for instance ladder photons in QED) in order to provide the leading order approximation. After doing so no spurious, gauge dependent terms, generated at every order in  $\alpha$  and cancelled in the resummation, will arise.

As we see, the problem lies on the existence in these diagrams of different hierarchically ordered physical scales entangled and contributing. For example, in NRQED those would be the mass  $m$  of a heavy particle, that is larger than the relative momentum  $p \sim mv$  of the bound state, which at the same time is larger than the bound state energy  $E \sim mv^2$  ( $v \ll 1$ ). In HQET we would have only the scale  $m$  which is larger than  $\Lambda_{QCD}$  and  $p \sim E \sim \Lambda_{QCD}$ . A non-relativistic EFT organizes itself as to power count correctly, so taking as starting point the evaluation of the non-relativistic Green function through a Schrödinger equation. Corrections coming from retardation or non-potential effects (given by interacting low-energy particles), relativistic effects (expansion of  $\frac{1}{m}$  in the energies and wave function) and higher order perturbative interactions, not only enter consistently at every stage of the calculation but are also incorporated in such a way that no unwanted IR divergences arise, UV divergences are per-

turbatively renormalized by the couplings at our disposal, non-perturbative contributions of the theory (read here QCD) are isolated and parametrized ...

But NREFTs do not restrict themselves to implementing technical facilities. They also broaden our knowledge about some conceptual issues. For example, we will see in the following pages that, once  $m$  has been integrated, we might take the NR formulation to a potential level whether it is the case that  $mv$  can also be integrated. This last step gives rise to the appearance of potentials as matching coefficients, so paving the way from a Field Theory formulation to a Quantum Mechanical setting.

In such spirit, this work is intended to be, more than a collection of different calculations performed in the common framework of NREFTs, my own learn-it-on-the-way report where every chapter, when focusing on a small range of theoretical aspects tightly related with problems of present concern in the field, reinforces the impression of unity. Besides providing answers to phenomenologically relevant questions, this set of contemporary examples aims at reviewing fundamental building blocks of NREFTs. So, in the first chapter, while tackling the calculation of ponium's -electromagnetically, loose bounded  $\pi^+$  and  $\pi^-$  system- decay, we gaze at the importance of different, more or less widely ranged, energy and momentum scales that give rise to a series of NREFT's Lagrangians, also characterized by their symmetries and counting rules, which constitute intermediate stages in the way to a quantum mechanical formulation. Other issues such as reparametrization invariance and field redefinitions, matching calculations and accuracy control, also enter our scope and are emphasized.

The second chapter, concerning the finite mass effects of vacuum polarization corrections in non-relativistic bound states, puts the stress on the integration of competing physical scales and on different fields of applicability of one and the same calculation.

The third section offers a brief review and our own approach to one of the issues that has become more controversial in the last years and has moved to considerable, and perhaps not enough rewarded, effort: that is, renormalizability in the context of Nuclear Physics EFTs and, to be more concrete, in NN interaction.

Finally, the last chapter is devoted to the calculation of the P-wave decays of heavy quarkonium. Potential Non-Relativistic QCD (pNRQCD), the ultrasoft EFT of a soft one, (the so-called NRQCD), will enable us to write the NRQCD colour-octet matrix elements in terms of derivatives of wave functions at the origin and non-perturbative universal constants. Thanks to this, we achieve a new set

of relations among hadronic inclusive decays' branching ratios for quarkonia with different quantum number and with different heavy flavour.

# Chapter 1

## Pionium's lifetime: last stage in a EFT's chain

### 1.1 Motivation

The striking simplicity of organizing corrections to one process and non-model dependency of calculations undertaken in NREFTs is perfectly well displayed in the following pages, that aim at offering a clear derivation of the  $\pi^+\pi^-$  (pionium) loosely, electromagnetically bounded ground state decay rate to neutral pions with a precision of 10%. This high accuracy is to be expected in DIRAC's experiment (see Appendix A), currently performed at CERN[4], so that theoretical predictions will be sternly tested and the nature of spontaneous chiral symmetry breaking will receive further enlightenment. Being pionium's lifetime proportional to the square of the difference between the strong scattering lengths for isospin 0 and 2,  $a_0-a_2$ , whose value is predicted to be, in the framework of Standard Chiral Perturbation Theory, equal to  $.265 \pm .004$ , any discrepancy coming from experimental values would signal the relevance of a Generalized Scenario[5] (where  $a_0-a_2$  is fitted to  $.29$  from  $K_{l4}$  decays and  $\pi\pi$  phase shifts).

It is of general knowledge that in the chiral limit where  $m_u = m_d = m_s = 0$ , QCD's flavour symmetry  $SU(3)_L \times SU(3)_R$  is spontaneously broken down to  $SU(3)_V$ , so arising eight massless Goldstone bosons coupled to the conserved axial-vector currents[6]. In the real world, where light quarks have small masses (in comparison with the typical hadronic mass scale  $\Lambda_\chi \sim 1$  GeV.) this approximate

symmetry serves us to establish  $\chi$ PTh, the low-energy effective theory obeyed by Goldstone bosons, as a systematic expansion in powers of external momenta and quark masses. Nevertheless, the usual assumption that the quark condensate mechanism is dominant as a symmetry breaking effect is somewhat controversial. It still holds the possibility that, instead of the Standard value of 2 GeV. ( $\sim \frac{m_\pi^2}{2m_q}$ ) for the quark condensate order parameter,  $B := -\frac{\langle \Omega | \bar{u}u | \Omega \rangle}{F_\pi^2}$ , the rather lower value  $\sim 100$  MeV. suits, so giving consistency to a less constricted picture that is called Generalized  $\chi$ PTh. The latter departs widely from Standard counting rules<sup>1</sup> :

$$\begin{aligned} S\chi PTh : \quad m_q &= \mathcal{O}(p^2) \quad , \quad B = \mathcal{O}(1) \\ G\chi PTh : \quad m_q &= \mathcal{O}(p) \quad , \quad B = \mathcal{O}(p) \end{aligned} \quad (1.1.1)$$

enlarges the number of parameters needed in order to calculate to a given order<sup>2</sup> and grants flexibility. For instance, the ratio  $r = \frac{m_s}{\hat{m}}$ , ( $\hat{m} = \frac{m_u + m_d}{2}$ ), which has a definite value  $\sim 26$  in Standard  $\chi$ PTh, can oscillate between 6.3 (8 when including higher order corrections) and 26 in the Generalized Scenario. Implications for the temperature of the Chiral Transition are exhibited in the following figure. Notice that  $S\chi$ PTh predicts  $T_c \sim 200$  MeV. whereas  $G\chi$ PTh would allow for a smaller value.

## 1.2 Scales intertwined in the non-relativistic approach

After pionium atoms were first observed in the late eighties[10] and the interest of measuring their lifetime became evident[11], propelled by DIRAC's high precision intended measurement, several papers tackling with such a calculation have appeared, showing the compelling necessity of a model independent, systematic method. So, first attempts in this direction, relativistic potential models where the strong interaction was modeled by square wells and the electromagnetic interaction was preliminary switched off to provide for a way of comparison with the purely hadronic situation, lacked completely from any of those desirable characteristics[12]. The situation was somewhat improved em-

<sup>1</sup>Somewhat restricting this counting to the case where the bilinear condensate  $B$  vanishes in the chiral limit, the authors of [7] have identified a pattern of Chiral Symmetry Breaking ( $\chi$ SB) where the Generalized Scenario is self-consistent. There, a custodial discrete subgroup  $Z_N$  of the axial  $SU(N_f)$  survives, so precluding the formation of a bilinear condensate, while the allowed quartic condensates become the natural order parameters. Regretfully, although this realization of  $\chi$ SB is not ruled out in gauge theories with scalar quarks and/or Yukawa couplings, it does enter in direct contradiction with exact QCD inequalities[8].

<sup>2</sup>Take the  $SU(2)_L \times SU(2)_R$  realization of  $\chi$ PT, where properties of pions are calculated. There the Generalized Scenario builds on the basis of a value of the effective coupling  $\ell_3$  which is completely unnatural from the Standard point of view.



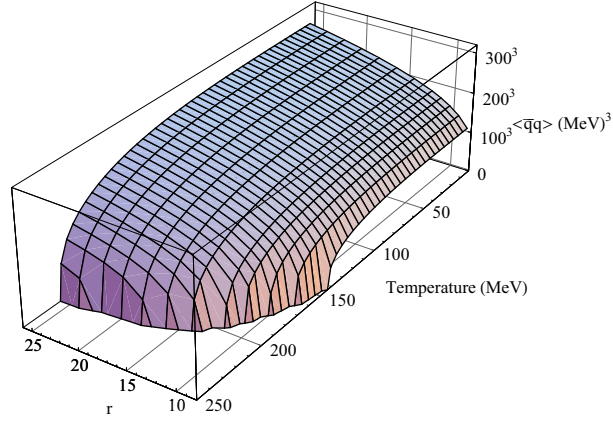


Figure : Quark condensate versus temperature and  $r$  [9].

ploying two-body wave equations of 3D constraint theory[13] and field theoretical approaches based on the Bethe-Salpeter equation[14]. Nevertheless we can state that the major breakthrough came by the hand of the non-relativistic EFT approach[15, 17, 18], that combined efficiency and simplicity with the abovementioned features.

Why a non-relativistic calculation is suited to our problem is well-understood once we assign numbers to the different energy-momentum scales involved in the lifetime. Pionium decays mainly by strong interaction to two neutral pions. In first approximation its associated lifetime is given by Deser's formula[19]:

$$\Gamma_{2\pi^0} = \frac{16\pi}{9m_\pi^3} \sqrt{2m_\pi \Delta m} (a_0 - a_2)^2 |\Psi_n(\mathbf{0})|^2, \quad (1.2.1)$$

whose derivation we will review when calculating its corrections, in the next few sections. Three physical scales appear in this expression: the higher one,  $m_\pi \sim 140$  MeV. will be in the following the mass of the charged pions;  $\Delta m \sim 5$  MeV. designates the mass difference between charged and neutral pions,  $m_{\pi^+} - m_{\pi^0}$ , with associated non-relativistic momentum  $\sqrt{2m\Delta m} \sim 40$  MeV.; the lower one is the inverse of the Bohr radius, which appears through the wave function at the origin,  $\frac{m\alpha}{2} \sim .5$  MeV. They all combine to give a value  $\Gamma_{2\pi^0}^{L0} \sim .2$  eV., where we have used the leading order value for the difference between isospin 0 and 2 scattering lengths ( $\frac{m^2}{8f_\pi^2}$ ), as calculated from the  $\chi$ -Lagrangian.  $\Gamma_{2\pi^0}$  is then, a quantity of order  $\alpha^3$ . The next relevant decay channel,  $\pi^+\pi^- \rightarrow \gamma\gamma$ , counts at leading order

as  $\Gamma_{2\gamma} = \frac{m\alpha^5}{4}$  and therefore it can be safely ignored at the 10% accuracy level.

The previous display of numbers suggests to proceed as following. As all scales involved are rather lower than the mass of the pion, a non-relativistic approach applies. Furthermore, if we want to reach the eV. level, two more intermediate scales, namely the mass difference  $\Delta m$  and bound state relative momenta  $mv$ , can be **sequentially** integrated out, so taking profit from the fact that they are four orders of magnitude apart. The following scheme describes our line of development:

QCD

$$\mathcal{L} = \frac{1}{2g^2} \text{Tr}[F^{\mu\nu}(x)F_{\mu\nu}(x)] + \frac{i}{2}\bar{q}^A(x)\gamma_\mu D^\mu q^A(x) - \frac{i}{2}\bar{D}^\mu q^A(x)\gamma_\mu q^A(x) - m_A\bar{q}^A(x)q^A(x) + \dots$$

↓

χ-Lagrangian

....  $4\pi f_\pi$  ....  $m_\rho$  ....

$$\mathcal{L} = \mathcal{L}_{p^2} + \mathcal{L}_{e^2} + \mathcal{L}_{p^4} + \mathcal{L}_{e^2p^2} + \mathcal{L}_{p^6} + \dots$$

$$\mathcal{L}_{p^2} = \frac{f^2}{4} \langle D_\mu U D^\mu U + \chi U^\dagger + \chi^\dagger U \rangle$$

$$\mathcal{L}_{e^2} = C \langle QUQU^\dagger \rangle$$

$$\mathcal{L}_{p^4} = l_1 \langle D_\mu U^\dagger D^\mu U \rangle^2 + l_2 \langle D_\mu U^\dagger D_\nu U \rangle \langle D^\mu U^\dagger D^\nu U \rangle + l_3 \langle D_\mu U^\dagger D^\mu U \rangle \langle \chi U^\dagger + \chi^\dagger U \rangle + \dots$$

$$\mathcal{L}_{e^2p^2} = k_1 \langle QUQU^\dagger \rangle^2 + k_2 \langle QUQU^\dagger \rangle \langle D_\mu U^\dagger D^\mu U \rangle + k_3 (\langle U^\dagger D_\mu U Q \rangle^2 + \langle D_\mu U U^\dagger Q \rangle^2) + \dots$$

↓

NRχLagrangian

.... **m** ....

$$\mathcal{L}_2 = \pi_+^\dagger (i\partial_0 + \frac{\nabla^2}{2m} + \frac{\nabla^4}{8m^3})\pi_+ + \pi_-^\dagger (i\partial_0 + \frac{\nabla^2}{2m} + \frac{\nabla^4}{8m^3})\pi_- + \pi_0^\dagger (i\partial_0 + \Delta m + \frac{\nabla^2}{2m} + \Delta m \frac{\nabla^2}{2m^2} + \frac{\nabla^4}{8m^3})\pi_0$$

$$\begin{aligned}
\mathcal{L}_4 &= R_{00}\pi_0^\dagger\pi_0^\dagger\pi_0\pi_0 + R_{cc}\pi_+^\dagger\pi_-^\dagger\pi_+\pi_- + (R_{0c}\pi_0^\dagger\pi_0^\dagger\pi_+\pi_- + h.c.) + \\
&+ S_{00}(\pi_0^\dagger\pi_0^\dagger\pi_0\nabla^2\pi_0 + h.c.) + S_{cc}(\pi_+^\dagger\pi_-^\dagger(\pi_+\nabla^2\pi_- + \pi_-\nabla^2\pi_+) + h.c.) + \\
&+ S_{0c}(\pi_0^\dagger\pi_0^\dagger(\pi_+\nabla^2\pi_- + \pi_-\nabla^2\pi_+) + 2\pi_+^\dagger\pi_-^\dagger\pi_0\nabla^2\pi_0 + h.c.) + \\
&+ P_{00}\pi_0^\dagger\partial_i\pi_0^\dagger\pi_0\partial_i\pi_0 + P_{cc}(\pi_+^\dagger\partial_i\pi_-^\dagger\pi_+\partial_i\pi_- + \pi_-^\dagger\partial_i\pi_+^\dagger\pi_-\partial_i\pi_+) \\
&\quad \Downarrow \\
&\dots \Delta m \dots \boxed{\text{NR}\chi \text{ Lagrangian (only charged sector)}} \dots \sqrt{2m\Delta m} \dots \\
&\mathcal{L}' = \pi_+^\dagger(iD_0 + \frac{\mathbf{D}^2}{2m})\pi_+ + \pi_-^\dagger(iD_0 + \frac{\mathbf{D}^2}{2m})\pi_- + \\
&\quad + R'_{cc}\pi_+^\dagger\pi_-^\dagger\pi_+\pi_- + P'\pi_+^\dagger\pi_-^\dagger i\partial_0\pi_+\pi_- \\
&\quad \Downarrow \\
&\dots m\alpha^2 \dots \boxed{\text{pNR}\chi \text{ Lagrangian}} \dots m\alpha \dots \\
&\mathcal{L} = \pi_+^\dagger(\mathbf{x}, t)(i\partial_0 + \frac{\nabla^2}{2m})\pi_+(\mathbf{x}, t) + \pi_-^\dagger(\mathbf{x}, t)(i\partial_0 + \frac{\nabla^2}{2m})\pi_-(\mathbf{x}, t) + \\
&\quad + R'_{cc}(\pi_+^\dagger\pi_-^\dagger\pi_+\pi_-)(\mathbf{x}, t) + P'(\pi_+^\dagger\pi_-^\dagger)(\mathbf{x}, t)i\partial_0(\pi_+\pi_-)(\mathbf{x}, t) - \\
&\quad - \int d^3\mathbf{y}(\pi_+^\dagger\pi_+)(\mathbf{x}, t)(V_0(|\mathbf{x} - \mathbf{y}|) + V_1(|\mathbf{x} - \mathbf{y}|))(\pi_-^\dagger\pi_-)(\mathbf{y}, t) \\
&\quad V_0(|\mathbf{x} - \mathbf{y}|) = -\frac{\alpha}{|\mathbf{x} - \mathbf{y}|} \\
&\quad V_1(|\mathbf{x} - \mathbf{y}|) = \int \frac{d^3\mathbf{k}}{(2\pi)^3} V_{vp}(\mathbf{k}) e^{i(\mathbf{x} - \mathbf{y})\mathbf{k}}
\end{aligned}$$

The first step consists in: (1) building to the level of accuracy required and containing all independent terms allowed by symmetries, a non-relativistic Lagrangian describing charged and neutral pions and, (2) matching[20], to the intended precision, its coefficients to the relativistic  $\chi$ -Lagrangian, by requiring that a convenient set of two and four point amplitudes, calculated by means of both Lagrangians, are equivalent at threshold for pion production. In order to meet the expected accuracy we must remember two things about expansions: (1) as for the non-relativistic Lagrangian, the next relevant scale we want to achieve is  $\Delta m$ , so in our power counting we will assign to any momenta the value  $\sqrt{2m\Delta m}$  and to any energy its associated non-relativistic energy  $\Delta m$ ; (2) since the  $\chi$ -Lagrangian is an expansion in  $\frac{m^2}{(4\pi f_\pi)^2} \sim .015$ ,  $\frac{p^2}{(4\pi f_\pi)^2}$  or, what comes to be the same, loops, we observe that, in

principle, one should expect only the  $\chi$ -Lagrangian to one-loop order to be relevant (therefore, only  $p^4$ ,  $p^2 e^2$  effects would be taken into account, if we use the standard counting  $e^2 \sim \frac{m^2}{(4\pi f_\pi)^2}$ ). Nevertheless, series do not converge so quickly. We further qualify in that respect in the future.

Next stage take us down to a Lagrangian which does not contain neutral pions. By integrating out the scale  $\Delta m$  imaginary parts are generated and coefficients inherit series in  $\left(\frac{\Delta m}{m}\right)^{\frac{1}{2}}$ . As this quotient is  $\sim .2$ , it is required to keep second order corrections in this variable.

Eventually, we reach the relative momentum scale. Coulomb photons are resummed and pionium is formed. Coefficients turn out to be potentials and calculations in this theory reduce to Quantum Mechanical ones. When computing, it is expected to find, besides the previous quotients and as most relevant contributions from the last integration performed, relevant corrections in  $\alpha$  and some in  $\frac{m\alpha^2}{\sqrt{2m\Delta m}} \sim 10^{-4}$  which will be beyond our scope.

### 1.3 Lagrangian for non-relativistic pions near threshold

We shall start by writing down the non-relativistic Lagrangian which, organized in powers of  $\frac{1}{m}$ , serves us to describe the dynamics of a two pion system whose off-shell energy is well below  $m$ . The next relevant scales for the problem at hand, that is,  $\Delta m$  for the energy and  $\sqrt{2m\Delta m}$  for its associated momentum, provide an estimation of the size of every operator and allow us to stop the expansion of the Lagrangian at the appropriate level of accuracy.

In constructing this Lagrangian attention must be payed on the symmetries (exact and approximate) inherited from the fundamental theory, in our case from the  $\chi$ -Lagrangian. Being  $m$  an integrated scale, our most characteristic internal symmetry, the chiral one, enters only through the parameters of the Lagrangian, which might be expanded in powers of  $\left(\frac{m}{4\pi f}\right)^2$ . No further algebraic implications constrain from this side the form of the theory.

On the contrary, isospin, the approximate internal symmetry explicitly broken by up and down quark mass difference,  $m_u - m_d$ , and electromagnetic interactions, generates the neutral to charged pion mass gap  $m_{\pi^+} - m_{\pi^0}$ , still a small quantity. Hence isospin symmetry is a good (approximate) symmetry for the non-relativistic Lagrangian. In order to implement it we shall use the vector  $\pi$ , defined as:

$$\pi = \left( \frac{\pi_+ + \pi_-}{\sqrt{2}}, \frac{\pi_- - \pi_+}{\sqrt{2}i}, \pi_0 \right), \quad (1.3.1)$$

where  $\pi_+$ ,  $\pi_-$  and  $\pi_0$  annihilate positive, negative and neutral pions respectively, as well as the  $T_3$ -proportional vectors  $\mathbf{Q} \sim (0, 0, e)$  and  $\mathbf{M} \sim (0, 0, m_u - m_d)$ , that take into account isospin breaking effects due to electromagnetic and strong interactions.

As for space-time and discrete symmetries, they are implemented in the standard way. In particular, the Lorentz subgroup requires the introduction of a non-linear implementation equivalent to imposing the so-called reparametrization invariance (see Appendix B), that turns out to be quite simple in the case of spin zero fields. That is, consider a composite spin zero field made up of tensor products of  $n$   $\pi$  and  $m$   $\pi^\dagger$  and define  $\omega = n - m$  as the weight of the field. If  $\omega \neq 0$ , then all derivatives acting on the field must be introduced through the combination:

$$D = i\partial_0 - \frac{1}{2\omega m} \partial_\mu \partial^\mu. \quad (1.3.2)$$

If  $\omega = 0$ , we are allowed to act with  $\partial_\mu$  on this field. Then all Lorentz indexes in the Lagrangian will appear contracted in a formally Lorentz invariant way.  $D$  must be considered a Lorentz invariant on its own.

With this simple rules in mind and considering in first place the limit of exact isospin symmetry, the following terms must be incorporated in the non-relativistic Lagrangian:

$$\begin{aligned} \mathcal{L} &= \mathcal{L}_2 + \mathcal{L}_4, \\ \mathcal{L}_2 &= \mathcal{L}_2^{(0)} + \mathcal{L}_2^{(1)} + \dots, \\ \mathcal{L}_4 &= \mathcal{L}_4^{(1/2)} + \mathcal{L}_4^{(3/2)} + \dots, \\ \mathcal{L}_2^{(0)} &= \pi^\dagger D \pi, \\ \mathcal{L}_2^{(1)} &= \pi^\dagger A_0 D^2 \pi, \\ \mathcal{L}_4^{(1/2)} &= B_1 (\pi^\dagger \pi)^2 + B_2 (\pi \pi) (\pi^\dagger \pi^\dagger), \\ \mathcal{L}_4^{(3/2)} &= A_1 (\pi D \pi) (\pi^\dagger \pi^\dagger) + h.c. + A_2 (\pi^\dagger D \pi) (\pi^\dagger \pi) + h.c. + \\ &\quad + A_3 (\pi^\dagger \pi^\dagger) D (\pi \pi) + A_4 \partial_\mu (\pi^\dagger \pi) \partial^\mu (\pi^\dagger \pi) + \\ &\quad + A_5 (\pi^\dagger{}^i \pi^\dagger{}^j) D (\pi^i \pi^j). \end{aligned} \quad (1.3.3)$$

Previous constants contain also information on isospin conserving electromagnetic interactions, both at quark level and those newly entering by matching from the relativistic Chiral Lagrangian. As for isospin breaking pieces, they are incorporated by making use of the previously introduced vectors

**Q** and **M**. Regarding that due to charge conjugation  $m_u - m_d$  contributions enter quadratically and are small[21] ( $\sim .1$  MeV., charged to neutral pion mass difference is mainly an electromagnetic effect), in the future we will ignore terms involving **M**. Remembering that **Q** must always appear in pairs, we include the following invariants in our Lagrangian:

$$\begin{aligned}
\Delta\mathcal{L} &= \Delta\mathcal{L}_2 + \Delta\mathcal{L}_4, \\
\Delta\mathcal{L}_2 &= \Delta\mathcal{L}_2^{(0)} + \Delta\mathcal{L}_2^{(1)}, \\
\Delta\mathcal{L}_4 &= \Delta\mathcal{L}_4^{(3/2)}, \\
\Delta\mathcal{L}_2^{(0)} &= \delta_1(\boldsymbol{\pi}^\dagger \mathbf{Q})(\mathbf{Q}\boldsymbol{\pi}), \\
\Delta\mathcal{L}_2^{(1)} &= \delta_2(\boldsymbol{\pi}^\dagger \mathbf{Q})D(\mathbf{Q}\boldsymbol{\pi}), \\
\Delta\mathcal{L}_4^{(3/2)} &= C_1(\boldsymbol{\pi}\mathbf{Q})(\boldsymbol{\pi}\mathbf{Q})(\boldsymbol{\pi}^\dagger \boldsymbol{\pi}^\dagger) + h.c. + C_2(\boldsymbol{\pi}\mathbf{Q})(\boldsymbol{\pi}^\dagger \mathbf{Q})(\boldsymbol{\pi}^\dagger \boldsymbol{\pi}) + \\
&\quad + C_3((\boldsymbol{\pi}^\dagger \times \boldsymbol{\pi}) \cdot \mathbf{Q})^2.
\end{aligned} \tag{1.3.4}$$

Before going on, let us discuss the general structure of the constants  $A_i$ ,  $B_i$ ,  $C_i$  and  $\delta_i$  above. Calling  $Z$  to any such a constant and  $z$  to its dimension, then the general form of  $Z$  will be:

$$\begin{aligned}
Z &= m^z \left( a_{-1} + a_0 \left( \frac{m}{4\pi f} \right)^2 + a_1 \left( \frac{m}{4\pi f} \right)^4 + a_2 \left( \frac{m}{4\pi f} \right)^6 + \dots \right. \\
&\quad \left. + b_1 \alpha + \dots \right)
\end{aligned} \tag{1.3.5}$$

$$\left. + c_{1,1} \alpha \left( \frac{m}{4\pi f} \right)^2 + c_{1,2} \alpha \left( \frac{m}{4\pi f} \right)^4 + \dots \right). \tag{1.3.6}$$

$a_i$ ,  $i=0,1,\dots$ , refers to pure strong interactions. Spontaneous chiral symmetry breaking implies that only those constants accompanying bilinear terms, that is  $A_0$  and  $\delta_i$ , can have  $a_{-1} \neq 0$ , as in the limit  $f \rightarrow \infty$  pions become free particles as regards to strong interactions. The subindex numbering keeps track of the higher number of loops that contributes to each four-boson term and, as you see, we have stopped at two loop order[22], which is the present stage of calculations.  $c_{1,i}$  combine leading electromagnetic with strong interactions[23]. As our future expressions will not make use of this chiral expansion, they contain in principle all number of loops. Nevertheless, let us mention for numerical purposes that the previous series, although displayed in terms of  $\left( \frac{m}{4\pi f} \right)^2$ , are seen to converge (that is, they have  $\mathcal{O} \sim 1$  coefficients) better as  $\left( \frac{m}{\pi f} \right)^2$ . To one loop order we have 20% corrections. To two loop order 5%. Although right now this is superfluous information, let us advance that, from final expressions, it is clearly observed that the 10% aimed accuracy require one combination of the above constants, that

enters quadratically in Deser's formula, to be provided at two loop level. Therefore, matching with  $\chi$ PTh involves  $\mathcal{L}_{p^2}$ ,  $\mathcal{L}_{p^4}$ ,  $\mathcal{L}_{p^6}$  and  $\mathcal{L}_{e^2 p^2}$ ,  $\mathcal{L}_{e^2 p^4}$ , if we keep counting  $e^2$  as standard  $\sim \left(\frac{m}{4\pi f}\right)^2$ .

The Lagrangian (1.3.3) and (1.3.4) contains time derivatives beyond leading order in the bilinear term. One can get rid of them, and draw the non-relativistic Lagrangian to its usual and more convenient minimal form, by using local field redefinitions. The price we pay when performing this rearrangement is that we cannot maintain Lorentz symmetry (and hence reparametrization invariance) explicit anymore. Nevertheless the constraints given by Lorentz symmetry somehow survive through a set of non-trivial relations among the parameters of the Lagrangian.

### 1.3.1 Local field redefinitions

Local field redefinitions exploit the freedom we have in field theory to choose the interpolating field we wish. We can take advantage of the fact that such redefinitions can be organized in powers of  $\Delta m/m$  to retain only those induced terms up to the relative order at which our Lagrangian was truncated, that is  $(\Delta m/m)^{\frac{3}{2}}$ . Furthermore, we can also neglect terms which do not contribute to the two particle sector (six pion terms and beyond).

We will begin by considering those local field redefinitions we can perform without loosing explicit Lorentz symmetry. In first place we can get rid of the  $A_0$  and  $\delta_2$  terms in (1.3.3) and (1.3.4) by:

$$\pi^i \mapsto \left[ \left(1 - \frac{DA_0}{2}\right) \delta^{ij} \pi^j + \left( \frac{\delta_1 A_0 \mathbf{Q}^i \mathbf{Q}^j}{2} - \frac{\delta_2 \mathbf{Q}^i \mathbf{Q}^j}{2} \right) \right] \pi^j. \quad (1.3.1.1)$$

By doing this, the bilinear terms become:

$$\mathcal{L}_2 + \Delta \mathcal{L}_2 = \pi^\dagger D\pi + \pi^\dagger \delta_1 \mathbf{Q}^i \mathbf{Q}^j \left[ 1 + (\delta_1 A_0 - \delta_2) \mathbf{Q}^2 \right] \pi^j, \quad (1.3.1.2)$$

and the following constants of the four pion terms get modified:

$$\begin{aligned} A_1 &\rightarrow A'_1 = A_1 - A_0 B_2, \\ A_2 &\rightarrow A'_2 = A_2 - A_0 B_1, \\ C_1 &\rightarrow C''_1 = C_1 - (\delta_2 - \delta_1 A_0) B_2, \\ C_2 &\rightarrow C''_2 = C_2 - 2(\delta_2 - \delta_1 A_0) B_1. \end{aligned} \quad (1.3.1.3)$$

We can also hide the  $A'_1$  and  $A'_2$  terms, while still keeping Lorentz invariance, by making:

$$\pi \mapsto \pi - A'_2{}^* \pi (\pi^\dagger \pi) - A'_1{}^* \pi^\dagger (\pi \pi), \quad (1.3.1.4)$$

which induces:

$$\begin{aligned} C_1'' &\rightarrow C_1''' = C_1'' - A_1' \delta_1, \\ C_2'' &\rightarrow C_2''' = C_2'' - (A_2' + A_2'^*) \delta_1. \end{aligned} \quad (1.3.1.5)$$

The remaining time derivatives in  $D$  and in the  $A_3$  and  $A_4$  terms can only be removed if we give up the explicit realization of Lorentz symmetry which we have kept so far. Notice that the time derivatives in the  $A_4$  term are higher order and can be dropped. Higher order time derivatives in the bilinear terms are removed by:

$$\pi^i \mapsto \left[ \left( 1 - \frac{i\partial_0}{4m} + \frac{\nabla^2}{8m^2} \right) \delta^{ij} + \frac{\delta_1 \mathbf{Q}^i \mathbf{Q}^j}{4m} \right] \pi^j. \quad (1.3.1.6)$$

Finally the time derivatives induced by this redefinition in the four pion terms together with the remaining time derivatives in  $A_3$  and  $A_4$  can be absorbed in:

$$\pi \mapsto \pi + \left( \frac{B_1}{2m} - A_5 \right) \pi (\pi^\dagger \pi) + \left( \frac{B_2}{2m} - A_3 \right) \pi^\dagger (\pi \pi). \quad (1.3.1.7)$$

In this way we obtain finally the Lagrangian in its minimal form:

$$\begin{aligned} \mathcal{L} &= \mathcal{L}_2 + \mathcal{L}_4, \\ \mathcal{L}_2 &= \pi^{\dagger j} \left[ \left( i\partial_0 + \frac{\nabla^2}{2m} + \frac{\nabla^4}{8m^3} \right) \delta_{ij} + \left( 1 + \frac{\nabla^2}{2m^2} \right) \Delta m \frac{\mathbf{Q}^i \mathbf{Q}^j}{\mathbf{Q}^2} \right] \pi^i, \\ \mathcal{L}_4 &= B_1 (\pi^\dagger \pi)^2 + B_2 (\pi \pi) (\pi^\dagger \pi^\dagger) + D_1 \left( \pi^\dagger \frac{\nabla^2}{2m} \pi + \pi \frac{\nabla^2}{2m} \pi^\dagger \right) (\pi^\dagger \pi) + \\ &\quad + D_2 \left[ \left( \pi \frac{\nabla^2}{2m} \pi \right) \pi^\dagger \pi^\dagger + \pi \pi \left( \pi^\dagger \frac{\nabla^2}{2m} \pi^\dagger \right) \right] + 2A_4 (\pi^\dagger \pi) \partial^i \pi^\dagger \partial^i \pi + \\ &\quad + C_1' (\pi \mathbf{Q}) (\pi \mathbf{Q}) (\pi^\dagger \pi^\dagger) + h.c. + C_2' (\pi \mathbf{Q}) (\pi^\dagger \mathbf{Q}) (\pi^\dagger \pi) + \\ &\quad + C_3 \left( (\pi^\dagger \times \pi) \cdot \mathbf{Q} \right)^2 + \frac{A_3}{2} (\pi^\dagger \pi^\dagger) \frac{\nabla^2}{2m} (\pi \pi) + \frac{A_5}{2} (\pi^{\dagger i} \pi^{\dagger j}) \frac{\nabla^2}{2m} (\pi^i \pi^j), \end{aligned} \quad (1.3.1.8)$$

where coefficients  $D_1$ ,  $D_2$ ,  $C_1'$  and  $C_2'$  are related with those from (1.3.3) and (1.3.4) by:

$$\begin{aligned} \Delta m &= \delta_1 \mathbf{Q}^2 \left[ 1 + \left( \delta_1 A_0 - \delta_2 + \frac{\delta_1}{2m} \right) \mathbf{Q}^2 \right], \\ D_1 &= \frac{B_1}{m} - A_5 + 2m A_4, \\ D_2 &= \frac{B_2}{m} - A_3, \\ C_1' &= C_1 - B_2 \delta_2 + \left( \frac{B_2}{m} - A_3 - A_1 + 2A_0 B_2 \right) \delta_1, \\ C_2' &= C_2 - 2B_1 \delta_2 + \left( \frac{2B_1}{m} - A_2 - A_2^* + 4A_0 B_1 - 2A_5 \right) \delta_1, \end{aligned} \quad (1.3.1.9)$$



Lorentz symmetry guarantees that the bilinear terms have the standard form including relativistic corrections. It also relates  $A_3$  and  $A_5$  in the two last terms to the remaining constants. Unfortunately, as these coefficients introduce terms related to the center of mass momentum, which is irrelevant to our problem, these relations have no practical consequences.

### 1.3.2 Zero charge sector

The zero charge sector in terms of the pion field reads:

$$\begin{aligned}
\mathcal{L}_2 = & \pi_+^\dagger \left( i\partial_0 + \frac{\nabla^2}{2m} + \frac{\nabla^4}{8m^3} \right) \pi_+ + \pi_-^\dagger \left( i\partial_0 + \frac{\nabla^2}{2m} + \frac{\nabla^4}{8m^3} \right) \pi_- + \\
& + \pi_0^\dagger \left( i\partial_0 + \Delta m + \frac{\nabla^2}{2m} + \Delta m \frac{\nabla^2}{2m^2} + \frac{\nabla^4}{8m^3} \right) \pi_0, \\
\mathcal{L}_4 = & R_{00} \pi_0^\dagger \pi_0^\dagger \pi_0 \pi_0 + R_{cc} \pi_+^\dagger \pi_-^\dagger \pi_+ \pi_- + \left( R_{0c} \pi_0^\dagger \pi_0^\dagger \pi_+ \pi_- + h.c. \right) + \\
& + S_{00} \left( \pi_0^\dagger \pi_0^\dagger \pi_0 \nabla^2 \pi_0 + h.c. \right) + S_{cc} \left[ \pi_+^\dagger \pi_-^\dagger \left( \pi_+ \nabla^2 \pi_- + \pi_- \nabla^2 \pi_+ \right) + h.c. \right] + \\
& + S_{0c} \left[ \pi_0^\dagger \pi_0^\dagger \left( \pi_+ \nabla^2 \pi_- + \pi_- \nabla^2 \pi_+ \right) + 2\pi_+^\dagger \pi_-^\dagger \pi_0 \nabla^2 \pi_0 + h.c. \right] + \\
& + P_{00} \pi_0^\dagger \partial_i \pi_0^\dagger \pi_0 \partial_i \pi_0 + P_{cc} \left( \pi_+^\dagger \partial_i \pi_-^\dagger \pi_+ \partial_i \pi_- + \pi_-^\dagger \partial_i \pi_+^\dagger \pi_- \partial_i \pi_+ \right),
\end{aligned} \tag{1.3.2.1}$$

whose constants are defined as:

$$\begin{aligned}
R_{00} = & B_1 + B_2 + e^2(C'_1 + C_1'^*) + e^2 C_2', \\
R_{0c} = & 2B_2 + 2e^2 C_1'^*, \\
R_{cc} = & 2B_1 + 4B_2 + 2e^2 C_3, \\
S_{00} = & \frac{D_1}{2m} + \frac{D_2}{2m}, \\
S_{0c} = & \frac{D_2}{2m}, \\
S_{cc} = & \frac{D_1}{2m} + \frac{D_2}{m}, \\
P_{00} = & 2A_4, \\
P_{cc} = & 2A_4.
\end{aligned} \tag{1.3.2.2}$$

Notice that since the origin of energies appears to be at the two charged pion threshold, the neutral pion shows a negative energy gap  $-\Delta m < 0$ . These terms in the Lagrangian can be combined in a more

standard form:

$$\left( i\partial_0 + \Delta m + \frac{\nabla^2}{2m} + \Delta m \frac{\nabla^2}{2m^2} + \frac{\nabla^4}{8m^3} \right) \sim \left( i\partial_0 + \Delta m + \frac{\nabla^2}{2(m - \Delta m)} + \frac{\nabla^4}{8(m - \Delta m)^3} \right). \quad (1.3.2.3)$$

Nevertheless, in order to keep the expansion systematic we shall not use the expression above.

The coupling to e.m. fields is done by promoting normal derivatives to covariant ones. None of the possible non-minimal couplings contributes at the order we are interested in and we will ignore them.

Before closing this section let us remark that we have assumed that the Lagrangian (1.3.3) and (1.3.4) is Hermitian. Although this is correct at the order we are interested in, in general the hermiticity constraint must be relaxed. Due to the fact that the  $\pi^+\pi^-$  atom may decay into degrees of freedom which do not appear in the non-relativistic Lagrangian, as the already mentioned two hard photons or hard electron-positron pairs, some non-hermitian pieces should be obtained in the matching to the Chiral Lagrangian at the same time as the hermitian ones, as it happens in NRQED.

## 1.4 Integrating neutral pions

Since  $\Delta m \gg m\alpha^2/4$  it is appropriated to integrate out this scale before tackling the electromagnetic bound state problem. This represents the main advantage of our approach with respect to previous non-relativistic proposals. The integration of neutral pions can be easily achieved by matching four point off-shell Green functions of the previous Lagrangian to a non-relativistic Lagrangian where neutral pions have been removed:

$$\begin{aligned} \mathcal{L}' = & \pi_+^\dagger \left( iD_0 + \frac{\mathbf{D}^2}{2m} \right) \pi_+ + \pi_-^\dagger \left( iD_0 + \frac{\mathbf{D}^2}{2m} \right) \pi_- + \\ & + R'_{cc} \pi_+^\dagger \pi_-^\dagger \pi_+ \pi_- + P' \pi_+^\dagger \pi_-^\dagger i\partial_0 \pi_+ \pi_- . \end{aligned} \quad (1.4.1)$$

Since the  $\pi^0$  energy gap is negative, the integration will produce imaginary parts in  $R'_{cc}$  and  $P'$ . By calculating the diagrams in fig. 1, we get in dimensional regularization:

$$\begin{aligned} R'_{cc} = & R_{cc} - |R_{0c}|^2 R_{00} \left( \frac{ms}{2\pi} \right)^2 + i |R_{0c}|^2 \frac{ms}{2\pi} \left( 1 + \frac{5}{8} \frac{s^2}{m^2} - \right. \\ & \left. - \frac{3}{4} \frac{s^2}{m^2} - \left( \frac{R_{00}ms}{2\pi} \right)^2 - \frac{2S_{0c}(R_{0c} + R_{0c}^*)s^2}{|R_{0c}|^2} \right), \end{aligned} \quad (1.4.2)$$

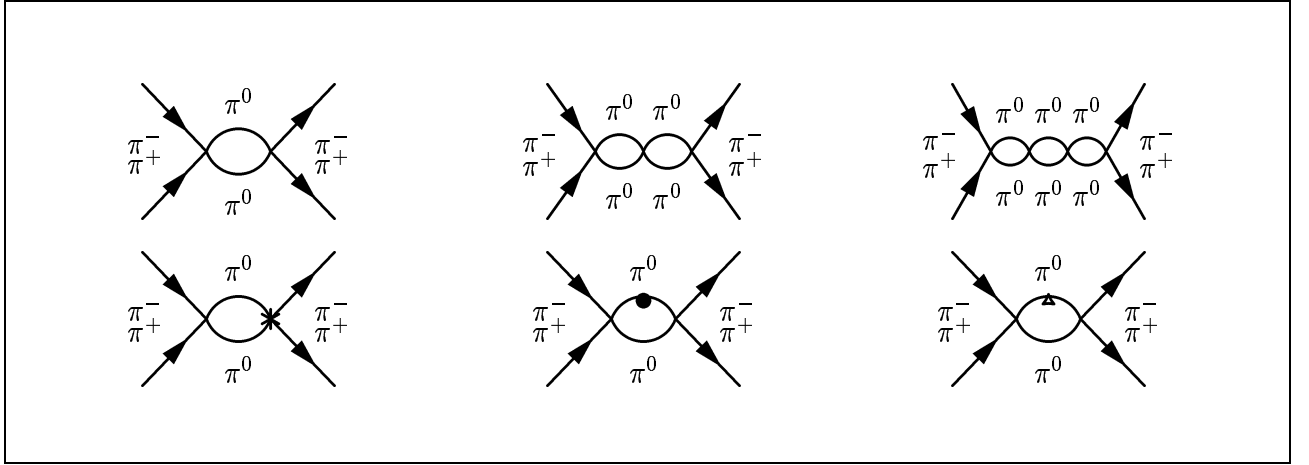


Figure 1: Diagrams contributing to the matching between  $L$  and  $L'$  up to corrections  $\mathcal{O}((\Delta m/m)^2)$ . No decorated vertices belong to  $R_{xy}$  insertions. \* corresponds to a  $S_{0c}$  interaction; • indicates a relativistic correction coming from  $\nabla^4/8m^3$ ;  $\Delta$  one of  $\Delta m \nabla^2/2m^2$  type.

$$P' = i|R_{0c}|^2 \frac{m^2}{4\pi s}, \quad (1.4.3)$$

where  $s = \sqrt{2m\Delta m}$ .  $R'_{cc}$  and  $P'$  contain the leading corrections in  $\Delta m/m$  and  $m\alpha^2/4\Delta m$  respectively. The electromagnetic contributions to  $L'$  coming from the energy scale  $\Delta m$  are negligible, as well as the relativistic corrections  $\sim \nabla^4/8m^3$  to the charge pions and the terms  $P_{cc}$  and  $S_{cc}$  in (1.3.2.1).

## 1.5 Integrating potential photons

The Lagrangian in the previous section is almost identical to NRQED (for spin zero particles) plus small local interactions. In refs. [24] it was shown that we can integrate out the next dynamical scale, namely,  $m\alpha/2$  in NRQED obtaining a further effective theory called potential NRQED (pNRQED), whose coefficients include the usual potential terms, where only the ultrasoft degrees of freedom ( $\sim m\alpha^2/4$ ) remain dynamical. We shall do the same here.

The (maximal) size of each term in (1.4.1) is obtained by assigning  $m\alpha$  to any scale which is not explicit. Apparently no corrections in  $\mathcal{O}(\alpha)$  to the Coulomb potential arise, since transverse photons start contributing to  $\mathcal{O}(\alpha^2)$ , which is beyond our present interest. However, as pointed out in ref. [27], below the pion threshold there are further light degrees of freedom apart from the photon. In particular, the electron mass  $m_e$  is  $\sim m\alpha/2$  and hence it must be integrated out here. This gives rise to a potential

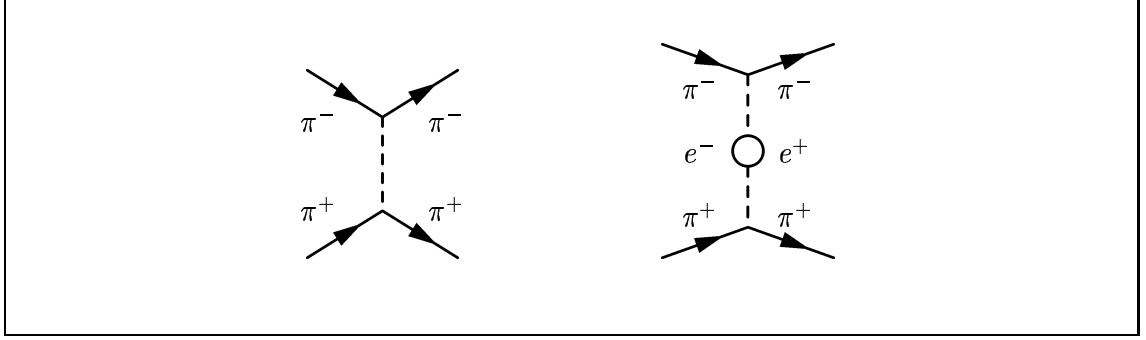


Figure 2: Diagrams contributing to the matching between  $L'$  and  $L''$  up to corrections  $\mathcal{O}(\alpha^2)$ . Dashed lines are longitudinal photon propagators in the Coulomb gauge.

term which is only  $\mathcal{O}(\alpha)$  suppressed with respect to the Coulomb one. By calculating the diagrams in fig. 2 we obtain:

$$\begin{aligned} \mathcal{L}'' = & \pi_+^\dagger(\mathbf{x}, t) \left( i\partial_0 + \frac{\nabla^2}{2m} \right) \pi_+(\mathbf{x}, t) + \pi_-^\dagger(\mathbf{x}, t) \left( i\partial_0 + \frac{\nabla^2}{2m} \right) \pi_-(\mathbf{x}, t) + \\ & + R'_{cc}(\pi_+^\dagger \pi_-^\dagger \pi_+ \pi_-)(\mathbf{x}, t) + P'(\pi_+^\dagger \pi_-^\dagger)(\mathbf{x}, t) i\partial_0(\pi_+ \pi_-)(\mathbf{x}, t) - \\ & - \int d^3\mathbf{y} (\pi_+^\dagger \pi_+)(\mathbf{x}, t) \left( V_0(|\mathbf{x} - \mathbf{y}|) + V_1(|\mathbf{x} - \mathbf{y}|) \right) (\pi_-^\dagger \pi_-)(\mathbf{y}, t), \\ & V_0(|\mathbf{x} - \mathbf{y}|) = -\frac{\alpha}{|\mathbf{x} - \mathbf{y}|}, \quad V_1(|\mathbf{x} - \mathbf{y}|) = \int \frac{d^3\mathbf{k}}{(2\pi)^3} V_{vpc}(\mathbf{k}) e^{i(\mathbf{x}-\mathbf{y})\mathbf{k}}, \end{aligned} \quad (1.5.1)$$

where  $V_{vpc}(\mathbf{k})$  (see Chapter 2 and [27]) is given by:

$$V_{vpc}(\mathbf{k}) = \int_0^1 dv \frac{-4\alpha^2 v^2 (1 - v^2/3)}{\mathbf{k}^2 (1 - v^2) + 4m_e^2}. \quad (1.5.2)$$

As the Lagrangian above contains no other degrees of freedom apart from the non-relativistic charged pions, what we have is totally equivalent to standard Quantum Mechanics. Nevertheless, we like better to stay within the lagrangian formalism and use the  $\pi^- \pi^+$  wave function field  $\phi(\mathbf{x}, \mathbf{X}, t)$ , where  $\mathbf{x}$  and  $\mathbf{X}$  are the relative and center of mass coordinates respectively. Dropping the center of mass kinetic term, we rewrite (1.5.2) as:

$$\mathcal{L}'' = \phi^\dagger(\mathbf{x}, \mathbf{X}, t) \left( i\partial_0 + \frac{\nabla^2}{m} - V_0(|\mathbf{x}|) - V_1(|\mathbf{x}|) + R'_{cc}\delta(\mathbf{x}) + P'\delta(\mathbf{x})i\partial_0 \right) \phi(\mathbf{x}, \mathbf{X}, t). \quad (1.5.3)$$

## 1.6 Quantum mechanical calculation

In order to calculate the corrections to the energy levels and decay width we shall consider the

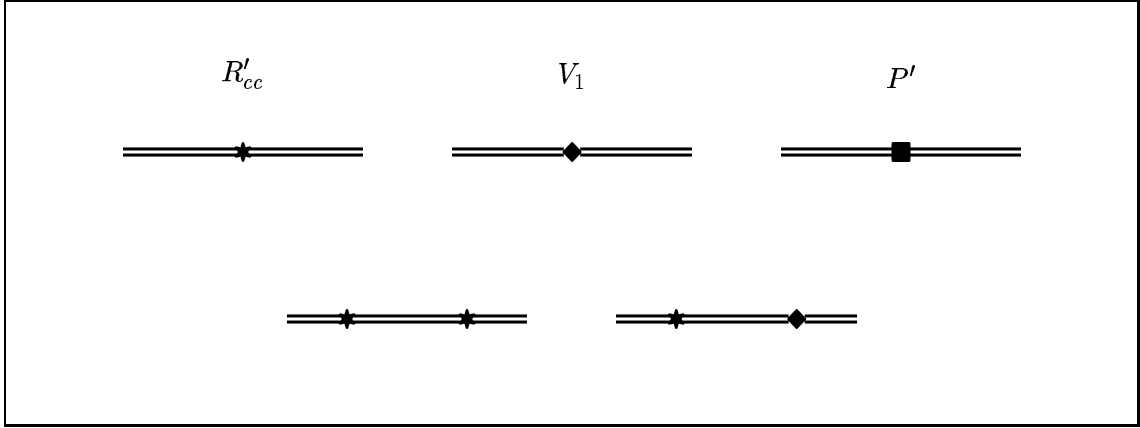


Figure 3: For the first line, diagrams contributing, respectively, to leading order in  $\Delta m/m$ ,  $\alpha$  and  $m\alpha^2/\Delta m$  to the energy and decay width. Second line are second order perturbation theory corrections. The double line is the Coulomb propagator of the  $\pi^+ \pi^-$  pair.

propagator of (1.5.3) and identify its pole. At the order we are interested in only the diagrams in fig. 3 contribute.

The diagrams in the first line of fig. 3 correspond to first order perturbation theory and can be easily evaluated, resulting in:

	$\delta E_n^{(1)}$	$\delta \Gamma_n^{(1)}$
$R'_{cc}$	$-\text{Re}(R'_{cc})  \Psi_n(\mathbf{0}) ^2$	$2 \text{Im}(R'_{cc})  \Psi_n(\mathbf{0}) ^2$
$P'$	---	$-\text{Im}(P')  \Psi_n(\mathbf{0}) ^2$
$V_1$	$\frac{11m\alpha^3}{18\pi} \left( 1 - \frac{9\pi}{22} \xi \frac{12}{11} \xi^2 - \frac{6\pi}{11} \xi^3 - \frac{3(2-\xi^2-4\xi^4)}{11\sqrt{\xi^2-1}} \tan^{-1} \sqrt{\xi^2-1} \right)$ $\xi := \frac{2m_e}{m\alpha}$	---

Table I

where  $\Psi_n(\mathbf{x})$  is the Coulomb wave function.

The diagrams in the second line of fig. 3 correspond to second order perturbation theory. While the second diagram gives a finite contribution which, for the ground state, is calculated in Chapter 2, the first diagram is UV divergent and requires to specify a suitable regularization and renormalization

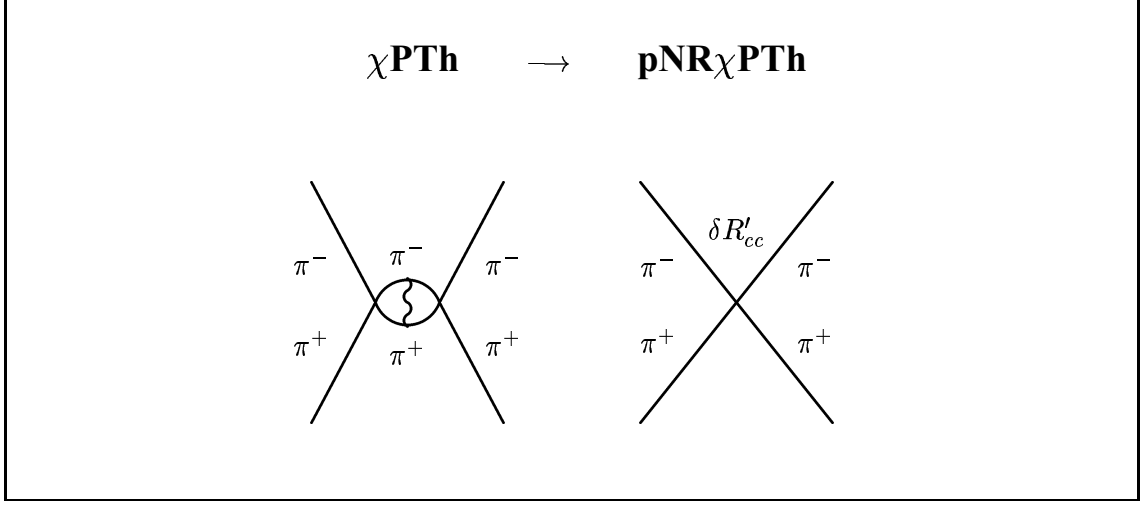


Figure 4: IR divergent relativistic diagram of order  $e^2 p^4$  in  $\chi\text{PTh}$  matches a delta type interaction in  $\text{pNR}\chi\text{PTh}$ .

scheme. The subtraction point dependence of the result will eventually cancel against those contained in the matching coefficients. Down from the Chiral Lagrangian,  $R'_{cc}$  inherits by the matching procedure an IR factorization scale that has been introduced through the calculation of the next figure's divergent, two loop diagram calculated at threshold in  $\chi\text{PTh}$ .

Both, the IR divergent previous diagram and the Quantum Mechanical UV divergence, must be regularized and renormalized using one and the same scheme, most efficiently in DR with  $\overline{MS}$  (or  $\overline{MS}$ ). That is what we have done with this first diagram of fig. 3, briefly sketched in next subsection.

### 1.6.1 Coulomb propagator in D space dimensions

First diagram in fig. 3 is given once we know  $G_c(\mathbf{0}, \mathbf{0}; E)$ , the Coulomb propagator at threshold in D ( $= 3 + 2\epsilon$ ) spatial dimensions. Although for the actual Coulomb potential in D dimensions:

$$V_c(r) = -\frac{\alpha c_D}{r^{D-2}} \quad ; \quad c_D = \frac{4\pi\Gamma\left(\frac{D}{2}\right)}{(D-2)2\pi^{\frac{D}{2}}}, \quad (1.6.1.1)$$

we were not able to find an explicit representation, a slight modification of it:

$$V'_c(r) = -\frac{\alpha c'_D}{r} \quad ; \quad c'_D = \frac{4\pi}{\Gamma\left(\frac{D-1}{2}\right)(4\pi)^{\frac{D-1}{2}}}, \quad (1.6.1.2)$$

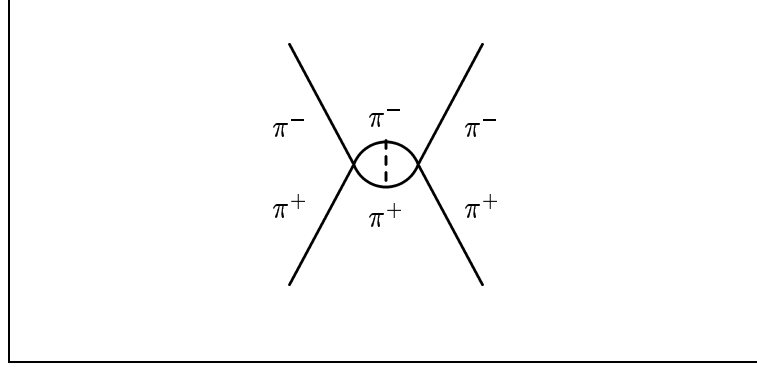


Figure 5: Logarithmically divergent diagram which is calculated with the two longitudinal photon propagators (1.6.1.4) for the dashed lines.

admits the following exact representation, which is a generalization of that presented in ref. [25]:

$$G'_c(\mathbf{x}, \mathbf{y}, E) = \sum_{l=0}^{\infty} G_l(x, y, E) \sum_{\{m_i\}} Y_l^{\{m_i\}}\left(\frac{\mathbf{x}}{x}\right) Y_l^{*\{m_i\}}\left(\frac{\mathbf{y}}{y}\right),$$

$$G'_l(x, y, E) = -m(2k)^{D-2} (2kx)^l (2ky)^l e^{-k(x+y)} \sum_{s=0}^{\infty} \frac{L_s^{2l+D-2}(2kx) L_s^{2l+D-2}(2ky) \Gamma(s+1)}{\left(s + \frac{2l+D-1}{2} - \frac{m\alpha}{2k} c'_D\right) \Gamma(s+2l+D-1)}, \quad (1.6.1.3)$$

where  $Y_l^{\{m_i\}}$  are the spherical harmonics in  $D$  dimensions and  $E = -k^2/m$ .

The potential  $V'_c(r)$  corresponds to the following modification of the longitudinal photon propagator in standard DR:

$$\frac{1}{\mathbf{k}^2} \longrightarrow \left(\frac{1}{\mathbf{k}^2}\right)^{\frac{D-1}{2}}. \quad (1.6.1.4)$$

So we can calculate using (1.6.1.3) and then translate the result to that of standard DR. This change of regularization scheme is obtained by calculating the logarithmically divergent diagram of fig. 5. Using  $MS$  in both cases we obtain:

$$\text{Log}\left(\frac{\mu'}{\mu}\right) = \frac{\gamma_E - 1 - \text{Log}(4\pi)}{2}. \quad (1.6.1.5)$$

The calculation of  $G'_c(0, 0; E)$  can be easily done using the formula 1.4.(1) of ref. [26]:

$$\sum_{n=-\infty}^{\infty} \frac{\Gamma(a+n)\Gamma(b+n)}{\Gamma(c+n)\Gamma(d+n)} = \frac{\pi^2 \Gamma(c+d-a-b-1)}{\sin(\pi a) \sin(\pi b) \Gamma(c-a)\Gamma(d-a)\Gamma(c-b)\Gamma(d-b)}, \quad (1.6.1.6)$$

that allow us to obtain:

$$(\mu')^{-2\epsilon'} G'_c \left( \mathbf{0}, \mathbf{0}, -\frac{k^2}{m} \right) = -2mk \frac{2\pi^{\frac{D}{2}}}{\Gamma\left(\frac{D}{2}\right)} \left(\frac{2k}{\mu'}\right)^{2\epsilon'} \sum_{s=0}^{\infty} \frac{\Gamma(s+D-1)\Gamma\left(s+\frac{D-1}{2}-\frac{m\alpha}{2k}c'_D\right)}{\Gamma(s+1)\Gamma\left(s+\frac{D+1}{2}-\frac{m\alpha}{2k}c'_D\right)\Gamma^2(D-1)} =$$

$$= \frac{mk}{4\pi} \left[ 1 + \right. \quad (1.6.1.7)$$

$$\left. + \frac{m\alpha}{2k} \left( \frac{1}{\epsilon'} + 2\text{Log}\left(\frac{2k}{\mu'}\right) + 2\gamma_E - 2\text{Log}(4\pi) - 2 \right) + \right. \quad (1.6.1.8)$$

$$\left. + \frac{m\alpha}{k} \left( \psi\left(1+\frac{m\alpha}{2k}\right) - \psi(1) + \frac{\pi \cos\left(\frac{m\alpha\pi}{2k}\right)}{\sin\left(\frac{m\alpha\pi}{2k}\right)} - \frac{2k}{m\alpha} \right) \right], \quad (1.6.1.9)$$

where (1.6.1.7), (1.6.1.8) and (1.6.1.9) correspond to zero, one and more than one longitudinal photon exchange respectively.

Finally, for  $E \rightarrow E_n = m\alpha^2/4n^2$  we have:

$$\lim_{E \rightarrow E_n} \left[ (\mu')^{-2\epsilon'} G'_c \left( \mathbf{0}, \mathbf{0}, -\frac{k^2}{m} \right) - \frac{\Psi_n(\mathbf{0})\Psi_n^*(\mathbf{0})}{E - E_n} \right] = \frac{m^2\alpha}{8\pi} \left[ \frac{1}{n} + \right.$$

$$\left. + \left( 2\text{Log}\left(\frac{m\alpha}{n\mu}\right) + \gamma_E - \text{Log}(4\pi) - 1 \right) + \right.$$

$$\left. + \left( 2\psi(n) + 2\gamma_E - \frac{3}{n} \right) \right] \quad (1.6.1.10)$$

$$=: \frac{m^2\alpha\Delta_n}{4\pi}$$

where we have used the MS renormalization scheme and changed  $\mu'$  by  $\mu$  according to (1.6.1.5), so that the results above are in standard DR with MS scheme (this result shows agreement with [16]). Clearly the singular part is local, independent of the principal quantum number  $n$ , and can be absorbed in a renormalization of  $R'_{cc}$ .

## 1.7 Results and numerics

The final outcome for the second order perturbation theory calculation is then:

$$\delta_{R'_{cc}} E_n^{(2)} = \text{Re} \left( R'_{cc} \right)^2 \frac{m^2\alpha\Delta_n}{4\pi} |\Psi_n(\mathbf{0})|^2,$$

$$\delta_{R'_{cc}} \Gamma_n^{(2)} = -2\text{Im} \left( R'_{cc} \right)^2 \frac{m^2\alpha\Delta_n}{4\pi} |\Psi_n(\mathbf{0})|^2, \quad (1.7.1)$$

for the first diagram of fig. 3. As for the second diagram, we can borrow  $\delta_{V_1} \Gamma_n^{(2)}$  from Chapter 2. Right now we can finally join first and second order contributions, to find the expression for leading



corrections in pionium's decay amplitude and energy shifts:

$$E_n = -\frac{m\alpha^2}{4n^2} - \frac{|\Psi_n(\mathbf{0})|^2}{2f^2} + \delta_{V_1} E_n^{(1)},$$

$$\Gamma_n = \Gamma_n^{(0)} \left( 1 + \Delta_{\chi PT} + \frac{5\Delta m}{12m} - \frac{m\alpha^2}{16\Delta m n^2} - \frac{m^2 \alpha \Delta_n}{4\pi f^2} \right) + \delta_{V_1} \Gamma_n^{(2)}, \quad (1.7.2)$$

$$\Gamma_n^{(0)} = \frac{9m\sqrt{2m\Delta m}}{64\pi f^4} |\Psi_n(\mathbf{0})|^2, \quad (1.7.3)$$

where, only due to numerical reasons,  $\delta_{V_1} \Gamma_n^{(2)}$  can be ignored for all purposes in our present analysis ( $\sim 3 \cdot 10^{-3} \Gamma_n^{(0)}$ ). We have substituted  $R_{00}$ ,  $R_{cc}$ ,  $R_{0c}$  and  $S_{0c}$  by their tree level values:

$$R_{00} \sim \frac{1}{16f^2},$$

$$R_{0c} \sim -\frac{3}{8f^2},$$

$$R_{cc} \sim \frac{1}{2f^2}, \quad (1.7.4)$$

$$S_{0c} \sim \frac{1}{32m^2 f^2},$$

and defined:

$$|R_{0c}|^2 = \left( \frac{3}{8f^2} \right)^2 (1 + \Delta_{\chi PT}). \quad (1.7.5)$$

In this way  $\Delta_{\chi PT}$  summarizes all contributions arising from one and two loop integration in the  $\chi$ -Lagrangian: not only the  $p^4$  and  $p^6$  terms, but also those coming from virtual electromagnetic corrections, real photon exchange and charged to neutral pion mass difference. So, formula (1.7.3) does not contain yet all leading corrections in  $\frac{\Delta m}{m}$ . There is one more, contained in  $\Delta_{\chi PT}$ , that can be deduced straightforwardly. That is, remind that the coefficient  $R_{0c}$  ( $R_{0c}^*$ ) is obtained at leading order by evaluating the  $p^2$  chiral amplitude at threshold for the process  $\pi^0 \pi^0 \rightarrow \pi^+ \pi^-$  ( $\pi^+ \pi^- \rightarrow \pi^0 \pi^0$ ). It holds then:

$$R_{0c} \cdot R_{0c}^*|_{LO} = \left( -\frac{s_{\pi^0\pi^0}^{thr} - m_{\pi^0}^2}{8m_{\pi^+}m_{\pi^0}f^2} \right) \cdot \left( -\frac{s_{\pi^+\pi^-}^{thr} - m_{\pi^0}^2}{8m_{\pi^+}m_{\pi^0}f^2} \right), \quad (1.7.6)$$

where the factors 2 and  $(4m_{\pi^+}m_{\pi^0})$  in the denominators take into account indistinguishability and non-relativistic normalization respectively. As  $s_{\pi^0\pi^0}^{thr} = 4m_{\pi^0}^2$  and  $s_{\pi^+\pi^-}^{thr} = 4m_{\pi^+}^2$ , we get:

$$R_{0c} \cdot R_{0c}^*|_{LO} \approx \left( -\frac{3}{8f^2} \right)^2 \left( 1 + \frac{2\Delta m}{3m} \right). \quad (1.7.7)$$

To sum up, all corrections of the form  $\frac{\Delta m}{m}$  to the decay width formula (1.7.3) turn out to be:

$$\frac{\delta\Gamma_n^{\frac{\Delta m}{m}}}{\Gamma_n^{(0)}} = \left( \frac{5}{12} \frac{\Delta m}{m} + \frac{2}{3} \frac{\Delta m}{m} \right) = \frac{13}{12} \frac{\Delta m}{m}, \quad (1.7.8)$$

in such a way that this last result coincides with formula (4.15) in ref.[17] once we substitute their expressions for  $\mathcal{A}$  and  $p^*$  and expand in  $\frac{\Delta m}{m}$ :

$$\begin{aligned} \Gamma_{2\pi^0} &= \frac{2}{9} \alpha^3 p^* \mathcal{A}^2 (1 + \mathcal{K}), \\ \mathcal{A} &= -\frac{3}{32\pi} \text{Re} \mathcal{A}_{thr}^{+-00} + o(\Delta m), \\ \mathcal{K} &= \frac{1}{9} \left( \frac{m_{\pi^+}^2}{m_{\pi^0}^2} - 1 \right) (a_0 + 2a_2)^2 - \frac{2\alpha}{3} (\ln \alpha - 1) (2a_0 + a_2) + o(\Delta m), \\ p^* &= \left( m_{\pi^+}^2 - m_{\pi^0}^2 - \frac{1}{4} \mu_{\pi^+}^2 \alpha^2 \right)^{\frac{1}{2}}. \end{aligned} \quad (1.7.9)$$

Notice that it seems, at first sight, that there is another contribution -identical to our  $R_{00}^2$ -proportional one in formula (1.4.2)- entering through  $\mathcal{K}$  but, as we have already pointed out, this is in fact of order  $\frac{\Delta m}{m} \left( \frac{m}{4\pi f} \right)^2 \sim 5 \cdot 10^{-4}$  and hence can be safely ignored.

Last reference provides us also with an explicit expression for the electromagnetic (including pion mass difference) part of  $\Delta_{\chi PT}$  up to order  $e^2 p^2$ :

$$\begin{aligned} \Delta_{\chi PT}^{\text{em}}|_{e^2 p^2} &= \frac{2\Delta m}{3m} \left( 1 + \frac{m^2}{6\pi^2 f^2} \left[ \frac{23}{8} + \bar{l}_1 + \frac{3}{4} \bar{l}_3 \right] \right) + \frac{3\alpha m^2}{256\pi^2 f^2} \mathcal{P}(K_i) + \dots, \\ \mathcal{P}(K_i) &= \frac{128\pi^2}{3} [-6(K_1^r + K_3^r) + 3K_4^r - 5K_5^r + K_6^r + 6(K_8^r + K_{10}^r + K_{11}^r)] - \\ &\quad - \left( 18 + \frac{7\Delta m m}{\pi \alpha f^2} \right) \text{Log} \frac{m^2}{\mu_{UV}^2} - \frac{\Delta m m}{2\pi \alpha f^2} \left( \text{Log} \frac{m_s B_0}{\mu_{UV}^2} + 1 \right) - 30, \end{aligned} \quad (1.7.10)$$

where  $K_i^r$  are the running couplings introduced by [28] and the numerical values are quoted from [29].

According to the same reference, and after using the following values for the different parameters that have appeared up to now:

$$\begin{aligned} a_0 - a_2 &= \frac{9m_{\pi^+}^2}{32\pi f^2} \left( 1 + \frac{1}{2} \Delta_{\chi PT}^{p^4} + \frac{1}{2} \Delta_{\chi PT}^{p^6} \right) = .265 \pm .004, \\ \bar{l}_1 &= -.4 \pm .6 & \bar{l}_3 &= 2.9 \pm 2.4, \\ K_1^r &= -6.4 \cdot 10^{-3} & K_3^r &= 6.4 \cdot 10^{-3}, \\ K_4^r &= -6.2 \cdot 10^{-3} & K_5^r &= 19.9 \cdot 10^{-3}, \end{aligned}$$

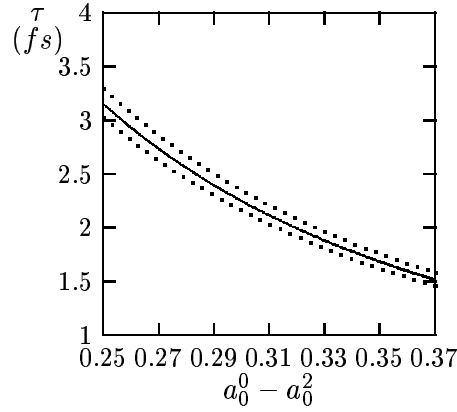


Figure 6: The pionium lifetime as a function of the combination  $(a_0^0 - a_0^2)$  analyzed in the framework of Generalized  $\chi$ PT. The band delineated by the dotted lines accounts for the uncertainties, coming from theoretical evaluations, low energy constants and  $a_1^1$ . Values of the lifetime lying below 2.4 fs. remain outside the domain of predictions of Standard  $\chi$ PT (large values of  $a_0^0$ ,  $\sim 0.28-0.36$  correspond to small values of the quark condensate parameter). (Thanks to H. Sazdjian hep-ph/9911520).

$$\begin{aligned} K_6^r &= 8.6 \cdot 10^{-3} & K_8^r = K_{10}^r &= 0, \\ K_{11}^r &= .6 \cdot 10^{-3}, \end{aligned} \quad (1.7.11)$$

where  $\Delta_{\chi PT}^{p^4}$  and  $\Delta_{\chi PT}^{p^6}$  denote respectively one and two loop contributions in the isospin symmetry limit ( $\alpha = 0$ ,  $m_u = m_d = 0$ ) to  $\Delta_{\chi PT}$  and  $\mu_{UV}$  has been chosen at  $M_\rho$ , then it is obtained:

$$\tau = \Gamma_1^{-1} = (2.9 \pm .1) \cdot 10^{-15} \text{ s}. \quad (1.7.12)$$

where the uncertainties are due mostly to the scattering lengths difference. In this 2.9 fs. value enters roughly a 6% correction to Deser's formula with a contribution from  $\Delta_{\chi PT} \sim 3.8\%$ .

## 1.8 Remarks and conclusions

We have presented an approach to pionium's lifetime calculation which consists of separating the various dynamical scales involved in the problem by using effective field theory techniques. The main advantage of this approach is, apart from its simplicity, that error estimates can be carried out very easily. Before closing this Chapter, a few remarks concerning other approaches are in order. First of all, relativistic ones[13, 14], besides being technically more involved, have all characteristic

physical scales of the problem entangled, which makes very difficult to estimate errors or to gauge the size of a given diagram. We also would like to emphasize that Lorentz symmetry, even though it is not linearly realized, it is implemented in our approach to the required order. Several non-relativistic approaches[15, 27] have appeared in the literature addressing particular aspects of the computation. Our analysis shows that a coupled channel approach to pionium is unnecessary because  $\Delta m$  is much larger than the bound state energy. It also shows that, although it is technically possible (trivial in fact) to make a resummation of bubble diagrams *à la* Lippmann-Schwinger, it does not make much sense since there are higher derivative terms in the effective Lagrangian, which have been neglected, that would give rise to contributions of the same order. In a way, our approach implements the already known remark that neutral pion loops give rise to important contributions in the non-relativistic and supplements it with relativistic corrections of the same order, which had been overlooked, in a full theoretical framework.

On the technical side we have worked out a new method to calculate the Coulomb propagator  $G_c(0, 0; E)$  in DR. The expressions for  $G_c(0, 0; E)$  when  $E \rightarrow E_n$  are easily obtained for any  $n$ . Using DR here it is not just a matter of taste. Eventually a two loop matching calculation is to be done in order to extract the parameters of the Chiral Lagrangian from the pionium width. These kind of calculations are only efficiently done in DR. Since the matching coefficients depend on the renormalization scheme, it is important to have our calculation in DR in order to be able to use the outcome of such a matching straight away.

Finally, a warning of caution must be put in reference with the conventional qualification of  $a_0^0$  and  $a_0^2$  as isospin 0 and 2 ‘strong scattering lengths’. As was already stated by the authors of [30], these quantities cannot be regarded as purely hadronic. In our formalism it is clearly seen that this difference, besides being proportional to  $m_{\pi^+}^2$ , inherits from QCD all electromagnetic interaction at quark level. Nevertheless it is completely meaningful to compute those parameters in the framework of  $\chi$ PT in the isospin symmetry limit as a series expansion in the physical charged pion mass<sup>3</sup>, which is in fact the underlying intention hidden under this ‘strong’ qualifier.

$$\begin{aligned} a_0^0 &= 0.159 \rightarrow 0.200 \rightarrow 0.216, \\ a_0^2 &= -0.0454 \rightarrow -0.0445 \rightarrow -0.0445, \end{aligned} \tag{1.8.1}$$

---

<sup>3</sup>Note that leading, next-to-leading[31] and next-to-next-to-leading order[32] calculations in the chiral limit are expressed in terms of the neutral pion mass.



## Chapter 2

# Light Fermion Finite Mass Effects in Non-relativistic Bound States

### 2.1 Motivation

As, when going from one link to another in the chain of EFTs described in last pages, we integrated out potential photons a new aspect of our formalism was entering that we wish to develop further in the present Chapter. The fact is that, whenever two or more physical scales are competing, as relative momenta and the mass of the electron were then, there is no chance of performing a step-by-step matching calculation: both must be taken into account at once, no approximations are allowed, and the matching coefficients' (potentials in our case) dependences usually lead to somewhat more involved calculations. At the same time, the EFT framework becomes the only reliable procedure capable of signaling when a non-perturbative (in  $m\alpha$  or  $m_e$ ) computation is compulsory. So, in view of the last calculation, someone might have claimed that for ponium, a system whose reduced mass is something like 70 MeV., a particle as light as the electron would have made a tiny correction, a negligible one in any case at the 10% accuracy level. Nevertheless our NREFT calculation relies precisely upon the existence in a bound state of other energy/momentum scales whose size must also be fixed in respect with the mass of any light degree of freedom.

The leading effect we are pursuing, -and we will see is not a particularity of the ponium system-, is a vacuum polarization correction to the energy and to the wave function at the origin, due to light

fermions whose mass (from now on  $m_l$ ) is of the order of the inverse Bohr radius of the Coulomb-like bound system. This effect, whose importance in the non-relativistic domain of both QED[36] and QCD[37] is known since long, has attracted lately considerable interest especially in relation with the  $\bar{b}b$  system. In fact, for QCD non-relativistic bound states,  $\Upsilon(1S)$  seems to be, in principle, the only one amenable to a weak coupling analysis[38]. In nowadays calculations at NNLO of that system, finite charm mass effects need to be taken into account if we aspire to extract with 1% accuracy the  $\overline{MS}$  bottom mass from  $M_\Upsilon$ . Sharp values of the running heavy quark mass serve us, for instance, to constrain the allowed parameter space for a given scenario of flavour generation in grand unification models[39].

Nevertheless, in spite of the fact that one would not say that excited  $\bar{b}b$  states are Coulombic<sup>1</sup>, following [42] one could formally assume we are in the perturbative regime  $mv \ll \Lambda_{QCD}$ , calculate by using NRQCD the quarkonium spectrum and, by comparison with known experimental levels, infer the size that non-perturbative corrections (together with higher orders in perturbation theory) caused by local or non-local gluon condensates might have. Perturbative calculations at NNLO including charm finite size effects show that, surprisingly, within 1-3% accuracy, levels are well reproduced. Although the net effect of taking into account charm finite mass corrections worsens the agreement by enlarging splittings, the picture still holds safely due to the uncertainties in  $\alpha_s^{(5)}(M_Z)$ .

Yet in weak coupling QCD's domain, we find another important field of application for the forthcoming displayed corrections in the computation of the total cross section for top quark pair production close to threshold in  $e^+e^-$  annihilation. This cornerstone of the Next Linear Collider's program has been recently calculated at NNLL<sup>2</sup> with the consequent reduction of the previous NNLO residual scale uncertainty ( $\approx 20\%$ ) down to only 3%. This improvement should lead to an accurate measure of the top width, the strong top coupling or the top Yukawa coupling in the case of a light Higgs. We will come back in our Discussion to that issue and will see that finite bottom mass effects in would-be toponium are right now a sizeable correction worth of being considered to find out the production cross section for  $\bar{t}t$ .

---

<sup>1</sup>In those relative momenta approaches  $\Lambda_{QCD}$  and it seems more natural to proceed by integrating out both  $mv$  and  $\Lambda_{QCD}$  at once, as done in [40, 41].

<sup>2</sup>The next-to-next to leading logarithm approximation includes a summation of potentially large logarithms of the scales  $m_t$  ( $\sim 175$  GeV.),  $m_tv$  ( $\sim 25$  GeV.) and  $m_tv^2$  ( $\sim 4$  GeV.), respectively called hard, soft and ultrasoft, by solving the renormalization group equations for the Wilson coefficients of vNRQCD (velocity NRQCD), as described in [43]. Quite recently the N<sup>3</sup>LO analysis of the heavy-quarkonium spectrum has also been presented [44].

Finally, it is obvious that any QED bound state built out of particles heavier than the electron may require to take into account its finite mass. Take for instance dimuonium, muonic hydrogen, pionium, pionic hydrogen and other simple hadronic atoms where  $m_e$  is such that  $m_e \sim \frac{\mu\alpha}{n}$ , being  $\mu$  the bound system's reduced mass and  $n$  its principle quantum number. We discovered in last Chapter the interest of those atoms, as they carry essential information on the QCD scattering lengths for several isospin channels, and also found out there that any NLO calculation in  $\alpha$  must take into account the existence of light degrees of freedom, whenever the mentioned condition holds.

That next results can be applied to such a variety of physical systems is a mere by-product of EFTs. All these non-relativistic bound states have at least three dynamical scales: the mass of the particles forming the bound state  $m$  (hard), its typical relative momentum  $mv$  (soft) and binding energy of order  $mv^2$  (ultrasoft). Once we integrate the hard scale NREFTs arise. For instance NRQED, NRQCD and NR $\chi$ L for QED, QCD and  $\chi$ PT<sup>3</sup>, respectively. Upon integrating out the soft scale effective theories which are local in time but non-local in space show up[24, 45]. The non-local terms in space are the usual quantum-mechanical potentials and only ultrasoft degrees of freedom are left dynamical. The corresponding non-relativistic effective field theories are named pNRQED, pNRQCD and pNR $\chi$ L in the previous cases. Since the leading (mass independent) coupling of the photon field to the non-relativistic charged particles as well as the one of the gluon field to the non-relativistic quarks is universal, it produces the same potential in both cases and can be discussed at once. It will be assumed in the following that we are in the situation in which a light (relativistic) charged particle in QED (or quark in QCD) whose mass is of the order of the soft scale is also integrated out when going from NR to pNR, so producing a light fermion mass dependent correction to the static potential.

When matching the NR theories to the pNR theories only the diagram of fig. 1 gives rise to a potential which contributes as a leading effect. For QED (on-shell scheme) it reads:

$$V_{vpc}(|\mathbf{x}|) = -\frac{\alpha}{\pi} \frac{\alpha}{|\mathbf{x}|} \int_0^1 dv \frac{v^2 \left(1 - \frac{v^2}{3}\right)}{(1-v^2)} e^{-\frac{m_l|\mathbf{x}|}{\sqrt{1-v^2}}}, \quad (2.1.1)$$

and for QCD ( $\overline{\text{MS}}$ ):

$$V_{vpc}(|\mathbf{x}|) = -\frac{C_F T_F \alpha_s}{\pi} \frac{\alpha_s}{|\mathbf{x}|} \left\{ \int_0^1 dv \frac{v^2 \left(1 - \frac{v^2}{3}\right)}{(1-v^2)} e^{-\frac{m_l|\mathbf{x}|}{\sqrt{1-v^2}}} + \frac{1}{3} \text{Log} \left( \frac{m_l^2}{\nu^2} \right) \right\},$$

<sup>3</sup>Note the slight departure from the expected NR $\chi$ PT name, that intends to stress that the calculation in the non-relativistic regime cannot longer be organized according to the chiral counting.



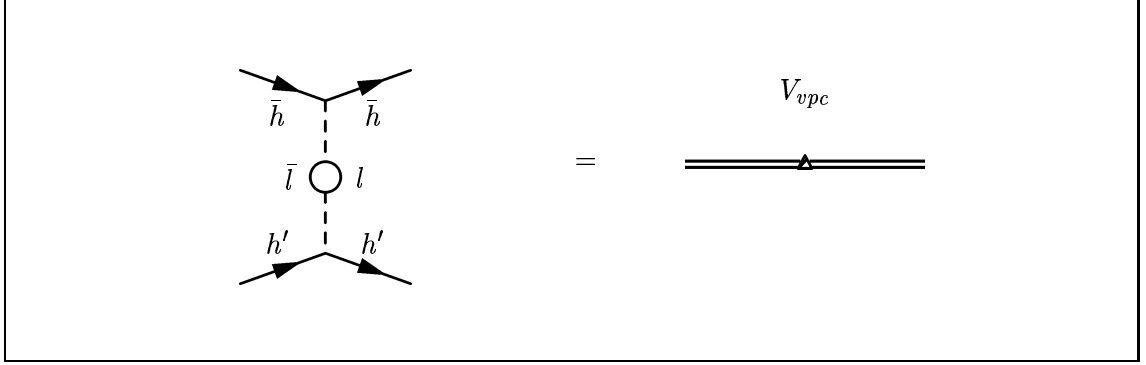


Figure 1: Matching between the non-relativistic theory and the potential one.

$$C_F = \frac{N_c^2 - 1}{2N_c} = \frac{4}{3}, \quad T_F = \frac{1}{2}. \quad (2.1.2)$$

If  $N_f$  is the number of flavours lighter than  $m_l$ , the  $\alpha_s(\nu)$  above runs with  $N_f + 1$  flavours. Notice that the difference between the QED and the QCD case is, apart from the trivial colour factors  $\alpha/|\mathbf{x}| \rightarrow C_F \alpha_s/|\mathbf{x}|$  and  $\alpha/\pi \rightarrow T_F \alpha_s/\pi$ , a term which can be absorbed in a redefinition of the Coulomb potential [46]. Hence for the actual calculation we shall only deal with (2.1.1) and use these facts to extend our results to the QCD realm.

## 2.2 Energy Shift

For the energy shift we obtain ( $\xi := \frac{nm_l}{\mu\alpha}$ ):

$$\begin{aligned} \delta E_{nl}(\xi) = & -\frac{2\alpha}{3\pi} E_n \left\{ \frac{5}{3} - \frac{3\pi}{2} n\xi + (n(2n+1) + (n+l)(n-l-1)) \xi^2 - \right. \\ & -\pi n \left( \frac{1}{3}(n+1)(2n+1) + (n+l)(n-l-1) \right) \xi^3 - \\ & - \frac{1}{(2n-1)!} \sum_{k=0}^{n-l-1} \binom{n-l-1}{k} \binom{n+l}{2l+1+k} \xi^{2(n-l-1-k)} \\ & \left. \frac{d^{2n-1}}{d\xi^{2n-1}} \left[ \xi^{2(k+l)+1} (2 - \xi^2 - \xi^4) F_1(\xi) \right] \right\}, \quad (2.2.1) \end{aligned}$$

$$F_1(\xi) := \begin{cases} \frac{1}{\sqrt{\xi^2-1}} \arccos \frac{1}{\xi} & \text{if } \xi > 1, \\ 1 & \text{if } \xi = 1, \\ \frac{1}{\sqrt{1-\xi^2}} \text{Log} \left[ \frac{1+\sqrt{1-\xi^2}}{\xi} \right] & \text{if } \xi < 1. \end{cases}$$

where  $E_n = -\mu\alpha^2/2n^2$  is the Coulomb energy. For  $\xi$  large, namely  $m_l \gg \mu\alpha/n$ , it reduces to:

$$\delta E_{nl}(\xi \rightarrow \infty) \rightarrow \frac{2\alpha}{3\pi} \frac{E_n}{\xi^{2l+2}} \left\{ \frac{(n+l)!}{(n-l-1)!(2l+1)!} \frac{(2l)!!}{(2l+1)!!} \left( 2 - \frac{(2l+2)}{(2l+3)} - \frac{(2l+2)(2l+4)}{(2l+3)(2l+5)} + \mathcal{O}\left(\frac{1}{\xi}\right) \right) \right\}, \quad (2.2.2)$$

whereas for  $\xi$  small, namely  $m_l \ll \mu\alpha/n$ , we obtain:

$$\delta E_{nl}(\xi \rightarrow 0) \rightarrow -\frac{2\alpha}{3\pi} E_n \left\{ \frac{5}{3} + 2(\psi(n+l+1) - \psi(1)) - 2\text{Log} \frac{2}{\xi} - \frac{3\pi}{2} n\xi + \frac{3}{2} (n(2n+1) + (n+l)(n-l-1)) \xi^2 - \pi n \left( \frac{1}{3} (n+1)(2n+1) + (n+l)(n-l-1) \right) \xi^3 + \mathcal{O}(\xi^4) \right\}, \quad (2.2.3)$$

where we have used (C.4). The key steps to obtain (2.2.1) are given in the Appendix D. We have done the following checks. For the 1S state (2.2.1) reduces to the result exhibited in Table I (formula (5.3) of ref. [18]). The energy shifts for the 1S, 2S, 2P, 3S, 3P and 3D states agree with the early analytical formulas of ref. [47]. For  $\xi$  large, we reproduce the well-known positronium like limit for  $l = 0$  (to be precise we agree with the correction to the energy obtained using formula (2.8) of [24]). We also agree for  $l = 1$  with formula (32) of ref. [48]. For  $\xi$  small, we can compare with known results for massless quarks in QCD. For arbitrary  $n$  and  $l$  we agree with formula (13) of ref. [46]. For  $l = n - 1$  we agree with  $\mathcal{O}(\xi^0)$  and  $\mathcal{O}(\xi^1)$  of formula (14) in ref. [49]<sup>4</sup> but disagree with their  $\mathcal{O}(\xi^2)$  result (the  $\mathcal{O}(\xi^3)$  is not displayed in [49]). Notice that for  $\xi$  large enormous cancellations occur in formula (2.2.1) and hence the analytic expansion (2.2.2) may prove very useful.

### 2.3 Wave Function at the Origin

The correction for the wave function at the origin for  $n = 1$  states reads:

$$\delta \Psi_{10}(\mathbf{0}) = -\frac{\alpha}{\pi} \Psi_{10}(\mathbf{0}) \left[ \left\{ \frac{5}{9} - \frac{\pi}{4} \xi + \frac{1}{3} \xi^2 - \frac{\pi}{6} \xi^3 + \frac{1}{3} (\xi^4 + \xi^2 - 2) F_1(\xi) \right\} + \right.$$

<sup>4</sup>Taking  $\epsilon_n = 0$  in that reference and upon correcting an obvious misprint  $\kappa_1 \rightarrow \kappa_n$ .

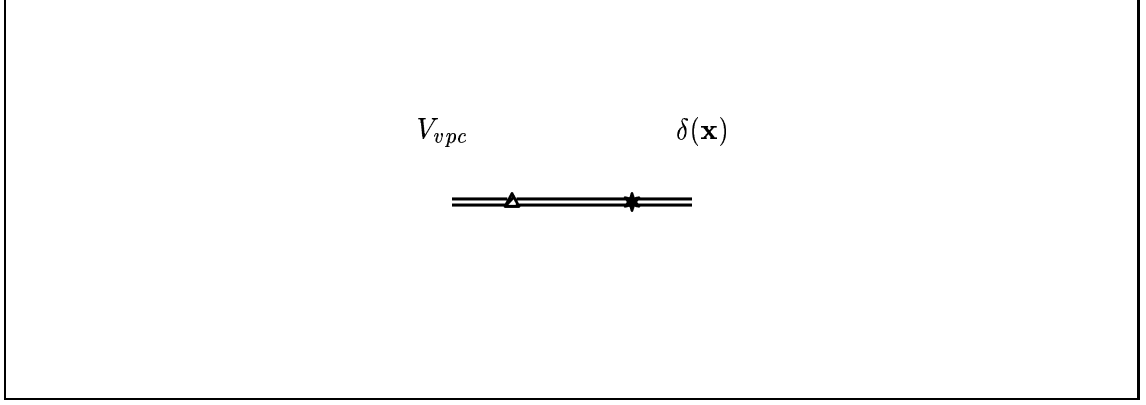


Figure 2: Diagram rendering the correction to the wave function at the origin. The double line is the Coulomb propagator of the non-relativistic pair and the star a local ( $\delta(\mathbf{x})$ ) potential.

$$\left\{ \frac{11}{18} - \frac{2}{3}\xi^2 + \frac{2\pi}{3}\xi^3 - \frac{1}{6}(12\xi^4 + \xi^2 + 2)F_1(\xi) - \frac{1}{6} \frac{(4\xi^4 + \xi^2 - 2)}{(\xi^2 - 1)} (1 - \xi^2 F_1(\xi)) \right\} +$$

$$+ \left\{ \frac{2}{3} + \frac{\pi}{4}\xi - \frac{1}{9}\xi^2 + \frac{13\pi}{18}\xi^3 - \frac{1}{9}(13\xi^4 - 11\xi^2 - 11)F_1(\xi) - \right.$$

$$\left. - \frac{1}{3}(4\xi^3 + 3\xi)F_2(\xi) + \frac{1}{3}(4\xi^4 + \xi^2 - 2)F_3(\xi) + \frac{1}{3} \left( 4\xi^2 + \frac{11}{3} \right) \text{Log} \frac{\xi}{2} \right\}, \quad (2.3.1)$$

where  $\Psi_{10}(\mathbf{x})$  is the Coulomb wave function. The first bracket corresponds to zero photon exchange and has already been calculated analytically in [27]. The second and third brackets correspond to the pole subtraction and multi-photon exchange contributions, respectively.  $F_i(\xi)$ ,  $i = 2, 3$  are defined as follows:

$$F_2(\xi) = \int_0^{\frac{\pi}{2}} d\theta \text{Log} \left[ \frac{\sin \theta + \xi}{\sin \theta} \right],$$

$$F_3(\xi) = \int_0^{\frac{\pi}{2}} d\theta \frac{1}{\sin \theta + \xi} \text{Log} \left[ \frac{\sin \theta + \xi}{\sin \theta} \right]. \quad (2.3.2)$$

$F_2(\xi)$  and  $F_3(\xi)$  can be expressed in terms of Clausen integrals and dilogarithms. We present the explicit formulas in Appendix C. The key steps in order to obtain (2.3.1) are given in Appendix D.

For  $\xi$  large, namely  $m_l \gg \mu\alpha$ , (2.3.1) behaves like:

$$\delta\Psi_{10}(\mathbf{0})_{\xi \rightarrow \infty} \rightarrow \frac{\alpha}{\pi} \Psi_{10}(\mathbf{0}) \left[ \frac{3\pi}{16\xi} + \frac{107}{225\xi^2} + \frac{4}{15\xi^2} \text{Log} \frac{\xi}{2} + \mathcal{O}\left(\frac{1}{\xi^3}\right) \right]. \quad (2.3.3)$$

This result must be compatible with the one obtained by integrating out the light fermion first and then calculating the electromagnetic potential. In the case  $m \gg m_l \gg \mu\alpha/n$  (for simplicity, we are assuming  $\hbar = \hbar'$ ,  $m$  being the mass of the non-relativistic particles) we expect that a local non-relativistic

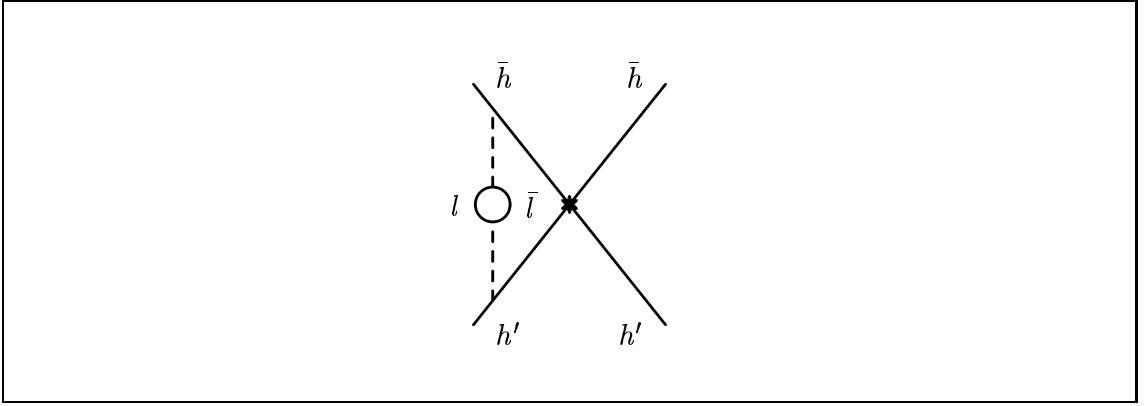


Figure 3: Vacuum polarization correction to the decay width at leading order in  $\frac{1}{\xi}$  when  $\xi \rightarrow \infty$ . Energies and momenta of order  $m_l$  and  $\sqrt{mm_l}$  respectively dominate the graph and hence the Coulomb resummation leads to subleading effects.

effective theory is obtained after integrating out the energy scale  $m_l$  and the associated three momentum scale  $\sqrt{mm_l}$  for the non-relativistic particle. The leading term in (2.3.3) corresponds to the contribution that would be obtained from the local term induced by the diagram in fig. 3. The logarithm in the subleading term corresponds to the iteration of two delta function potentials in quantum mechanics (see formula (1.7.1)). The second delta function is due to the contribution to the electromagnetic potential of the dimension six photon operator (see [24]) which arises after integrating out a heavy particle[50].

For  $\xi$  small, namely  $m_l \ll \mu\alpha$ , we obtain:

$$\delta\Psi_{10}(\mathbf{0})(\xi \rightarrow 0) \rightarrow -\frac{\alpha}{\pi}\Psi_{10}(\mathbf{0}) \left[ \frac{3}{2} - \frac{\pi^2}{9} - \text{Log}\frac{2}{\xi} - \frac{3}{2}\xi^2 + \mathcal{O}(\xi^3) \right]. \quad (2.3.4)$$

We have made the following checks. For  $\xi$  large and small, the leading term of (2.3.3) and (2.3.4) agree with formulas (22) and (23) of ref. [48], respectively, (the next-to-leading terms are not displayed in [48]). For  $\xi$  small we can also compare with known results for massless quarks in QCD. We agree with the  $\mathcal{O}(\alpha_s)$  correction of formula (69) of ref. [51]. We have also checked that the formula (2.3.1) reproduces the numerical results obtained for dimuonium and pionium in refs. [52] and [27] respectively, and we also agree numerically with the analytical result in terms of a non-trivial integral of ref. [48].

## 2.4 Applications

### 2.4.1 Exotic Atoms

We have listed in Table II and Table III the corrections to some energy splittings and to the wave function at the origin, respectively, of simple exotic atoms of current interest. This purely electromagnetic corrections must be conveniently taken into account if one wants to obtain precise information of the strong scattering lengths from hadronic atoms.

	$\frac{\delta E_{21} - \delta E_{10}}{\alpha(E_2 - E_1)}$	$\frac{\delta E_{31} - \delta E_{10}}{\alpha(E_3 - E_1)}$	$\frac{\delta E_{21} - \delta E_{20}}{\alpha E_2}$
$pK^-$	.44593	.38629	-.10453
$p\pi^-$	.18103	.15388	-.056337
$p\mu^-$	.13616	.11548	-.044443

**Table II.** Vacuum polarization induced energy splittings for some exotic atoms

	$\xi = \frac{m_e}{\mu\alpha}$	$\frac{\delta_{zph}\Psi(\mathbf{0})}{\alpha\Psi(\mathbf{0})}$	$\frac{\delta_{ps}\Psi(\mathbf{0})}{\alpha\Psi(\mathbf{0})}$	$\frac{\delta_{mph}\Psi(\mathbf{0})}{\alpha\Psi(\mathbf{0})}$	$\frac{\delta\Psi(\mathbf{0})}{\alpha\Psi(\mathbf{0})}$
$K^-p$	.21648	.34290	.15454	.09650	.59394
$K^+K^-$	.28369	.29837	.12958	.08785	.51581
$\pi^-p$	.57635	.19613	.07285	.06166	.33064
$K^+\pi^-$	.64357	.18237	.06549	.05741	.30527
$\mu^-p$	.73738	.16627	.05703	.05222	.27552
$\pi^+\pi^-$	1.00344	.13338	.04052	.04099	.21490
$\mu^+\mu^-$	1.32550	.10793	.02876	.03184	.16853

**Table III.** Vacuum polarization correction to the ground state wave function at the origin of some exotic atoms.

### 2.4.2 $\Upsilon(1S)$ and $\bar{t}t$

The current calculations of heavy quarks near threshold assume that the remaining lighter quarks are massless. This approximation is far from being justified at least in two cases. For the  $\Upsilon(1S)$  system the typical relative momentum  $m_b\alpha_s/2 \sim 1.3$  GeV. [53] is of the same order as the charm mass  $m_c \sim 1.5$  GeV. The effects of a finite charm mass in the binding energy have been quantified in [54]. We

give in Table IV the size of these effects in the wave function at the origin. For the  $\bar{t}t$  production near threshold at a relative momentum  $m_t\alpha_s/2 \sim 18$  GeV. the effects of a finite bottom mass  $m_b \sim 5$  GeV. should be noticeable. In order to estimate them, we also show in Table IV the size of this effect, both for bottom and charm, in the wave function at the origin for the would-be-toponium (1S) state.

	$\xi = \frac{m_c}{C_F\alpha_s\mu}$	$\xi = \frac{m_b}{C_F\alpha_s\mu}$	$\frac{\delta\Psi(\mathbf{0})_{\xi\neq 0} - \delta\Psi(\mathbf{0})_{\xi=0}}{\alpha_s\Psi(\mathbf{0})}$
$\bar{b}b$	1.4		.088
$\bar{t}t$		.28	.011
$\bar{t}t$	.10		.0019

**Table IV.** Vacuum polarization correction to wave function at the origin in quarkonia.  $\overline{\text{MS}}$  has been used.

Were the corrections organized in a series of  $\frac{\alpha_s}{\pi}$  multiplied by  $\mathcal{O} \sim 1$  numbers, could we conclude that the leading effects of a finite quark mass would be:

1. In the  $\Upsilon(1s)$  system for charm more important than the next to leading corrections in  $\alpha_s$  [51];
2. In the  $\bar{t}t$  system near threshold for bottom (charm) as important as (less important than) the next to leading corrections in  $\alpha_s$ [55].

However, as relativistic corrections do not have the  $\pi$  suppression and some radiative corrections are enhanced by factors of  $\beta_0$ , in practice the next to leading corrections are comparable to the leading ones, even for the  $\bar{t}t$  system (see [56] for a discussion). Nevertheless, once these convergence issues are solved, following the lines of [39, 43], our evaluation of the finite mass effects' size for the above systems still applies.

## 2.5 Related works

We would like to conclude this Chapter by commenting briefly on some other works whose aim was quantifying the effects of the finite charm quark mass in bottom quark mass determinations, as well as bottomonium spectra. With this, our purpose is to show some other applications that serve us to provide an appropriate framework for our own work.

The determination of the bottom  $\overline{MS}$  mass is a delicate issue, as illustrated in [39]. In sum rule analyses at NNLO in the non-relativistic expansion, special care must be taken to eliminate the strong linear sensitivity to small momenta and its associated (artificially) large perturbative corrections, as well as large correlations with the choice of the strong coupling constant. This is done by using as expansion parameter, instead of the bottom quark pole mass, any ‘low-virtuality short-distance’ mass such as the kinetic mass (Melnikov-Yelkhovsky), the  $1S$  mass (Hoang), the  $PS$  mass (Beneke-Singer) or the  $RS$  mass (Pineda). After this, uncertainties are automatically reduced to a 2% level and further to merely 1% or less just by taking into account some other corrections of straightforward implementation, among which figures out our charm mass effects.

By formulating observables in terms of a short-distance bottom quark mass, which is expanded around the light quark massless limit, all IR linear charm mass sensitivity that entered through the bottom pole mass vanishes, and the first correction to the massless case is of order  $(\frac{\alpha_s}{\pi})^2 \frac{m_c^2}{m_b}$ , which represents a shift of only a few MeV. and, up to the intended accuracy (tens of MeV.), can be safely neglected. But the dynamical charm mass effects, filtering through the  $\xi$  parameter, which is not a small quantity, represent no negligible corrections as we have just seen. Beware, then, of extractions of the running bottom mass, which does not show  $\xi$ -dependence and so must remain after being related to a short-mass parameter, actually affected by  $\xi$  corrections, that is the one fitted from sum rule analyses for the masses and electronic decay widths of  $\Upsilon$  mesons. That is, the leading effect coming from the finite charm quark mass in the bottom  $\overline{MS}$  mass as obtained from the bottom  $1S$  mass<sup>5</sup> arises at order  $\alpha_s^2$  from the fact that one can expand in the charm mass in the bottom pole- $\overline{MS}$  mass relation, but not in the pole- $1S$  mass one. Schematically:

$$m_{b,NNLO}^{1S} = m_b^{pole} \left[ 1 - \Delta^{LO}(\alpha_s) - \left( \Delta_{massless}^{NLO}(m_b^{pole}, \alpha_s, \mu) + \Delta_{massive}^{NLO}(m_c, m_b^{pole}, \alpha_s) \right) - \left( \Delta_{massless}^{NNLO}(m_b^{pole}, \alpha_s, \mu) + \Delta_{massive}^{NNLO}(m_c, m_b^{pole}, \alpha_s, \mu) \right) \right], \quad (2.5.1)$$

$$m_{b,three-loop}^{pole} = \bar{m}_b(\bar{m}_b) \left[ 1 + \delta^{(1)}(\alpha_s) + \left( \delta_{massless}^{(2)}(\alpha_s) + \delta_{massive}^{(2)}(m_c, \bar{m}_b(\bar{m}_b), \alpha_s) \right) + \left( \delta_{massless}^{(3)}(\alpha_s) + \delta_{massive}^{(3)}(m_c, \bar{m}_b(\bar{m}_b), \alpha_s) \right) \right], \quad (2.5.2)$$

$$\delta_{massive}^{(2)}(m_c, \bar{m}_b(\bar{m}_b), \alpha_s) \approx \frac{\alpha_s^2}{6} \frac{m_c}{\bar{m}_b(\bar{m}_b)}, \quad (2.5.3)$$

<sup>5</sup>The  $1S$  mass was first introduced to address the aforementioned problems for bottom and top quark mass extractions from  $\Upsilon$  sum rules and from top-antitop quark pair production close to threshold at NLC. It is defined as half of the perturbative contribution to the mass of a  $J^{PC} = 1^{-}, {}^3S_1$  quark-antiquark bound state, assuming that the heavy quark is stable.

$$\delta_{massive}^{(3)}(m_c, \bar{m}_b(\bar{m}_b), \alpha_s) \approx \frac{\alpha_s^2}{12} \left( \frac{\alpha_s}{\pi} \right) \frac{m_c}{\bar{m}_b(\bar{m}_b)} \left[ \text{Log} \frac{m_c^2}{\bar{m}_b^2}, \text{ct.} \right], \quad (2.5.4)$$

where  $\Delta_{massive}^{NLO}(m_c, m_b^{pole}, \alpha_s)$  corresponds to (2.2.1) divided by 2 once the massless contribution therein contained is subtracted, and  $\Delta_{massive}^{NNLO}(m_c, m_b^{pole}, \alpha_s)$  is a massive  $\mathcal{O}(\alpha_s^2)$  second order correction whose expression is given in formulas (64)-(74) of [39].  $\alpha_s$  is shorthand for  $\alpha_s^{n_f=4}(\mu)$ .

Although very interesting, at this point we do not wish to describe the whole procedure needed in order to extract both  $m_b^{1S}$  and  $\bar{m}_b(\bar{m}_b)$ . The final outcome of the calculation undertaken in [39] reads:

$$\begin{aligned} m_b^{1S} &= 4.69 \pm .03 \text{GeV}, \\ \bar{m}_b(\bar{m}_b) &= 4.16 \pm .05 \text{GeV}, \end{aligned} \quad (2.5.5)$$

where the net effect of the massive charm contributions is to shift about -20 MeV. the  $m_b^{1S}$  mass and something like -30 to -35 MeV. the  $\bar{m}_b(\bar{m}_b)$  one.

In our Motivation we have already presented the approach of [42], where heavy quarkonia spectroscopy was computed in perturbative QCD up to order  $\alpha_s^4$ , once the  $\mathcal{O}(\Lambda_{QCD})$  renormalon was cancelled between the static potential and the pole mass. Taking care of this leading renormalon, the perturbative series turns out to be convergent and reproduces reasonably well the structure of the bottomonium spectrum up to some of the  $n = 3$  levels. Sketching the procedure rather roughly, the energy eigenvalues (X's) of the NNLO pNRQCD Hamiltonian take the form:

$$\begin{aligned} E_X(\mu, \alpha_s^{(n_l)}(\mu), m_{b,pole}) &= 2m_{b,pole} + E_{bin,X}^{n_l}(\mu, \alpha_s^{(n_l)}, m_{b,pole}), \\ E_{bin,X}^{n_l}(\mu, \alpha_s^{(n_l)}, m_{b,pole}) &= -\frac{8}{9n^2} \alpha_s^{(n_l)}(\mu)^2 m_r \sum_{k=0}^2 \varepsilon^{k+1} \left( \frac{\alpha_s^{(n_l)}(\mu)}{\pi} \right)^k P_k(L_{nl}), \end{aligned} \quad (2.5.6)$$

where  $\varepsilon = 1$  is the parameter that serves us to keep track of the leading renormalon cancellation and  $P_k(L_{nl})$  is a  $k^{th}$ -degree polynomial of  $L_{nl} \equiv \text{Log} \left[ \frac{3n\mu}{8\alpha_s^{(n_l)}(\mu)m_r} \right] + S_1(n+l) + \frac{5}{6}$ . The series expansion of  $E_X$  is then written in terms of  $\overline{MS}$  masses by use of:

$$m_{b,pole} = \bar{m}_b \left[ 1 + \frac{4}{3} \varepsilon \frac{\alpha_s^{(n_l)}(\bar{m}_b)}{\pi} + \varepsilon^2 \left( \frac{\alpha_s^{(n_l)}(\bar{m}_b)}{\pi} \right)^2 d_1^{(n_l)} + \varepsilon^3 \left( \frac{\alpha_s^{(n_l)}(\bar{m}_b)}{\pi} \right)^3 d_2^{(n_l)} \right], \quad (2.5.7)$$

where both  $d_1^{(n_l)}$  and  $d_2^{(n_l)}$  are known. To incorporate the renormalon cancellation it is necessary to expand  $m_{b,pole}$  and  $E_{bin,X}^{n_l}$  in the same coupling,  $\alpha_s^{(n_l)}(\mu)$ , by using:

$$\alpha_s^{(n_l)}(\bar{m}_b) = \alpha_s^{(n_l)}(\mu) \left[ 1 + \varepsilon \frac{\alpha_s^{(n_l)}(\mu)}{\pi} \frac{\beta_0^{(n_l)}}{2} \text{Log} \left( \frac{\mu}{\bar{m}_b} \right) + \right.$$



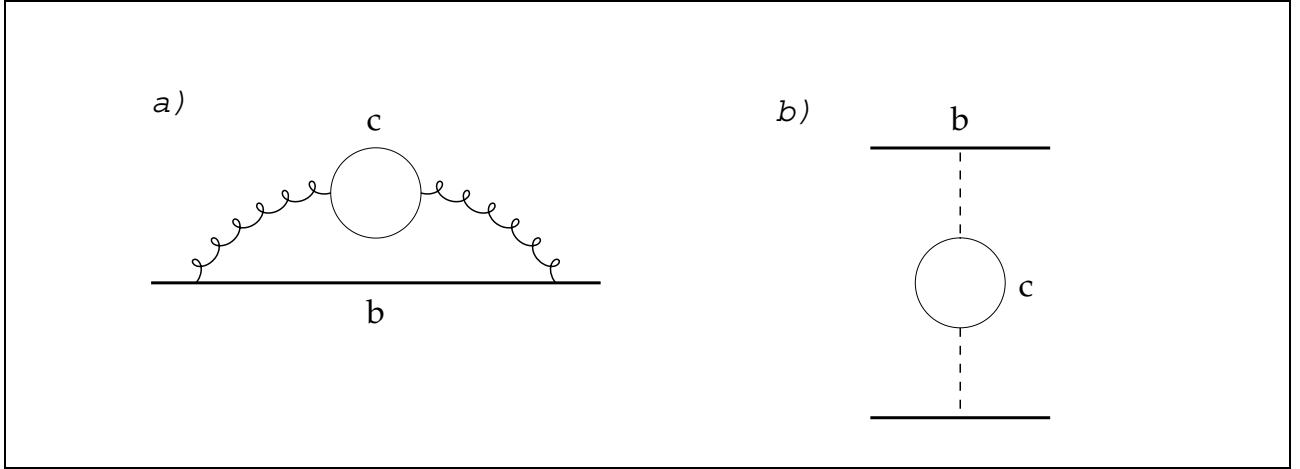


Figure 4: Feynman graphs responsible for the leading charm mass effects to the pole mass a) and to the Coulomb potential b).

$$+\varepsilon^2 \left( \frac{\alpha_s^{(n_l)}(\mu)}{\pi} \right)^2 \left( \frac{\beta_0^{(n_l)2}}{4} \text{Log}^2 \left( \frac{\mu}{\bar{m}_b} \right) + \frac{\beta_1^{(n_l)}}{8} \text{Log} \left( \frac{\mu}{\bar{m}_b} \right) \right) \Big]. \quad (2.5.8)$$

So the energy levels take the form:

$$\begin{aligned} E_X(\mu, \alpha_s^{(n_l)}(\mu), \bar{m}_b) &= 2\bar{m}_b + E_X^{n_l(1)}(\mu, \alpha_s^{(n_l)}(\mu), \bar{m}_b)\varepsilon + E_X^{n_l(2)}(\mu, \alpha_s^{(n_l)}(\mu), \bar{m}_b)\varepsilon^2 + \\ &+ E_X^{n_l(3)}(\mu, \alpha_s^{(n_l)}(\mu), \bar{m}_b)\varepsilon^3 + \dots, \end{aligned} \quad (2.5.9)$$

form that explicitly realizes the first renormalon cancellation and where, since  $\alpha_s$  and  $\bar{m}$  are short range quantities, the obtained perturbative expansion is expected to show a better convergence. Until here no charm mass effects have been taken into account. To do so at first and second order ( $\varepsilon^2$  and  $\varepsilon^3$ ), we consider:

$$\begin{aligned} (\delta E_{\bar{b}b}) &= \varepsilon^2 (\delta E_{\bar{b}b})_{m_c}^{(1)} + \varepsilon^3 (\delta E_{\bar{b}b})_{m_c}^{(2)}, \\ (\delta m_b)_{m_c} &= \varepsilon^2 (\delta m_b)_{m_c}^{(1)} + \varepsilon^3 (\delta m_b)_{m_c}^{(2)}. \end{aligned} \quad (2.5.10)$$

The term  $(\delta E_{\bar{b}b})_{m_c}^{(1)}$  is given in (2.2.1) (b),  $(\delta m_b)_{m_c}^{(1)}$  has been calculated in [57] (a), the quantity  $(\delta E_{\bar{b}b})_{m_c}^{(2)}$  is only known for  $1S$  bottomonium, and  $(\delta m_b)_{m_c}^{(2)}$  has been calculated in the limit  $m_c \rightarrow 0$  (linear contribution) in [39].

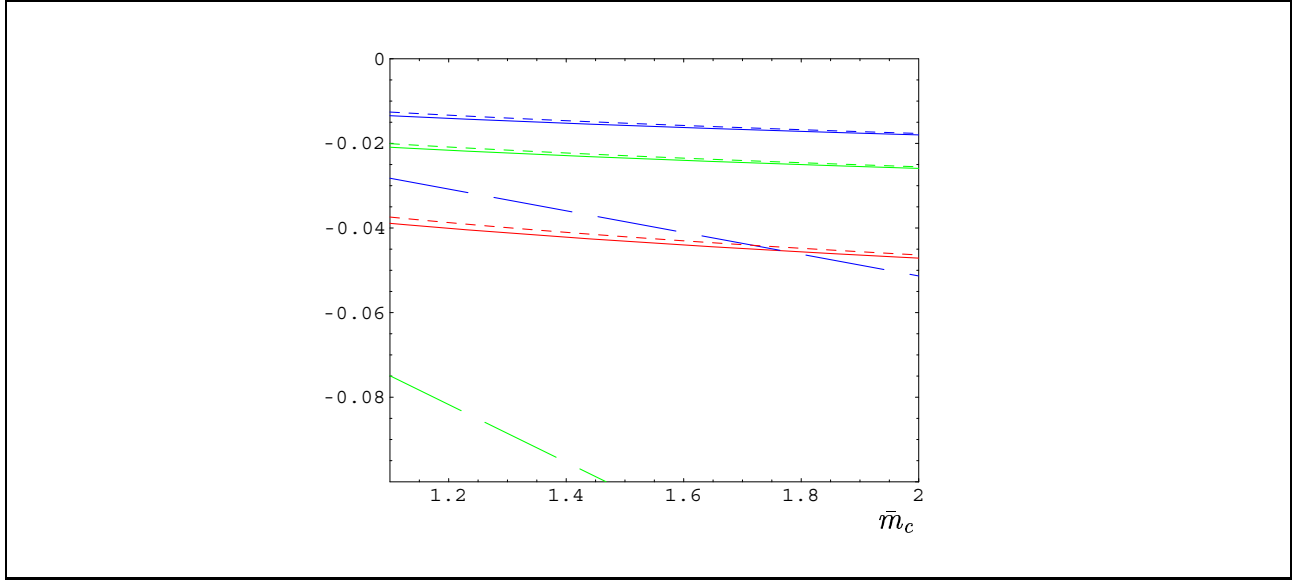


Figure 5:  $(\delta E)_{m_c}^{(1)}$  (continuous line),  $(\delta E)_{m_c \rightarrow 0}^{(1)}$  (dashed line),  $(\delta E)_{m_c \rightarrow \infty}^{(1)}$  (dotted line), as a function of  $\bar{m}_c$  for  $\bar{m}_b = 4.201$  GeV. Going down, the first set of lines corresponds to the  $1S$  state with  $\mu = 2.446$  GeV, the second one to the  $2S$  state with  $\mu = 1.065$  GeV, and the third one to the  $3S$  state with  $\mu = 0.724$  GeV. Lines, which are not displayed, fall outside the plot range. The units are GeV.

As both  $(\delta m_b)_{m_c}^{(1,2)}$  are functions of  $\rho = \frac{\bar{m}_c}{\bar{m}_b}$ , a small quantity, the linear approximation turns out to be very accurate to take into account charm mass effects in the running bottom mass. The substitution  $(\delta m_b)_{m_c}^{(1)}$  for  $(\delta m_b)_{m_c \rightarrow 0}^{(1)} = \frac{(\alpha_s^{(4)}(\bar{m}_b))^2}{6} \bar{m}_c$  induces an error that is only about 15% at the value  $\rho = .294$ , and the agreement persists when the scale in the strong coupling constant moves in a rather wide range of values (between 1 and 3 GeV).

On the contrary, both  $(\delta E_{\bar{b}\bar{b}})_{m_c}^{(1,2)}$ , as we have seen, are functions of  $\bar{\xi} = \frac{2n\bar{m}_c}{C_F \bar{m}_b \alpha_s^{(4)}(\mu)}$ , which is a quantity  $\sim 2$  in most cases of bottomonium spectra. The substitution  $(\delta E_{\bar{b}\bar{b}})_{m_c}^{(1,2)}$  for  $(\delta E_{\bar{b}\bar{b}})_{m_c \rightarrow \infty}^{(1,2)}$  should provide an excellent approximation (in the worst situation, the  $1S$  level,  $(\delta E_{\bar{b}\bar{b}})_{m_c \rightarrow \infty}^{(1)}$  is only 5% away from the full result), as it is clearly seen in the next figure and table:

$$(\delta E_{\bar{b}\bar{b}})_{m_c \rightarrow \infty}^{(1)} = \bar{m}_b \frac{C_f (\alpha_s^{(4)}(\mu))^2 \alpha_s^{(4)}}{4n^2 3\pi} \left[ 2 \text{Log} \frac{2}{\bar{\xi}} - \frac{5}{3} - 2(\psi(n+l+1) - \psi(1)) \right]. \quad (2.5.11)$$

The reason why this expansion around  $m_c \rightarrow \infty$  works so well is understood in view of (2.2.2):

$$\frac{(\delta E_{\bar{b}\bar{b}})_{m_c}^{(1)} - (\delta E_{\bar{b}\bar{b}})_{m_c \rightarrow \infty}^{(1)}}{(\delta E_{\bar{b}\bar{b}})_{m_c}^{(1)}} \sim -\frac{1}{\bar{\xi}^{2l+2}} \frac{1}{2\psi(n+l+1) - 2\psi(1) + 5/3}, \quad (2.5.12)$$

which also clarifies that:

State	$\mu$	$\alpha_s^{(4)}(\mu)$	$\bar{\xi}$	$(\delta E_{\bar{b}b})_{\bar{m}_c}^{(1)}$	$(\delta E_{\bar{b}b})_{\bar{m}_c \rightarrow 0}^{(1)}$	$(\delta E_{\bar{b}b})_{\bar{m}_c \rightarrow \infty}^{(1)}$
$1^3S_1$	2.446	0.277	1.59	-0.0143	-0.032	-0.0136
$1^3P_0$	1.140	0.428	2.06	-0.0210	-0.076	-0.0210
$1^3P_1$	1.111	0.437	2.02	-0.0221	-0.079	-0.0221
$1^3P_2$	1.086	0.445	1.99	-0.0232	-0.082	-0.0232
$2^3S_1$	1.065	0.452	1.96	-0.0219	-0.084	-0.0211
$2^3P_0$	0.726	0.695	1.91	-0.0426	-0.199	-0.0424
$2^3P_1$	0.703	0.733	1.81	-0.0490	-0.222	-0.0488
$2^3P_2$	0.678	0.782	1.70	-0.0581	-0.252	-0.0579
$3^3S_1$	0.724	0.698	1.90	-0.0405	-0.201	-0.0392

**Table V.**  $(\delta E_{\bar{b}b})_{\bar{m}_c}^{(1)}$ ,  $(\delta E_{\bar{b}b})_{\bar{m}_c \rightarrow 0}^{(1)}$  and  $(\delta E_{\bar{b}b})_{\bar{m}_c \rightarrow \infty}^{(1)}$  for  $\bar{m}_b = 4.201$  GeV. and  $\bar{m}_c = 1.237$  GeV.;  $\alpha_s^{(4)}$  is calculated from  $\Lambda_{\overline{MS}}^{(4)} = 0.292$  GeV. at four loops. All dimensionful quantities are expressed in GeV.

1. states with high  $l$  are expected to be reproduced better by the asymptotic approximation;
2. higher  $n$  are also, in principle, well reproduced, as  $\xi$  grows like  $\frac{n}{\alpha_s^{(4)}(\mu)}$  and the growing of the strong coupling constant does not compensate that of  $n$ ;
3. charm mass effects can be taken into account in the energy level expansion very effectively by taking the situation with only three active and massless quarks:

$$(\delta E_{\bar{b}b})_{\bar{m}_c} \underset{95\%}{\simeq} (\delta E_{\bar{b}b})_{\bar{m}_c \rightarrow \infty} = E_{\text{bin},\bar{b}b}^3(\mu, \alpha_s^{(3)}(\mu), m_{b,\text{pole}}) - E_{\text{bin},\bar{b}b}^4(\mu, \alpha_s^{(4)}(\mu), m_{b,\text{pole}}) \quad (2.5.13)$$

The previous expansions seem to imply that, up to the present level of accuracy, both  $\varepsilon^2$  and  $\varepsilon^3$  corrections can be safely expanded for small (large)  $\bar{m}_c$  in the bottom mass (bottomonium binding energy), so resulting in:

$$E_{\bar{b}b} = \left[ 2\bar{m}_b \left\{ 1 + \frac{4}{3}\varepsilon \frac{\alpha_s^{(4)}(\bar{m}_b)}{\pi} + \varepsilon^2 \left( \frac{\alpha_s^{(4)}(\bar{m}_b)}{\pi} \right)^2 d_1^{(4)} + \varepsilon^3 \left( \frac{\alpha_s^{(4)}(\bar{m}_b)}{\pi} \right)^3 d_2^{(4)} \right\} + \right. \\ \left. + E_{\text{bin},\bar{b}b}^3 \left( \mu, \alpha_s^{(3)}(\mu), \bar{m}_b \left\{ 1 + \frac{4}{3}\varepsilon \frac{\alpha_s^{(4)}(\bar{m}_b)}{\pi} + \varepsilon^2 \left( \frac{\alpha_s^{(4)}(\bar{m}_b)}{\pi} \right)^2 d_1^{(4)} \right\} + \right) \right. \\ \left. + \varepsilon^2 2(\delta m_b)_{\bar{m}_c}^{(1)} + \varepsilon^3 \left\{ 2(\delta m_b)_{\bar{m}_c}^{(2)} - \frac{1}{4} \left( \frac{C_F \alpha_s^{(4)}(\mu)}{n} \right)^2 (\delta m_b)_{\bar{m}_c}^{(1)} \right\} \right] \quad \alpha_s(\bar{m}_b) = \text{Eq. (2.5.8)}$$

$$\alpha_s^{(4)} = \text{Eq. (2.5.15)}$$

$$\equiv 2\bar{m}_b + E_{\bar{b}b}^{(1)}(\mu, \alpha_s^{(3)}(\mu), \bar{m}_c, \bar{m}_b)\varepsilon + E_{\bar{b}b}^{(2)}(\mu, \alpha_s^{(3)}(\mu), \bar{m}_c, \bar{m}_b)\varepsilon^2 \\ + E_{\bar{b}b}^{(3)}(\mu, \alpha_s^{(3)}(\mu), \bar{m}_c, \bar{m}_b)\varepsilon^3 + \dots, \quad (2.5.14)$$

State $X$	$E_X^{\text{exp}}$	$E_X$	$E_X^{\text{exp}} - E_X$	$E_X^{(1)}$	$E_X^{(2)}$	$E_X^{(3)}$	$\mu_X$	$\alpha_s^{(3)}(\mu_X)$
$\Upsilon(1^3S_1)$	9.460	9.460	0	0.866	0.208	0.006	2.14	0.286
$\Upsilon(1^3P_0)$	9.860	$9.995^{+75}_{-62}$	$-0.135^{+62}_{-75}$	1.534	0.101	-0.021	1.08	0.459
$\Upsilon(1^3P_1)$	9.893	$10.004^{+78}_{-63}$	$-0.111^{+63}_{-78}$	1.564	0.081	-0.022	1.05	0.468
$\Upsilon(1^3P_2)$	9.913	$10.012^{+81}_{-65}$	$-0.099^{+65}_{-81}$	1.591	0.063	-0.022	1.034	0.477
$\Upsilon(2^3S_1)$	10.023	$10.084^{+93}_{-75}$	$-0.061^{+75}_{-93}$	1.618	0.096	-0.010	1.02	0.486
$\Upsilon(2^3P_0)$	10.232	$10.548^{+196}_{-151}$	$-0.316^{+151}_{-196}$	2.421	-0.356	0.102	0.778	0.710
$\Upsilon(2^3P_1)$	10.255	$10.564^{+200}_{-153}$	$-0.309^{+153}_{-200}$	2.472	-0.404	0.116	0.770	0.726
$\Upsilon(2^3P_2)$	10.268	$10.578^{+203}_{-155}$	$-0.310^{+155}_{-203}$	2.518	-0.449	0.129	0.762	0.740
$\Upsilon(3^3S_1)$	10.355	$10.645^{+218}_{-168}$	$-0.290^{+168}_{-218}$	2.472	-0.348	0.140	0.770	0.726
$\Upsilon(4^3S_1)$	10.580	*	*	*	*	*	*	*
$B_c(1^1S_0)$	$6.4 \pm 0.4$	$6.307^{+4}_{-2}$	$0.1 \pm 0.4$	0.675	0.188	0.017	1.62	0.334

**Table VI.** Theoretical predictions for the bottomonium and  $B_c$  masses. The  $c$ -quark and  $b$ -quark  $\overline{MS}$  masses are fixed on the experimental values of the  $J/\psi$  and  $\Upsilon(1S)$  masses, respectively. The uncertainties in the third and fourth columns refer to the uncertainties in  $\alpha_s^{(5)}(M_Z)$  only. All the other data refer to  $\alpha_s^{(5)}(M_Z) = 0.1181$  and to the  $\overline{MS}$  quark masses fixed on the central values  $\overline{m}_c = 1237^{+16}_{-16}$  MeV. and  $\overline{m}_b = 4201^{+19}_{-18}$  MeV. All dimensionful numbers are in GeV.

with

$$\alpha_s^{(4)}(\mu) = \alpha_s^{(3)}(\mu) \left\{ 1 + \varepsilon \frac{\alpha_s^{(3)}(\mu)}{3\pi} \text{Log} \left( \frac{\mu}{\overline{m}_c} \right) + \varepsilon^2 \left( \frac{\alpha_s^{(3)}(\mu)}{\pi} \right)^2 \left[ \frac{1}{9} \text{Log}^2 \left( \frac{\mu}{\overline{m}_c} \right) + \frac{19}{12} \text{Log} \left( \frac{\mu}{\overline{m}_c} \right) - \frac{11}{72} \right] \right\}. \quad (2.5.15)$$

So, after fixing the scale  $\mu$  by demanding that:

$$\frac{d}{d\mu} E_X(\mu, \alpha_s^{(n_i)}(\mu), \overline{m}_b) |_{\mu=\mu_X} = 0, \quad (2.5.16)$$

the predictions given in Table VI are obtained. This table should be compared with Table VII, where no finite charm mass effects were taken into account.

We see that the effect of a finite charm mass is to increase the level spacings, being the effects larger among the higher levels. As the effective coupling becomes larger at the relevant scale when the decoupling of the charm quark is incorporated, the binding energy increases. Since  $\overline{m}_b \equiv m_b^{\overline{MS}}(m_b^{\overline{MS}})$  was fixed on  $\Upsilon(1S)$ ,  $\overline{m}_b$  was decreased by about 11 MeV.  $n = 2$  and  $n = 3$  levels were then increased by about 70-100 MeV. and 240-280 MeV., respectively.

State $X$	$E_X^{exp}$	$E_X$	$E_X^{exp} - E_X$	$E_X^{(1)}$	$E_X^{(2)}$	$E_X^{(3)}$	$\mu_X$	$\alpha_s(\mu_X)$
$J/\psi$	3.097	3.097	0	0.362	0.205	0.043	1.07	0.448
$\eta_c(1^1S_0)$	2.980	3.056	-0.076	0.333	0.195	0.042	1.23	0.399
$\Upsilon(1^3S_1)$	9.460	9.460	0	0.837	0.204	0.013	2.49	0.274
$\Upsilon(1^3P_0)$	9.860	9.905	-0.045	1.38	0.115	0.003	1.18	0.409
$\Upsilon(1^3P_1)$	9.893	9.904	-0.011	1.40	0.098	0.002	1.15	0.416
$\Upsilon(1^3P_2)$	9.913	9.916	-0.003	1.42	0.086	0.003	1.13	0.422
$\Upsilon(2^3S_1)$	10.023	9.966	+0.057	1.46	0.093	0.009	1.09	0.433
$\Upsilon(2^3P_0)$	10.232	10.268	-0.036	2.37	-0.66	0.15	0.693	0.691
$\Upsilon(2^3P_1)$	10.255	10.316 <sup>#</sup>	-0.061 <sup>#</sup>	3.97	-3.56	1.50	0.552 <sup>#</sup>	1.20
$\Upsilon(2^3P_2)$	10.268	10.457 <sup>#</sup>	-0.189 <sup>#</sup>	4.55	-5.03	2.53	0.537 <sup>#</sup>	1.39
$\Upsilon(3^3S_1)$	10.355	10.327	+0.028	2.34	-0.583	0.163	0.698	0.684
$\Upsilon(4^3S_1)$	10.580	11.760 <sup>#</sup>	-1.180 <sup>#</sup>	5.45	-6.47	4.38	0.527 <sup>#</sup>	1.61
$B_c(1^1S_0)$	$6.4 \pm 0.4$	6.324	$0.08 \pm 0.4$	0.668	0.187	0.022	1.64	0.329

**Table VII.** Comparisons of the theoretical predictions of perturbative QCD and the experimental data.  $n_l = 4$  for  $\bar{b}b$  systems and  $n_l = 3$  for  $\bar{c}c$  and  $\bar{c}b$  systems. All dimensionful numbers are in GeV. units.

As the uncertainties originating from the error of the input  $\alpha_s^{(5)}(M_Z)$  are as large (even larger) than other uncertainties, both unknown high-order corrections and next-to-leading order renormalons are expected to contribute some  $\pm(5-30)$  MeV. in the case of  $1S$ ,  $\pm(20-130)$  MeV. for  $n = 2$  states and about  $\pm(40-220)$  MeV. in  $n = 3$  ones.

## Chapter 3

# Renormalization issues in Nucleon-Nucleon EFT

### 3.1 Motivation

Until the moment we have discussed different applications of non-relativistic EFT's well-grounded corpus. Let us now deviate our attention to not so solid terrain. Non-perturbative renormalization, as it is required to treat nucleon-nucleon (NN) interaction, remains a controversial issue, mainly due to our partial lack of understanding of the underlying dynamics and, as a consequence, our inability to consistently organize the EFT calculation. That is why our first approach to the subject is going to focus on power counting and the binomial iterated versus perturbative interactions. We consider that, from that viewpoint, the renormalization problem is presented in the right perspective and its inherent complexity is gazed at in all its depth.

Weinberg's original suggestion[58] that NN scattering and nuclear physics problems could fruitfully benefit from a EFT approach was followed by a huge amount of work undertaken, not to improve the fits of the already successful semi-phenomenological models (Paris, Bonn or Nijmegen potentials), but to provide a better understanding of the relationships among related processes and the underlying physics. NN EFTs were expected to disentangle the various physical scales therein involved:  $M$ , the nucleon mass, vector and scalar meson masses as  $m_\rho$  and  $m_\omega$  and some nucleon resonances' splittings were tagged as large ( $\sim 1$  GeV); whereas Goldstone boson (GB) masses,  $m_\pi$  basically, and the splitting

$M_\Delta$ - $M$  were categorized as the low energy, dynamical part of the spectrum ( $\sim 200$  MeV). Furthermore, NN EFTs were expected to correctly implement the constraints derived from chiral symmetry in the nucleon-pion interaction. This program, invaluable for reproducing low-energy characteristics of NN scattering, has found in the non-perturbative nature of nuclear forces its most serious difficulty to prosper.

Consider in first place what happens in a long-tradition EFT such as  $\chi$ PT, which is perturbatively renormalizable (in a EFT sense). There, we can truncate the expansion of any observable quantity and assign an error estimate to its amplitude just by declaring which is next order in the perturbative series (say, for instance,  $\mathcal{O}(p^{2n+2})$  if we wish a  $p^{2n}$  accuracy in our calculation). By performing some power counting on diagrams, –remember that whenever we have  $L$  loops,  $V_i$  vertices of type  $i$  which contain  $d_i$  derivatives and  $f_i$  fermion fields, our graph is order  $p^\nu$ ,

$$\nu = 2(L + 1) + \sum_i V_i \Delta_i, \quad \Delta_i \equiv d_i + \frac{f_i}{2} - 2, \quad (3.1.1)$$

– we learn up to which order our Lagrangian is required. That is, we would need the set of interactions  $\{ \mathcal{L}^\Delta \}$ ,  $\Delta = 0, \dots, 2n - 2$  where  $n \geq 1$ , in the previous case. As our Lagrangian is an expansion in powers of momenta, loops are going to be increasingly divergent as we keep including higher order vertices. Nevertheless they can be regulated (let us refer to a cutoff  $\Lambda$  for convenience, although dimensional regularization is the optimal way to work at in this context) and the severe cutoff dependence coming from the high momenta region, which otherwise is not correctly described by the EFT, can be removed by lumping these terms together with the unknown bare parameters  $\{ l_i^{\Delta, B} \}$  into renormalized coefficients  $\{ l_i^{\Delta, r} \}$ . As you see, for the most divergent dependence we have at our disposal the brand-new group of vertices  $\{ l_i^{2n-2, B} \}$ . Those ensure renormalization scale independence at every order in the EFT expansion of observables.

Unfortunate complications arise whenever we face in a EFT with the presence of shallow bound (quasi-bound) states. As, to generate them, some interactions must be resummed using a Schrödinger or Lippmann-Schwinger equation, first of all, one should try to work out some criteria that allow us to decide which terms are leading order and, therefore, must be iterated, and which ones are mere perturbations. Accordingly, contact interactions would be ordered in ever growing powers of the inverse cutoff. Large scattering lengths in NN interactions require, indeed, some of the latter to be tagged as leading order potentials, with the consequent appearance of more acute divergences as we keep

increasing the order of the iteration. That is the point where the regularization and non-perturbative renormalization issues enter.

As we notice, so proceeding, any justification on the power counting is made a posteriori, once we compute our phase shifts or any other observables and verify that they are reasonably well reproduced (up to the intended accuracy), while cutoff dependence is being removed in this order-by-order expansion of the amplitude. To provide for a solid, consistent renormalization program of NN interactions has become, as it is shown in the next section, a most debated object and, at the same time, a most desirable one if one is interested in lending EFT's sound techniques to nuclear calculations. Only after we have attained a fair comprehension of the hierarchies involved and low-energy constants fine-tuning, will be able to relate different NN low-energy processes model-independently.

So, before going on, it would be most interesting to review briefly what is the status of matter reached after several studies which tested various regularization schemes, power countings and more or less rigorous approaches. Nevertheless, in view of the huge amount of bibliography this question has generated, regrettably we better opt to focus only on three or four recent works chosen, not only in regard to their intrinsic value, but also because we consider they are useful in providing a way of comparison with our own work.

### 3.1.1 Reporting on previous work

Although our final purpose is to consider NN interactions as mediated by exchanged pions plus local sources of short-distance repulsion, in order to have a nodding acquaintance with the complexity of the problem, let us consider first, following refs. [59] a simplified EFT for NN interaction in the  $^1S_0$  channel, a theory in which all exchanged particles have been integrated out:

$$V(p', p) = C + C_2(p^2 + p'^2). \quad (3.1.1.2)$$

This should deliver a reasonable description of the NN scattering amplitude at low-energy ( $p, p' \ll m_\pi$ ), as

$$A(k) = A_0 + iA_1k + A_2k^2 + A_4k^4 + \dots, \quad (3.1.1.3)$$

is the effective range expansion. Nevertheless, our first surprise comes when we realize that although these  $A_n$  coefficients are naively expected to scale as  $m_\pi^{(-2n-2)}$ , they are fixed by a rather lower scale,



on the order of  $\mathcal{O} \sim 10$  MeV. Such a behaviour is associated to this channel's large scattering length:

$$a_{np}^{1S_0} = -23.75 \text{ fm}, \quad r_{np}^{1S_0} = 2.75 \text{ fm}, \quad (3.1.1.4)$$

or, what comes to be equivalent, to its low lying nearly-bound state. In fact also the spin triplet channel suffers from the same particularity, with the difference that what is found now is a real bound state:

$$a^{3S_1} = 5.42 \text{ fm}, \quad r^{3S_1} = 1.75 \text{ fm}. \quad (3.1.1.5)$$

But perhaps, following Weinberg's suggestion, one may expect that making an EFT expansion of the potential and iterating it through a Lippmann-Schwinger equation one could still generate these loosely bound states, while maintaining natural coefficients in the potential:

$$A(p, p'; E) = V(p, p') + \int \frac{d^3 p''}{(2\pi)^3} V(p, p'') \frac{1}{E - \frac{p''^2}{M} + i\nu} T(p'', p'; E). \quad (3.1.1.6)$$

After inserting (3.1.1.2) above it is evident that what we are doing in fact is generating new difficulties. That is, severe divergences arise and demand a sensible procedure to regularize and renormalize them non-perturbatively, so conditioning the existence of the EFT. To be concrete, our solution of the T-matrix:

$$\begin{aligned} \frac{1}{A(k)} &= \frac{(C_2 \mathcal{I}_3 - 1)^2}{C + C_2^2 \mathcal{I}_5 + k^2 C_2 (2 - C_2 \mathcal{I}_3)} - \mathcal{I}_1, \\ \mathcal{I}_5 &= -M \int \frac{d^3 p''}{(2\pi)^3} p''^2; \quad \mathcal{I}_3 = -M \int \frac{d^3 p''}{(2\pi)^3}; \quad \mathcal{I}_1 = M \int \frac{d^3 p''}{(2\pi)^3} \frac{1}{k^2 - p''^2 + i\nu}, \end{aligned} \quad (3.1.1.7)$$

where  $k$  is the on-shell momentum, contains the power-law divergent integrals  $\mathcal{I}_5$ ,  $\mathcal{I}_3$  and  $\mathcal{I}_1$ , that can be regularized either using a cutoff (sharp or smooth), by dimensional regularization with minimal subtraction (DR<sup>MS</sup>) or any other appropriated choice. In DR<sup>MS</sup> the divergent pieces of every integral vanish by prescription and it is straightforward to match both coefficients  $C$  and  $C_2$  to the experimental scattering length and effective range by means of the effective range expansion:

$$\frac{1}{A(k)} = -\frac{M}{4\pi} \left( -\frac{1}{a} + \frac{1}{2} r_e k^2 + \mathcal{O}(k^4) - ik \right), \quad (3.1.1.8)$$

so yielding:

$$\frac{1}{A^{\text{DR}^{\text{MS}}}(k)} = -\frac{M}{4\pi} \left( -\frac{1}{-a - \frac{1}{2} a^2 r_e k^2} - ik \right),$$

$$\begin{aligned}
C^{\text{DR}^{\text{MS}}} &= \frac{4\pi a}{M} \left( \sim - \left( \frac{1}{25 \text{ MeV.}} \right)^2 \right) \quad ({}^1\text{S}_0 \text{ value}), \\
\frac{2C_2^{\text{DR}^{\text{MS}}}}{C^{\text{DR}^{\text{MS}}}} &= \frac{1}{2} r_e a \left( \sim - \left( \frac{1}{35 \text{ MeV.}} \right)^2 \right) \quad ({}^1\text{S}_0 \text{ value}).
\end{aligned} \tag{3.1.1.9}$$

Due to the large scattering length, the radius of convergence of the theory  $\mathbf{p}^2 \sim 1/(ar_e)$  is helplessly small. On the other hand, choosing a cutoff and sending it to infinity at the end, we get:

$$\frac{1}{A^{\text{cutoff}}(k)} = -\frac{M}{4\pi} \left( -\frac{1}{a} + \frac{1}{2} r_e k^2 + \mathcal{O}(k^4) - ik \right), \tag{3.1.1.10}$$

with the constraint  $r_e \leq 0$  if  $C$  and  $C_2$  are real. The conclusion is that whereas perturbatively we can prove the equivalence between  $\text{DR}^{\text{MS}}$  and other methods of regularization, it appears that in the non-perturbative setting we cannot longer assert this. The difficulty stems on the fact that, when applied perturbatively,  $\text{DR}^{\text{MS}}$  trusts on the absorption of all power-law divergences by higher order counterterms. As here the renormalization conditions are no longer linear, this causes both amplitudes to differ. What's more,  $\text{DR}^{\text{MS}}$ 's removal of power-law divergences seems to be throwing some crucial information of the amplitude. What has been found in the cutoff case is in agreement with Wigner's theorem, that states that whenever a potential goes to zero beyond some range  $R$ , then:

$$r_e \leq 2 \left( R - \frac{R^2}{a} + \frac{R^3}{3a^2} \right). \tag{3.1.1.11}$$

As you see, apparently we are not able to describe positive range interactions unless we keep the cutoff finite ( $R \neq 0$ ).

That possibility, which had been advanced by Lepage[60] and has become most popular since then, led the path to a somewhat more relaxed conception of renormalizing procedures. Last encountered difficulties clearly indicate that low-energy physics can be very sensitive to short-distance interactions. Nevertheless we know there exist infinite many theories which can mimetize the right behaviour, being the power of EFTs its skill to design the most economic theory in terms of interactions, while keeping the capability of systematic improvement. This last feature advises us to proceed so:

1. First the correct long-range behaviour is incorporated.
2. Then an ultraviolet cutoff is introduced to exclude the high-momentum states and to deal with possible sources of irregularity as  $r \rightarrow 0$ .

3. We add, respecting the symmetries of the underlying theory, local correction terms to the effective Hamiltonian to account for those high-virtuality states previously extracted. Long-range and smeared delta (and its derivatives) interactions are iterated via a Schrödinger equation.
4. Coupling constants are made to vary with the cutoff (tuning) so as to maintain observables independent of the cutoff with a precision which must be higher order in the momentum expansion  $\left(\mathcal{O}\left(\left(\frac{p^2}{\Lambda^2}\right)^{n+1}\right)\right)$ . The dependence of the effective theory on its couplings becomes highly non-linear when the short-distance interactions are strong. Nevertheless another source of non-linear behaviour sets in when the cutoff distance is made too small. If this is reduced below the range  $r_e$  of the true potential high-momentum states are included that are sensitive to its structure. Then results degrade and in extreme cases, the theory may become unstable or untunable.

It is worth emphasizing that, although here the cutoff is kept finite, it is not a parameter to be fitted by data to account for some known physical effect, as it was traditionally done in nuclear physics. Indeed what must be checked in every numerical simulation of a EFT is that errors decrease when  $\Lambda$  is enlarged until we reach some scale  $M$ , frontier of new physics, beyond which there is no further improvement.

Extending already our framework to somewhat higher energy physics, let us outline what is Lepage's treatment of NN interaction at leading order. It features a long-range potential that at large  $r$  we identify with one pion exchange:

$$\begin{aligned} V_{1\pi} &= \alpha_\pi \tau_1 \cdot \tau_2 \frac{\sigma_1 \cdot \nabla \sigma_2 \cdot \nabla}{m_\pi^2} v_\Lambda(r), \\ v_\Lambda(r) &\longrightarrow \frac{e^{-m_\pi r}}{r}, \end{aligned} \quad (3.1.1.12)$$

where  $\alpha_\pi \approx \frac{g_A^2 m_\pi^2}{16\pi f_\pi^2}$ . Projecting into different spin-orbit channels we get:

$$\begin{aligned} V_{1\pi} &\longrightarrow -\alpha_\pi [bv_\Lambda(r) + b_T v_T(r)], \\ v_T(r) &= \frac{1}{m_\pi^2} \left( v_\Lambda'' - \frac{v_\Lambda'}{r} \right), \end{aligned} \quad (3.1.1.13)$$

where the constants  $b$  and  $b_T$  will depend on the analyzed channel. Now we introduce an ultraviolet smooth cutoff,  $(e^{-\frac{q^2}{2\Lambda^2}})$ , in the Fourier transform of the spatial potential to obtain:

$$v_\Lambda(r) \equiv \frac{1}{2r} \left[ e^{m_\pi r} \operatorname{erfc} \left( -\frac{(r\Lambda - \frac{m_\pi}{\Lambda})}{\sqrt{2}} \right) - (r \rightarrow -r) \right], \quad (3.1.1.14)$$

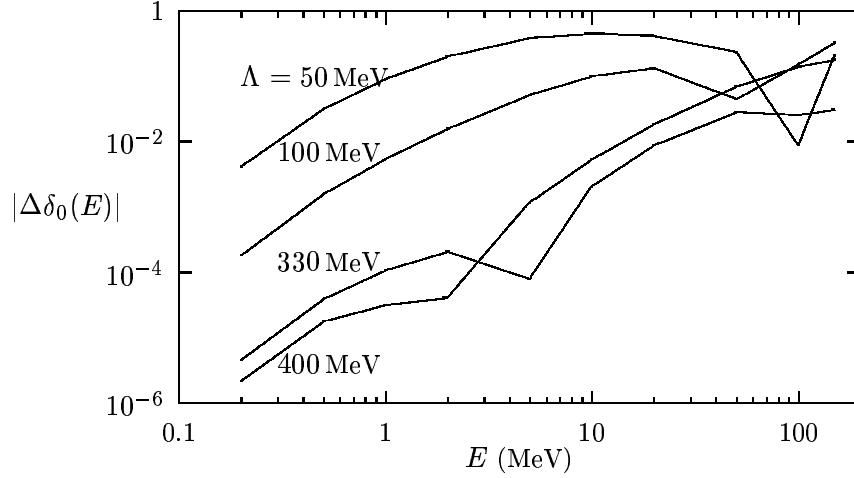


Figure 1: Errors in the  $^1S_0$  phase shifts (in radians) versus energy for the full effective theory with different values of the cutoff  $\Lambda$ .

and the function  $\text{erfc}(x)$  stands for  $1-\text{erf}(x)$  (error function). The short distance terms in the potential are smeared delta functions (and its derivatives):

$$\delta_{1/\Lambda}^{(3)}(\mathbf{r}) \equiv \frac{\Lambda^3 e^{-r^2 \frac{\Lambda^2}{2}}}{(2\pi)^{\frac{3}{2}}}. \quad (3.1.1.15)$$

In all, nine constants account for two S and four P waves up to order  $\mathcal{O}(\mathbf{p}^2)$ .

Take  $^1S_0$  channel at this accuracy. It requires the tuning of two short distance couplings to, let's say, the phase shifts at two different energies. Our potential is:

$$V(r) = -\alpha_\pi v_\Lambda(r) + c \frac{\delta_{1/\Lambda}^{(3)}(\mathbf{r})}{\Lambda^2} - d \nabla^2 \frac{\delta_{1/\Lambda}^{(3)}(\mathbf{r})}{\Lambda^4}. \quad (3.1.1.16)$$

The errors obtained in the phase shift as a function of the center of mass energy are found in fig. 1. Errors decrease until  $\Lambda \sim 300$  MeV. and afterwards no further improvement is seen. The low radius of convergence of the theory can perhaps be explained by two-pion exchange role, isospin breaking effects,  $\Delta$  (the baryonic resonance with  $I=3/2$ ) contributions or some tuning of  $\alpha_\pi$ .

So, should we content with this new viewpoint or should we pursue in trying to find out a more conventional renormalization program -a program where one merely regulates the integrals and then renormalizes the couplings of the theory so absorbing all terms that diverge as the cutoff is removed?

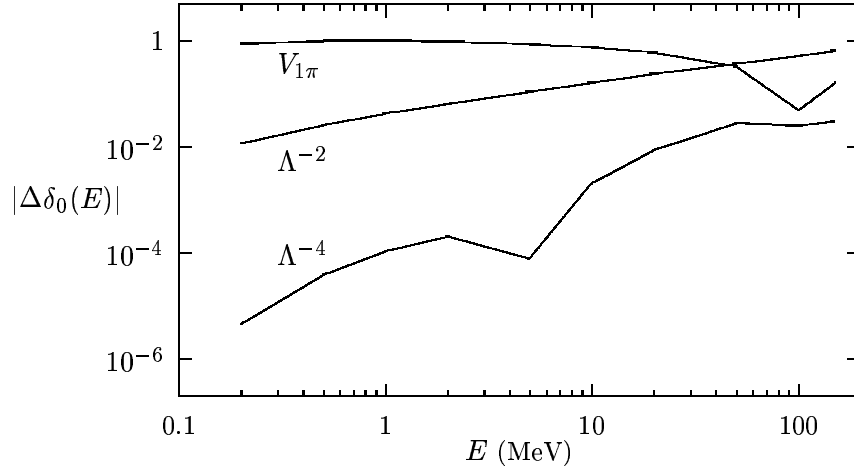


Figure 2: Errors in the  $^1S_0$  phase shifts (in radians) versus energy for the effective theory through orders  $\Lambda^{-2}$  and  $\Lambda^{-4}$ . Results from the theory with just pion exchange ( $V_{1\pi}$ ) are also shown. The cutoff was  $\Lambda = 330$  MeV in each case.

Firstly, we want to review DR's treatment of NN interaction to see where lies exactly the problem and whether there is any possibility of circumventing it. Let's borrow for a while that opinion (page 34 in [61]) which states that constraint (3.1.1.11) although 'unusual it is doubtful of much relevance to EFTs applied consistently to a certain order', as it is 'a regularization-scheme-dependent issue'.

So take once more  $^1S_0$  channel in the pionless theory and remember what we did in order to get DR's result: we expanded the potential up to order  $\mathbf{p}^2$  (terms of  $\mathcal{O} \sim V_2$  and iterated it through a Schrödinger/LS equation. Now we want to do something quite different. After Kaplan, Savage and Wise suggestion (KSW, [63]), we will expand the inverse of Feynman's amplitude. This is shown diagrammatically in fig. 3.

$$\frac{1}{\mathcal{A}} = \frac{1}{\mathcal{A}_0} \left[ 1 - \left( \frac{\mathcal{A}_2}{\mathcal{A}_0} \right) - \left( \frac{\mathcal{A}_3}{\mathcal{A}_0} \right) + \left( \frac{\mathcal{A}_2^2 - \mathcal{A}_0 \mathcal{A}_4}{\mathcal{A}_0^2} \right) + \dots \right]. \quad (3.1.1.17)$$

$\mathcal{A}_0$  and  $\mathcal{A}_2$  are found to be:

$$\begin{aligned} \mathcal{A}_0 &= -\frac{C}{1 + i\frac{CM|\mathbf{p}|}{4\pi}} = \frac{4\pi}{M} \frac{1}{a} + i|\mathbf{p}|, \\ \mathcal{A}_2 &= \left( \frac{C}{1 + i\frac{CM|\mathbf{p}|}{4\pi}} \right)^2 \left( \frac{2C_2 \mathbf{p}^2}{C^2} \right) = \left( \frac{M\mathcal{A}_0}{4\pi} \right) \frac{1}{2} r_e \mathbf{p}^2, \end{aligned} \quad (3.1.1.18)$$

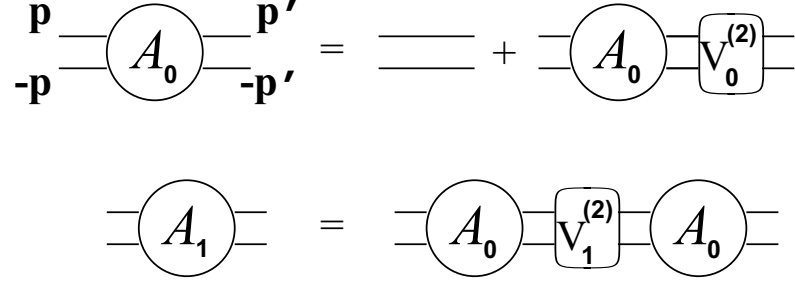


Figure 3: The first two terms in the EFT expansion for the Feynman amplitude ( $T$ -matrix) for nucleon-nucleon scattering in the center of mass frame. The leading amplitude  $\mathcal{A}_0$  consists of the sum of ladder diagrams with the leading 2-nucleon potential  $V_0^{(2)}$  at every rung; the subleading amplitude  $\mathcal{A}_1$  consists of one insertion of  $V_1^{(1)}$  (1-loop nucleon wavefunction renormalization) or one insertion of the subleading 2-nucleon potential  $V_1^{(2)}$ , dressed by all powers of the leading interaction  $V_0^{(2)}$ .

which reproduces exactly the effective range expansion (see formulas (3.1.1.9) and (3.1.1.10)):

$$\frac{1}{T(k)} = -\frac{M}{4\pi} \left( -\frac{1}{a} + \frac{1}{2} r_e k^2 - ik \right). \quad (3.1.1.19)$$

This demonstrates that the amplitude's expansion allows us to extend the range of validity of the EFT beyond the scale set by the derivative expansion of the potential. At the same time it illustrates the importance of power counting in a non-perturbative context: it is crucial to treat leading order ( $V_0$ ) and perturbations ( $V_2$ ) in the right footing. That will be one of the main points in the presentation of our own work.

Here is the right place to introduce pions in order to extend the range of validity of the theory. Therefore we must decide in first place how one pion exchange should count as for the amplitude. Perturbatively (as  $V_2$ )? Iteratively (in  $V_0$ )? If this introduction was intended to be a fair report, at this point we would feel compelled to start a new chapter that displayed the huge amount of debate this question has risen. Nevertheless that is far beyond our intentions. Let's only state that both alternatives have been carefully explored, being nowadays the non-perturbative role of pions (at least in  ${}^3S_1$  channel) of general belief.

In [63], pions in  ${}^1S_0$  channel of NN scattering were included at leading order:

$$\begin{aligned} V(\mathbf{p}, \mathbf{p}') &= C - \left( \frac{g_A^2}{4f_\pi^2} \right) \frac{(\mathbf{p} - \mathbf{p}') \cdot \sigma_1 (\mathbf{p} - \mathbf{p}') \cdot \sigma_2}{(\mathbf{p} - \mathbf{p}')^2 + m_\pi^2} (\tau_1 \cdot \tau_2) = \tilde{C} - V_\pi(\mathbf{p}, \mathbf{p}'), \\ \tilde{C} &=: \left( C + \frac{g_A^2}{2f_\pi^2} \right), \end{aligned}$$

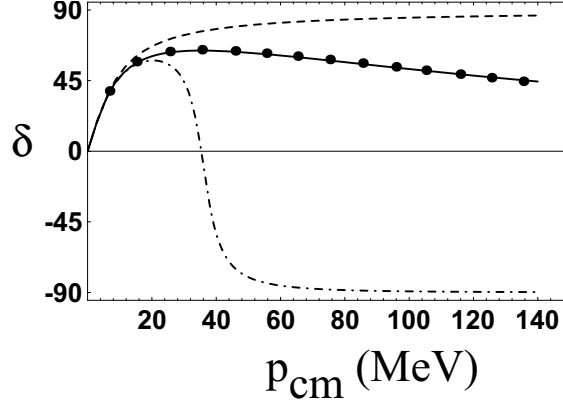


Figure 4:  $^1S_0$   $np$  phase shifts in degrees plotted versus center of mass momentum. The dots are the  $^1S_0$  phase shift data from the Nijmegen partial wave analysis; the dashed, dash-dot and solid lines are EFT calculations in a theory without pions. The dashed line is the result from eq. (3.1.1.9) with  $C_2 = 0$ ; the dash-dot line is the EFT result when the potential is expanded to second order eq. (3.1.1.9); the solid line (which lies along the dots) is the EFT result when the invers of the amplitude is expanded to second order, eq. (3.1.1.19).

$$V_\pi(\mathbf{p}, \mathbf{p}') = -\frac{4\pi\alpha_\pi}{((\mathbf{p} - \mathbf{p}')^2 + m_\pi^2)}, \quad \alpha_\pi =: \left( \frac{g_A^2 m_\pi^2}{16\pi f_\pi^2} \right), \quad (3.1.1.20)$$

where  $g_A = 1.25$  is the axial coupling constant. The ladder of all possible interactions containing any number of contact interactions and pion exchanges in whatever order was summed up so yielding:

$$i\mathcal{A}_0 = i\mathcal{A}_\pi - i \frac{\tilde{C} |\chi_{\mathbf{p}}(\mathbf{0})|^2}{1 - \tilde{C} \tilde{G}_E(\mathbf{0}, \mathbf{0})}, \quad (3.1.1.21)$$

where  $\mathcal{A}_\pi$  resums all possible pion exchanges and the quantity  $\tilde{G}_E(\mathbf{0}, \mathbf{0})$  describes the chain of two contact interactions joined by any number of pion exchanges. We will review in our exposition how the divergences contained in  $\tilde{G}_E(\mathbf{0}, \mathbf{0})$ , arising from no pion and one pion exchange, get renormalized by replacing the bare  $\tilde{C}$  by the renormalized  $\tilde{C}_{\overline{\text{MS}}}^r(\mu)$ . In the meanwhile is enough with saying that this last quantity can be fitted so as our amplitude to reproduce the correct scattering length.

$$\tilde{C}_{\overline{\text{MS}}}^r(m_\pi) = - \left( \frac{1}{79 \text{ MeV}} \right)^2. \quad (3.1.1.22)$$

Once we do so, the effective range can be computed:

$$r_e = 1.3 \text{ fm}, \quad (3.1.1.23)$$

that is approximately half the actual value.

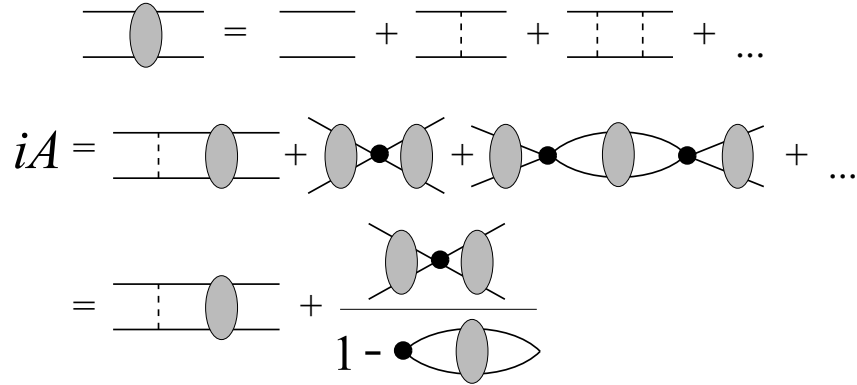


Figure 5: Ladder diagrams for the leading order contribution to the Feynman amplitude ( $\mathcal{A}_0$ ) are formally resummed by expressing the kernel  $V_0$  as a sum of a contact interaction proportional to  $\tilde{C}$  and a nonlocal interaction  $V_\pi$ . The shaded blobs consist of the ladder sum of  $V_\pi$  interactions (dashed lines), while the black vertices correspond to a factor of  $\tilde{C}$ .

Next step to be done within that framework (non-perturbative pion exchange) is to compute the perturbative effect of a  $V_2$  insertion with any number of leading order interactions, as it was done in the pionless case. We do not wish to go into detail about this.  $\tilde{C}$  and  $C_2$  need to be renormalized in order to have a finite amplitude, the cutoff is therefore removed from the theory and a subtraction point is introduced. Fitting both constants at a scale  $m_\pi$  so as to reproduce the measured scattering length and effective range, it is obtained:

$$\tilde{C}_{\text{MS}}(m_\pi) = -\frac{1}{(100 \text{ MeV})^2}, \quad C_2 = \frac{1}{(110 \text{ MeV})^4}. \quad (3.1.1.24)$$

The message of all this is that we can indeed renormalize ‘the old way’ NN interaction in the singlet channel, being the only dark point the fact that, at least apparently, the radius of convergence of the theory ( $|\mathbf{p}| \sim 121 \text{ MeV}$ .) is pretty small. Nevertheless, had we (inconsistently with any power counting) iterated  $V_2$  potential to all orders, the radius would have been roughly of  $|\mathbf{p}| \sim 43 \text{ MeV}$ . This is shown in fig. 6.

But the last word about this convergence problem had not been said. In ’98 these same authors [64] presented a new expansion for NN interactions. The trend now was renormalizing in a conventional manner, but with the counting of pion exchange as a perturbative potential. The observation that in the singlet channel this expansion offered a fairly good convergence, triggered the purpose of extending this analysis to the coupled channel  ${}^3S_1$ - ${}^3D_1$ . Did it work, this would provide for analytical expressions of



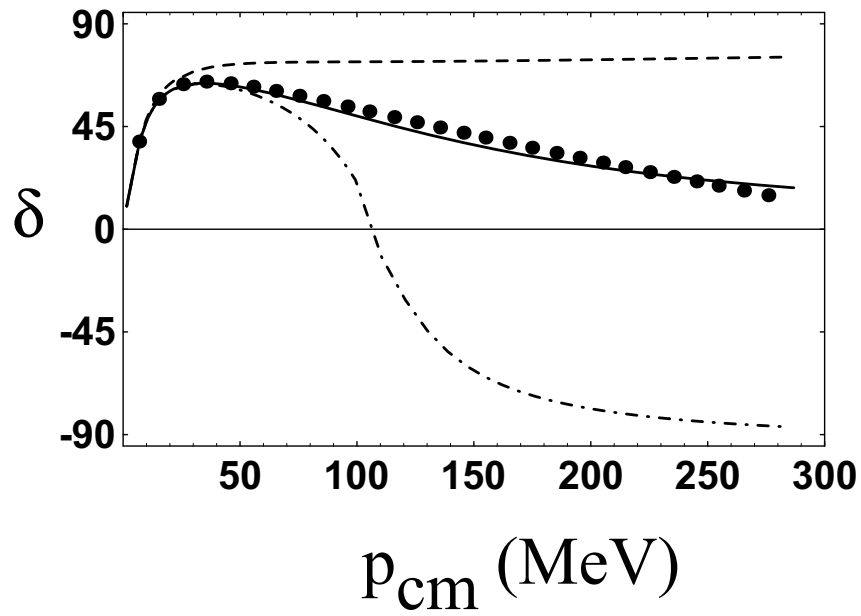


Figure 6:  $^1S_0$   $np$  phase shifts in degrees plotted versus center of mass momentum. The dots are the data from the Nijmegen partial wave analysis; the dashed, dash-dot and solid lines are EFT calculations in a theory with one pion exchange. The dashed line is the leading order; the dash-dot line is the EFT result when the potential is expanded to second order and iterated; the solid line (which lies along the dots) is the EFT result when the invers of the amplitude is expanded to second order.

scattering amplitudes, as we will see in the forthcoming sections that when pions are included non-perturbatively a numerical treatment is compulsory. But soon it was found out that such a procedure breaks down completely in the triplet case, what is no surprise since, from the viewpoint of counting rules and scaling, a perturbative treatment of pions is far from evident.

But let's come back to KSW's suggestion. After all the criticism ([59, 60]) blamed on Dimensional Regularization as an appropriate tool in NN interaction, it was time to demonstrate that the method worked also when pions were perturbative. The fact is that, once OPEP is relegated to a  $V_2$  insertion, we must provide somehow for a large radius of convergence (at least of the order of the pion mass). As it is seen in fig. 5, in DR with  $MS$  the pionless theory, that is now our starting point, is a pretty bad approximation for momenta larger than  $\sim 25$  MeV. Otherwise DR is not guilty for the failure. It is mere artifice of  $MS$ , that adds a counterterm that eliminates the poles at four space-time dimensions and sends to zero all power divergent integrals. Then, had we subtracted in the linearly divergent integral:

$$\begin{aligned} \mathcal{I}_0 &= -i \left(\frac{\mu}{2}\right)^{4-D} \int \frac{d^D q}{(2\pi)^D} \frac{i}{\frac{E}{2} - q^0 - \frac{\mathbf{q}^2}{2M} + i\nu} \frac{i}{\frac{E}{2} + q^0 - \frac{\mathbf{q}^2}{2M} + i\nu} = \\ &= -M(-ME - i\nu)^{\frac{D-3}{2}} \Gamma\left(\frac{3-D}{2}\right) \frac{\left(\frac{\mu}{2}\right)^{4-D}}{(4\pi)^{\frac{(D-1)}{2}}}, \end{aligned} \quad (3.1.1.25)$$

not only the pole at  $D=4$ , but also the one at  $D=3$ , the outcome would have been something quite different:

$$\mathcal{I}_0^{\text{PDS}} = \left(\frac{M}{4\pi}\right) (\mu + ip), \quad (3.1.1.26)$$

where we have introduced the PDS (after Power Divergent Subtraction) scheme. Working out the leading order amplitude within the new framework, we get:

$$i\mathcal{A}_{-1} = \frac{-i}{\frac{1}{C} + \frac{M(\mu+ip)}{4\pi}}, \quad (3.1.1.27)$$

that allows us to extract the value of  $C$  by matching to the effective range expansion:

$$C(\mu) = \frac{4\pi}{M} \left( \frac{1}{-\mu + \frac{1}{a}} \right). \quad (3.1.1.28)$$

From above's expression it becomes apparent that, in a system with a scattering length of natural size,  $\mu$  can be sent to zero and we still have natural size coefficients. On the contrary, always  $a$  is large it is

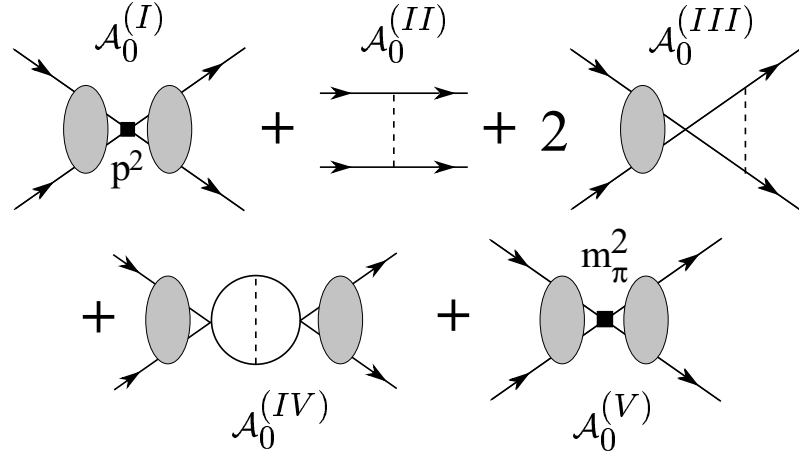


Figure 7: The five sub-graphs contributing to  $\mathcal{A}_0$ . The gray blob is defined as the iteration of contact  $C$  interactions. The dashed line is the exchange of a potential pion.

convenient to take a non-zero  $\mu$ . That way coefficients are made to scale like  $C_{2n} \sim \frac{4\pi}{M\Lambda_\chi^n \mu^{n+1}}$ , where  $\Lambda_\chi$  is a natural scale of NN interactions (take  $m_\pi$  or  $\left(\frac{g_A^2 M}{8\pi f^2}\right)^{-1}$ , for instance). Furthermore we can set  $\mu = \Lambda$  and then we reobtain the cutoff results. Or we can replace  $\mu$  by  $\frac{1}{a}$  and then we meet again those large coefficients we found when using  $MS$ .

Taking as leading order  $\mathcal{A}_{-1}$ , and with the help of our new power counting and associated renormalization scheme, we are in position of computing first corrections to the amplitude. These come from local, order two insertions,  $\mathcal{O} \sim \mathbf{p}^2$  and from OPEP. The whole group is shown in fig. 8 under the name  $\mathcal{A}_0$ .

It should be noted that now the mass-proportional constant  $D_2$  serves to cure the logarithmic divergence we found when we were treating pions non-perturbatively (3.1.1.22).<sup>1</sup> The coupled channel  ${}^3S_1$ - ${}^3D_1$  is amenable to a similar analysis. The S-matrix in this channel is usually given in terms of two phase shifts  $\delta_0$  and  $\delta_2$  and a mixing angle  $\epsilon_1$  (barred parametrization<sup>2</sup>):

$$S = \begin{pmatrix} e^{2i\delta_0} \cos 2\epsilon_1 & i e^{i(\delta_0 + \delta_2)} \sin 2\epsilon_1 \\ i e^{i(\delta_0 + \delta_2)} \sin 2\epsilon_1 & e^{2i\delta_2} \cos 2\epsilon_1 \end{pmatrix}. \quad (3.1.1.29)$$

It should be warned that at leading order  $\mathcal{A}_{20} = \mathcal{A}_{02} = \mathcal{A}_{22} = 0$ , which implies that  $\epsilon_1$  and  $\delta_2$  are zero.

<sup>1</sup>The fact that in the non-perturbative situation  $\frac{1}{C}$  must contain a term  $\sim \left(\frac{M m_\pi}{4\pi f}\right)^2 \Gamma(4 - D)$ , in order to get rid of the ‘one pion-two contacts’ divergence, is known in the literature as the ‘inconsistency of Weinberg’s power counting’. In the next pages we will come back to the issue.

<sup>2</sup>Although the barred parametrization is quite convenient whenever mixing is small, as it happens in the NN triplet channels, the physically relevant parametrization is Blatt-Biedenharn’s.

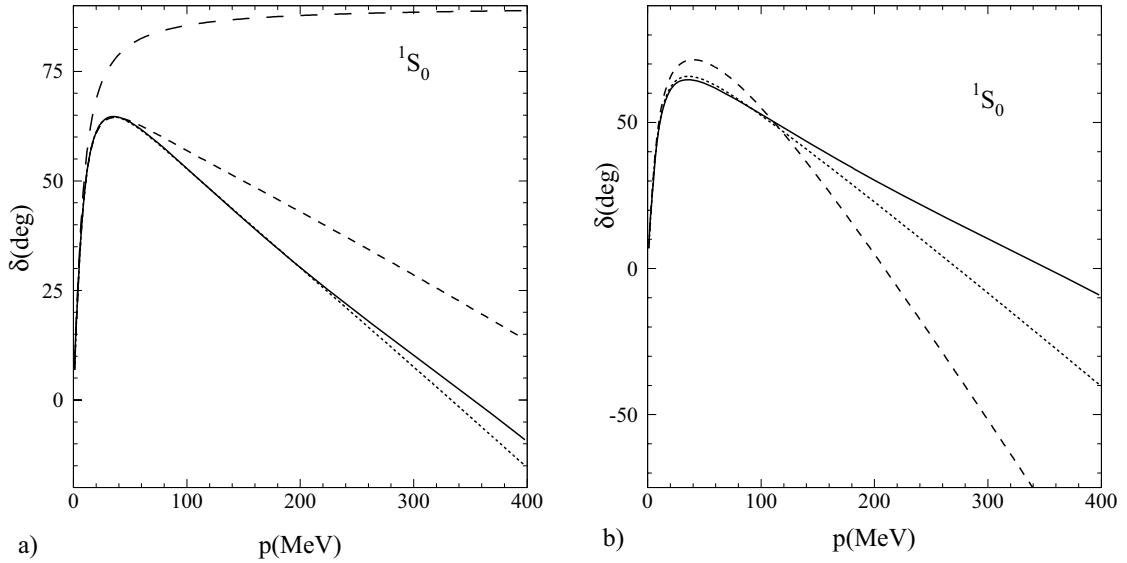


Figure 8: Fit to the  $^1S_0$  phase shift  $\delta$ . The solid line is the Nijmegen fit to the data. In a), the long dashed, short dashed, and dotted lines are the LO, NLO, and NNLO results respectively. In b) we show two other NNLO fits with a different choice of parameters.

The task of studying the possible convergence of the expansion based on KSW counting was undertaken mainly by Fleming, Mehen and Stewart[65]. Their results, from which we include two illustrating examples in fig. 8, show that in the singlet channels  $^1S_0$ ,  $^1P_1$  and  $^1D_2$  and up to NNLO the fits are converging. Agreements of 1%, 13% and 33% at  $p = m_\pi$  appear as a byproduct of the smallness of two potential pion exchange contribution (the box graph). In those channels single pion exchange (remember that this is NLO in KSW counting and enters with  $\mathcal{O} \sim p^2$  contact terms) provides a similar accuracy as the LO Weinberg calculation, which treats potential pions non-perturbatively.

As for the behaviour in triplet channels, it is more or less erratic. While the NNLO predictions for  $^3P_1$  and  $^3D_2$  at  $p = m_\pi$  have errors of the expected size (15% and 8%, which is less than  $\mathcal{O} \sim \left(\frac{g_A^2}{4f^2} \frac{Mm_\pi}{4\pi}\right)^2 \sim .25$ , the estimated accuracy error), in the  $^3P_0$  and  $^3P_2$  channels errors are much bigger than expected (170% and 52%). It is worth emphasizing that the coupled  $^3S_1$ - $^3D_1$  channel at NNLO does worst in fitting the data than the NLO prediction. Here also the appearance of non-analytic contributions that grow with  $p$  entering through the box graph make compulsory the non-perturbative (Weinberg counting) treatment of one pion exchange interaction.

Then, although KSW program was very appealing (amplitudes could be analytically calculated and renormalization worked perturbatively in pion exchange diagrams), it was not suitable in triplet

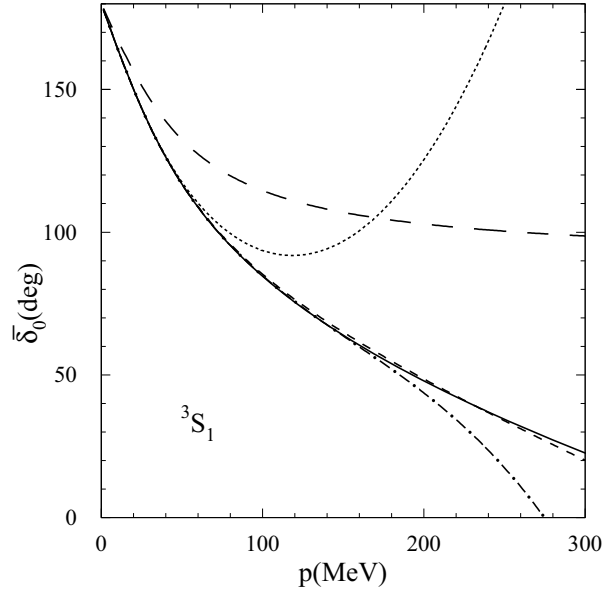


Figure 9: The  ${}^3S_1$  phase shift for NN scattering. The solid line is the Nijmegen multi-energy, the long dashed line is the LO effective field theory result, the short dashed line is the NLO result, and the dotted line is the NNLO result. The dash-dotted line shows the result of including the parameter  $\zeta_5$  which is *higher order* in the power counting.

channels. In fact, during the time KSW power counting was still under discussion, different studies[66], some of them more rigorous than others, claimed that a non-perturbative treatment of pion exchange was not a matter of debate, but rather an unavoidable fact. Nevertheless, besides its partial success, this proposal taught us quite a lot about the intimate interplay between power counting and non-perturbative renormalization, the ingredients and procedure a solid program that treated NN interaction should include.

So, let us finish this rather brief account here. As it was warned at the beginning of the subsection, the intention was not at all to give a complete description of the field, but to provide the background and main motivations of our own analysis. In spite of the interest of the subject and in regard to the length and difficulty that a rigorous display would require, we will go directly to the last two works that connect to a certain extent with our study, mainly focused on these triplet channels that still lack from a well-grounded formalism.

First one is a '99 paper of Frederico et al[67]. There the Lippmann-Schwinger equation was regulated by means of the replacement of the potential by  $T(-\mu^2)$ , the  $T$ -matrix at a scale  $\mu$ , which

was intended to be sent eventually to infinity. Then, the authors discussed, it was justified to constrain  $T(-\mu^2)$  to be equal to our potential, that is, OPEP plus non-derivative contact interactions:

$$\begin{aligned} T(E) &= T(-\mu^2) + T(-\mu^2)G_R^{(+)}(E; -\mu^2)T(E), \\ G_R^{(+)}(E; -\mu^2) &:= G_0^{(+)}(E) - G_0(-\mu^2) = \frac{(\mu^2 + E)}{(\mu^2 + H_0)}G_0^{(+)}(E), \end{aligned} \quad (3.1.1.30)$$

$$T_s^{(00)}(p', p; -\mu^2) = V_{\pi,s}^{(00)}(p', p) + \Lambda_{\mathcal{R},s}(\mu), \quad (3.1.1.31)$$

$$T_t^{(ll')}(p', p; -\mu^2) = V_{\pi,t}^{(ll')}(p', p) + \Lambda_{\mathcal{R},t}(\mu)\delta_{l0}\delta_{l'0}, \quad (3.1.1.32)$$

where  $\Lambda_{\mathcal{R},s}(\mu)$  and  $\Lambda_{\mathcal{R},t}(\mu)$  are the two subtraction point dependent contact interactions that belong to the singlet and triplet channel respectively. Their results are compared to ours in the Discussion at the conclusion of the chapter.

$\mu$ (fm <sup>-1</sup> )	$\lambda_{\mathcal{R},s}$ (fm)	$r_{0,s}$ (fm)	$\lambda_{\mathcal{R},t}$ (fm)	$r_{0,t}$ (fm)	$B_D$ (MeV)	$\eta_D$
4	-0.8806	1.332	-0.2281	1.364	1.977	0.02808
10	-0.7570	1.345	21.741	1.536	2.084	0.02904
30	-0.6977	1.347	-0.3776	1.582	2.114	0.02933
Nijmegen	-	2.73	-	1.75	2.2246	0.0256

**Table VIII.** Low energy n-p and deuteron observables compared with data. Singlet ( $r_{0,s}$ ) and triplet ( $r_{0,t}$ ) effective ranges, deuteron binding energy ( $B_D$ ) and ratio  $\eta_D$  are given for several values of the single parameter  $\mu$ . The  $\lambda_{\mathcal{R},s}(\mu)$  and  $\lambda_{\mathcal{R},t}(\mu)$  are the strengths of the  $\delta$ -interactions which were added to the OPEP and adjusted to the corresponding scattering lengths,  $a_s = -23.7$  fm and  $a_t = 5.4$  fm.

The second paper that has recently undertaken an apparently similar task, appeared under the title ‘Towards a Perturbative Theory of Nuclear Forces’[68]. There the authors argue, basing on numerical simulations, that while Weinberg’s non-perturbative treatment of pion exchange is formally inconsistent in the  $^1S_0$  channel, the coupled  $^3S_1$ - $^3D_1$  system requires such an approach, although calculations can be simplified by making use of the chiral limit  $m_\pi \rightarrow 0$ . Sketching their procedure only very roughly, they depart from the substitution of the usual delta interaction in the  $^1S_0$  channel by a square well of radius  $R$ :

$$C_0 \delta^{(3)}(\mathbf{r}) \longrightarrow \frac{3C_0\theta(R-r)}{4\pi R^3} \equiv V_0 \theta(R-r), \quad (3.1.1.33)$$

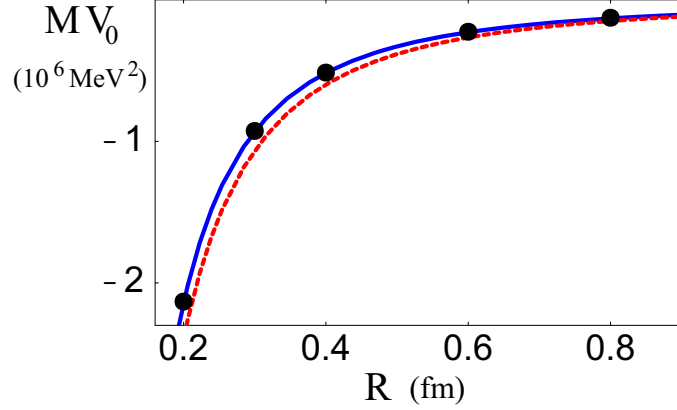


Figure 10: The solid line represents the running of  $V_0$  as a function of the cutoff  $R$  (in fermis), taken from eq. (3.1.1.35) with  $n = 1$ , for the physical value of  $m_\pi$ , while the dotted line neglects the  $R^{-1}$  part of the running. The dots are extracted directly from a numerical solution of the Schrödinger equation for the physical value of  $m_\pi$ .

and cut the OPE potential at the radius  $R \equiv 1/\Lambda$ . Matching the wavefunctions corresponding to both interactions at  $R$ , they find a multibranch condition on  $V_0$  as a function of  $R$ :

$$\sqrt{-MV_0} \cot(\sqrt{-MV_0}R) = -m_\pi^2 M \alpha_\pi \text{Log}\left(\frac{R}{R_*}\right) + \mathcal{O}(R), \quad (3.1.1.34)$$

where  $R_*$  should be numerically determined and  $\alpha_\pi$  is now  $\frac{g_A^2}{16\pi f^2}$ . Then they further expand the left hand side near its zeros to get:

$$V_0(R; n) = -(2n+1)^2 \frac{\pi^2}{4MR^2} - \frac{2m_\pi^2 \alpha_\pi}{R} \text{Log}\left(\frac{R}{R_*}\right) + \mathcal{O}(R^0). \quad (3.1.1.35)$$

This running is presented in fig. 10 for  $n = 1$  in connection with the phase shift produced. Here, following the authors, the formal inconsistency of Weinberg's power counting in this channel is perfectly well displayed. This is seen in the fact that  $V_0$  must contain a  $m_\pi^2$ -proportional term in order to keep cutoff (in the sense of Lepage) independence.

Triplet  ${}^3S_1$ - ${}^3D_1$  channel is handled in a similar fashion. Outside a square well of radius  $R$  we still have the tensor potential given by OPE, while inside what we find is the energy-dependent interaction:

$$\mathcal{V}_S(r) = \begin{pmatrix} -M(V_0 + k^2 V_2) & 0 \\ 0 & -M(V_0 + k^2 V_2) - 6/r^2 \end{pmatrix}. \quad (3.1.1.36)$$

Taking the chiral limit of the tensor force and neglecting the angular-momentum barrier outside the well ( $R < r < M\alpha_\pi$ ) and treating energy-dependence as a perturbation, the long range potential is

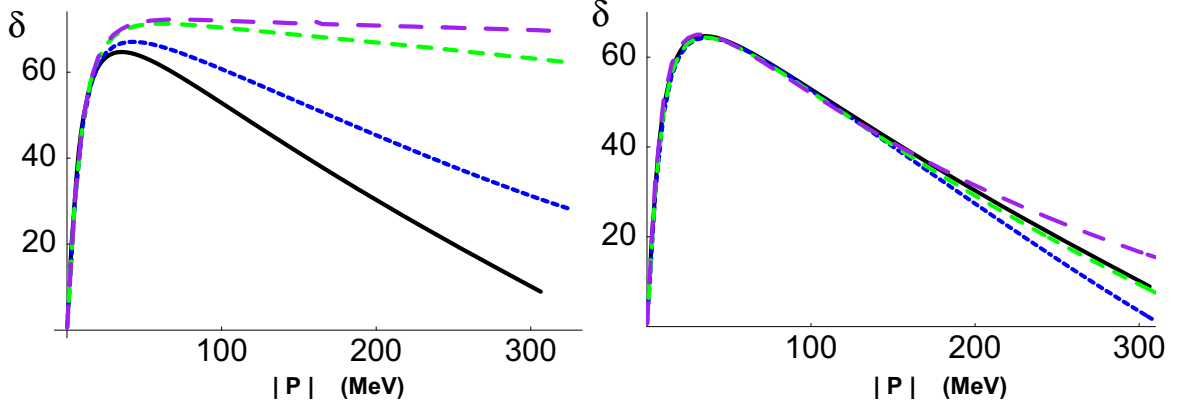


Figure 11: The  $^1S_0$  phase-shift plotted versus center of mass momentum. The solid lines are the Nijmegen phase-shift analysis. The long-dash lines corresponds to  $R = 0.2$  fm. ( $\Lambda = 985$  MeV.), the medium-dash lines correspond to  $R = 0.4$  fm. ( $\Lambda = 492$  MeV.), and the dotted lines correspond to  $R = 1.4$  fm. ( $\Lambda = 140$  MeV.). The left panel corresponds to setting  $V_2 = 0$ , while the right panel includes  $V_2$  in such a way to reproduce the measured effective range.

diagonalized and its Schrödinger equation decouples in an attractive and a repulsive piece. The solution to the attractive singular potential (Bessel functions) can be matched at  $R$  to that of the square well of height  $V_0 + k^2 V_2$ . This yields two equations:

$$\begin{aligned} \sqrt{-MV_0}R \cot(\sqrt{-MV_0}R) &= \frac{3}{4} + \sqrt{\frac{6M\alpha_\pi}{R}} \tan\left(2\sqrt{\frac{6M\alpha_\pi}{R}} + \phi_0\right), \\ \frac{MV_2 - 1}{MV_0} \left[ \sqrt{-MV_0} \cot(\sqrt{-MV_0}R) + MV_0 R \csc^2(\sqrt{-MV_0}R) \right] &= \\ = \frac{R^{\frac{3}{2}}}{\sqrt{6M\alpha_\pi}} \tan\left(2\sqrt{\frac{6M\alpha_\pi}{R}} + \phi_0\right) - \left(\frac{2}{5}R + \frac{2}{R}\sqrt{\frac{6M\alpha_\pi}{R}}\phi_1\right) \sec^2\left(\sqrt{\frac{6M\alpha_\pi}{R}} + \phi_0\right) \end{aligned} \quad (3.1.1.37)$$

where the phases  $\phi_0$  and  $\phi_1$  are determined so to fit the experimental values of the scattering length and effective range.

Considerations about this regularizing procedure are also postponed till the Discussion. Nevertheless it is worth warning already that:

i) what the authors are pursuing is regularization, not renormalization (in the GellMann-Low or Wilsonian sense). In a misunderstood and unfortunate way, they resort to Lepage's aforementioned lectures[60], that accurately describe how to handle **renormalizable** theories, in order to dismiss the limit  $\Lambda \rightarrow \infty$ .

ii) phase-shifts and mixing angles calculated in the chiral-limit obviously differ from those



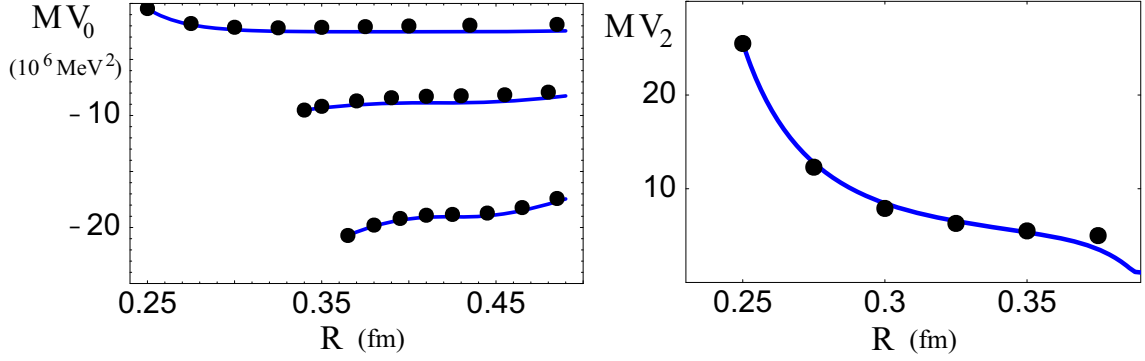


Figure 12: The solid lines represent the running of  $MV_0$  and  $MV_2$  as a function of the cutoff  $R$ , taken from eq. (3.1.1.37). The dots are extracted directly from a numerical solution of the Schrödinger equation. The different branches in the left panel correspond to a different number of nodes in the square well, i.e. an artifact of this particular regulator. The curves continue to smaller values of  $R$ , but we have not shown them. Further, analogous branches exist for  $MV_2$ . For each branch, the ultraviolet phase is fit to the smallest  $R$  data point to produce the theoretical curve.

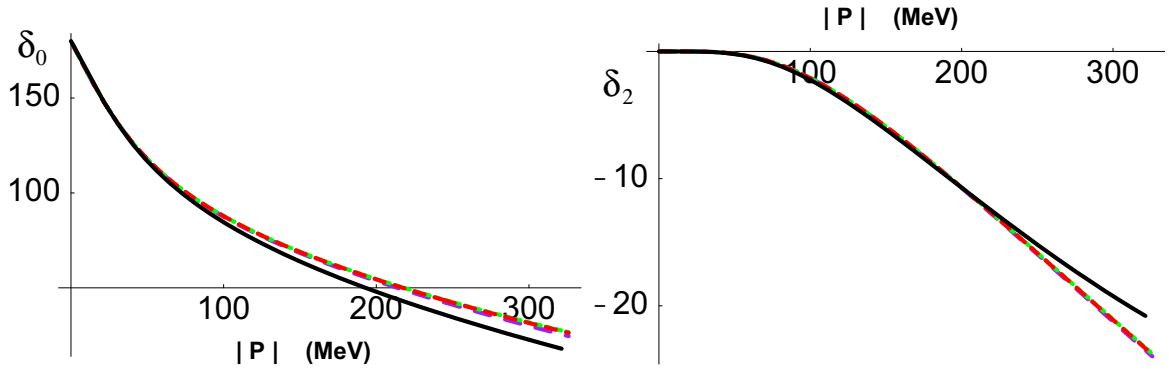


Figure 13: The  ${}^3S_1$ - ${}^3D_1$  phase-shifts as a function of the center of mass momentum. The solid line is the Nijmegen phase-shift analysis. The long-dash line corresponds to  $R = 0.45$  fm. ( $\Lambda = 438$  MeV.), the medium-dash line corresponds to  $R = 0.21$  fm. ( $\Lambda = 938$  MeV.), and the dotted line corresponds to  $R = 0.10$  fm. ( $\Lambda = 1970$  MeV.).  $V_2$  was kept equal to zero.

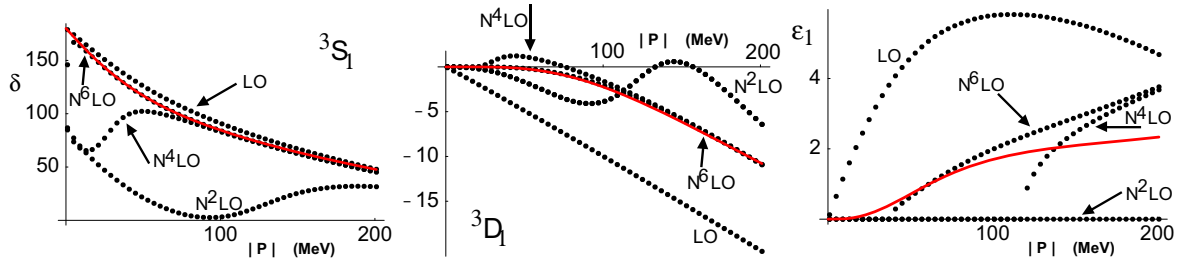


Figure 14: The  $\delta_0$ ,  $\delta_2$  phase-shifts and  $\varepsilon_1$  mixing angle in perturbation theory out to  $N^8$ LO in  $V(r; m_\pi) - V(r; 0)$ . The solid line is the result of the Nijmegen phase-shift analysis, while the dotted curves correspond to the LO,  $N^2$ LO,  $N^4$ LO and  $N^6$ LO results, as indicated on each panel. These results were obtained for a square well of radius of  $R = 0.25$  fm., with  $MV_0 = 1.01 \times 10^6$  MeV.<sup>2</sup> and  $MV_2 k^2 = 23.54 k^2$ .

which keep the mass of the pion finite; the expansion around  $m_\pi = 0$  turns out to be quite wild behaved (see fig. 14).

Finally, we would like to stress that, in spite of the rooted beliefs of some people, also in quantum theories the limit  $\Lambda \rightarrow \infty$  is the relevant one (see ref. [69]).

After this brief account of related/previous work, which provides the subjective context of our interests, we finally are in the right position to present our own contribution to the subject. In the following pages our aim will be the making up of an analytically clear response to the concrete question: can the One Pion Exchange Potential (OPEP) be renormalized (in the conventional sense, that is, sending the cutoff to infinity)? We have just shown, when pursuing the tangled thread of controversies this issue has arised, the subtlety of our, apparently, simple question. So, as we do not desire that any intricacy of the renormalization procedure, that may deliver a valid solution, is lost due to more or less widely accepted conjectures, we will proceed in the most general fashion. That is, we will take the OPEP potential, will analyze its behaviour when iterated through a Lippmann-Schwinger equation and will be so open-minded as to allow all couplings in the potentials (even the ones in front of the non-local terms) to vary so as to absorb all cutoff dependence in the limit  $\Lambda \rightarrow \infty$ . That is the usual<sup>3</sup>, most general approach from a Field Theory perspective, one that, by recognizing our hopeless inability to perform a non-perturbative matching between the NN Lagrangian and QCD, indulges to consider more freedom than perhaps necessary. Note, however, that the standard choice ‘only local terms should renormalize

<sup>3</sup>Not only it is found in theoretical works on renormalization of singular potentials (see for instance [70]), but also there are known examples in a non-relativistic EFT of QCD (pNRQCD) where the renormalization of non-local potentials is required in order to absorb certain divergences [71], the most spectacular of which being the renormalization of the static potential [45, 72].

divergences' is also studied as a restricted subset in a larger ensemble of possibilities we examine.

Anyway, allowing for the renormalization of non-local potentials in the NN system should not represent any problem, even if their coupling constants are fixed to definite values when their potentials are computed from the HB $\chi$ L. What matters for the low energy properties of NN systems is not the precise values those constants take at the scale of the HB $\chi$ L, but only the *form* of the potentials themselves. Hence, any of those (bare) constants with a non-trivial flow will just provide a free parameter (the analogous to a renormalized coupling constant), which may be eventually fixed by low energy data or, alternatively, related to its (higher energy) HB $\chi$ L value by a matching procedure. There is no need of elaborating further on this point because, eventually, it will not be needed. Let us only mention that it has some implications. Mainly, it becomes irrelevant whether a certain potential, which first arises at a given order of  $\chi$ PT, receives also contributions from higher orders, since this will amount to a re-definition of (unknown) counterterms. In particular, for the lower energy EFT there is no inconsistency at all in the so-called Weinberg counting for the  $^1S_0$  channel we have been referring to all during this section. It only reflects the fact that the low energy calculation, or NN EFT, is not organized in terms of the chiral counting anymore<sup>4</sup>.

So, as we pose this study, at the same time the regularization analysis tells us whether a constant does flow, relevant information about the actual form of the cutoff dependence, as well as the way its subleading behaviour in  $\Lambda$  enters into observables (and therefore is fixed by experiment), is easily attained. By regarding NN renormalization as a theoretical matter, not only are we avoiding the so-conspicuous model-dependency of previous works, but are also leading the way to a deeper insight on the power counting and organization of the theory. That is, our results, although perhaps phenomenologically less spectacular than some commonly accepted numerical treatments, are not intended to affect their very successful achievements. Even a way of comparison is sometimes difficult, taking into account that their flows/solutions fail to consider the strict limit of  $\Lambda \rightarrow \infty$ , which furthermore explains why some of their observables behave more or less wildly when approaching this limit. Let us advance right now some of the main points we reach after the next demonstration, as we regard they are worth of

---

<sup>4</sup>In other words, HB $\chi$ PT is a local theory with pions and non-relativistic nucleons as explicit degrees of theory. It has an energy cutoff ( $\Lambda_E$ ) such that  $E \sim m_\pi \ll \Lambda_E \ll M \sim 4\pi f_\pi$  and a momentum cutoff ( $\Lambda_p$ ) which verifies  $p \ll \Lambda_p \ll M \sim 4\pi f_\pi$ . Therefore its Lagrangian can be organized according to the chiral counting since this (and its breaking) is an explicit symmetry. But the NN lower energy EFT we are handling has an energy cutoff ( $\tilde{\Lambda}_E$ ) such that  $E \ll \tilde{\Lambda}_E \ll m_\pi$  and a momentum cutoff ( $\tilde{\Lambda}_p$ ) such that  $p \lesssim m_\pi \ll \tilde{\Lambda}_p \ll M$ . Namely, it consists of non-relativistic nucleons interacting via a (non local) potential. No pion fields exist and chiral counting is not a natural way to organize the theory anymore.

being emphasized from the very beginning. It is going to be clearly shown that, in order to renormalize the non-perturbatively handled full OPEP, the coupling ( $c_1$ ) accompanying the tensor-like, non-local interaction describing pion exchange does need to flow so as to produce a non-trivial scattering amplitude. Nevertheless, we will find out that the strong cutoff dependence of  $c_1$ , otherwise obliged in order to regularize the spin conserving part of the interaction, induces as a solution a T-matrix that lacks from partial wave mixing. This unphysical, undesirable feature leads us to conclude that, in order to renormalize, one should distinguish between spin symmetry conserving (SS) and breaking (SSB) terms of the interaction. While the first ones (diagonal part in a  $2 \times 2$  matrix notation) are tagged as LO and must be resummed, the second ones are handled out perturbatively and begin contributing at NLO. We further demonstrate, in first order perturbation theory, that this way, no non-local term coupling constant does need to flow. At the same time this proposal seems to be consistent with the fact that partial wave mixings are observed to be rather small in all triplet channels. Finally, while a possible power counting that ensures renormalizability is proposed, a future line of further study is pointed out.

### 3.2 A convenient decomposition

We start from the LO NN potential:

$$V(\mathbf{k}, \mathbf{k}') = - \left( \frac{g_A}{2f_\pi} \right)^2 \tau_1 \cdot \tau_2 \frac{\sigma_1 \cdot (\mathbf{k} - \mathbf{k}') \sigma_2 \cdot (\mathbf{k} - \mathbf{k}')}{(\mathbf{k} - \mathbf{k}')^2 + m_\pi^2} + C_S + C_T \sigma_1 \cdot \sigma_2. \quad (3.2.1)$$

This potential acts on a wave function  $\Psi_{\alpha\beta}^{ab}(\mathbf{k}, \mathbf{k}')$ , where  $a, b$  and  $\alpha, \beta$  are nucleon isospin and spin indices respectively, which can be decomposed into irreducible representations of spin and isospin as follows:

$$\begin{aligned} \Psi_{\alpha\beta}^{ab}(\mathbf{k}) &= \frac{1}{2} \left[ (\tau_2)^{ab} (\sigma_2)_{\alpha\beta} \psi_{SS}(\mathbf{k}) + (\tau_2)^{ab} (\sigma_{k'} \sigma_2)_{\alpha\beta} \psi_{SV}^{k'}(\mathbf{k}) + \right. \\ &\quad \left. + (\tau_k \tau_2)^{ab} (\sigma_2)_{\alpha\beta} \psi_{VS}^k(\mathbf{k}) + (\tau_k \tau_2)^{ab} (\sigma_{k'} \sigma_2)_{\alpha\beta} \psi_{VV}^{kk'}(\mathbf{k}) \right]. \end{aligned} \quad (3.2.2)$$

The potential (3.2.1) reduces for each isospin-spin channel to:

$$\begin{aligned} V_{SS}(\mathbf{k}, \mathbf{k}') &= -3 \left( \frac{g_A}{2f_\pi} \right)^2 \frac{(\mathbf{k} - \mathbf{k}')^2}{(\mathbf{k} - \mathbf{k}')^2 + m_\pi^2} + C_S - 3C_T, \\ V_{SV}^{i'j'}(\mathbf{k}, \mathbf{k}') &= 3 \left( \frac{g_A}{2f_\pi} \right)^2 \frac{(\mathbf{k} - \mathbf{k}')^2 \delta^{i'j'} - 2(\mathbf{k} - \mathbf{k}')^{i'} (\mathbf{k} - \mathbf{k}')^{j'}}{(\mathbf{k} - \mathbf{k}')^2 + m_\pi^2} + (C_S + C_T) \delta^{i'j'}, \end{aligned}$$

$$\begin{aligned}
V_{VS}^{ij}(\mathbf{k}, \mathbf{k}') &= \left(\frac{g_A}{2f_\pi}\right)^2 \frac{(\mathbf{k} - \mathbf{k}')^2 \delta^{ij}}{(\mathbf{k} - \mathbf{k}')^2 + m_\pi^2} + (C_S - 3C_T) \delta^{ij}, \\
V_{VV}^{ij,i'j'}(\mathbf{k}, \mathbf{k}') &= -\left(\frac{g_A}{2f_\pi}\right)^2 \delta^{ij} \frac{(\mathbf{k} - \mathbf{k}')^2 \delta^{i'j'} - 2(\mathbf{k} - \mathbf{k}')^{i'}(\mathbf{k} - \mathbf{k}')^{j'}}{(\mathbf{k} - \mathbf{k}')^2 + m_\pi^2} + (C_S + C_T) \delta^{ij} \delta^{i'j'} \quad (3.2.3)
\end{aligned}$$

We still have to implement Fermi symmetry. This implies that the irreducible wave functions (3.2.2) must fulfill (isospin and spin indices will be omitted for the rest of this section):

$$\begin{aligned}
\psi_{SS}(\mathbf{k}) &= -\psi_{SS}(-\mathbf{k}), \\
\psi_{SV}(\mathbf{k}) &= \psi_{SV}(-\mathbf{k}), \\
\psi_{VS}(\mathbf{k}) &= \psi_{VS}(-\mathbf{k}), \\
\psi_{VV}(\mathbf{k}) &= -\psi_{VV}(-\mathbf{k}), \quad (3.2.4)
\end{aligned}$$

which is implemented in the LS equation if we choose:

$$\begin{aligned}
T_{SS}(\mathbf{k}, \mathbf{k}'; E) &= \frac{1}{2} (V_{SS}(\mathbf{k}, \mathbf{k}') - V_{SS}(-\mathbf{k}, \mathbf{k}')) + \\
&+ \frac{1}{2} \int^\Lambda \frac{d^3 k''}{(2\pi)^3} (V_{SS}(\mathbf{k}, \mathbf{k}'') - V_{SS}(-\mathbf{k}, \mathbf{k}'')) \frac{1}{E - \frac{\mathbf{k}''^2}{M} + i\eta} T_{SS}(\mathbf{k}'', \mathbf{k}'; E) \quad (SS \longleftrightarrow VV), \\
T_{SV}(\mathbf{k}, \mathbf{k}'; E) &= \frac{1}{2} (V_{SV}(\mathbf{k}, \mathbf{k}') + V_{SV}(-\mathbf{k}, \mathbf{k}')) + \\
&+ \frac{1}{2} \int^\Lambda \frac{d^3 k''}{(2\pi)^3} (V_{SV}(\mathbf{k}, \mathbf{k}'') + V_{SV}(-\mathbf{k}, \mathbf{k}'')) \frac{1}{E - \frac{\mathbf{k}''^2}{M} + i\eta} T_{SV}(\mathbf{k}'', \mathbf{k}'; E) \quad (SV \longleftrightarrow VS), \quad (3.2.5)
\end{aligned}$$

It is the advantage of the above decomposition that we will not need to specify which (coupled) partial waves we are analyzing.

If the LS equation for the potentials (3.2.3) was well defined, using (3.2.5) would be equivalent to solving the LS equation:

$$\widehat{T}_{xy}(\mathbf{k}, \mathbf{k}'; E) = V_{xy}(\mathbf{k}, \mathbf{k}') + \int^\Lambda \frac{d^3 k''}{(2\pi)^3} V_{xy}(\mathbf{k}, \mathbf{k}'') \frac{1}{E - \frac{\mathbf{k}''^2}{M} + i\eta} \widehat{T}_{xy}(\mathbf{k}'', \mathbf{k}'; E), \quad (3.2.6)$$

( $x, y=S, V$ ) namely, ignoring the statistics and then using the standard formulas:

$$\begin{aligned}
T_{SS}(\mathbf{k}, \mathbf{k}'; E) &= \frac{1}{2} \left( \widehat{T}_{SS}(\mathbf{k}, \mathbf{k}'; E) - \widehat{T}_{SS}(-\mathbf{k}, \mathbf{k}'; E) \right) \quad (SS \rightarrow VV), \\
T_{SV}(\mathbf{k}, \mathbf{k}'; E) &= \frac{1}{2} \left( \widehat{T}_{SV}(\mathbf{k}, \mathbf{k}'; E) + \widehat{T}_{SV}(-\mathbf{k}, \mathbf{k}'; E) \right) \quad (SV \rightarrow VS). \quad (3.2.7)
\end{aligned}$$

However, the LS equation for  $\widehat{T}_{xy}$  is not well defined in any channel and hence using (3.2.5) or (3.2.6)-(3.2.7) may not be totally equivalent. In particular, for the SS and VV channels, the UV divergences one finds using (3.2.5) are softer than those from (3.2.6)-(3.2.7), so we shall work with (3.2.5). For the SV and VS channels, however, the UV divergences found using (3.2.5) are as strong as the ones that stem from (3.2.6)-(3.2.7). For convenience, we have chosen to work with the latter for these channels.

The LS equation in the isoscalar-scalar channel is already in (3.2.5) well defined, as it is apparent from the antisymmetrization of the corresponding potential (3.2.3). On the contrary, the other three channels require regularization. Searching for the systematics to tackle them will be the aim of the next three sections. For notation simplicity, the energy dependence of the T-matrices as well as of other auxiliary functions will not be displayed explicitly for the rest of the chapter.

### 3.3 The isovector-singlet channel

The LS equation for this channel reads:

$$\widehat{T}_{VS}^{ij}(\mathbf{k}, \mathbf{k}') = V_{VS}^{ij}(\mathbf{k}, \mathbf{k}') + \int^\Lambda \frac{d^3 k''}{(2\pi)^3} V_{VS}^{ik}(\mathbf{k}, \mathbf{k}'') \frac{1}{E - \frac{\mathbf{k}''^2}{M} + i\eta} \widehat{T}_{VS}^{kj}(\mathbf{k}'', \mathbf{k}'),$$

where

$$\begin{aligned} V_{VS}^{ij}(\mathbf{k}, \mathbf{k}') &= \left\{ c_0 + \frac{c_2}{(\mathbf{k} - \mathbf{k}')^2 + m_\pi^2} \right\} \delta^{ij}, \\ c_0 &:= C_S - 3C_T + \left( \frac{g_A}{2f_\pi} \right)^2, \\ c_2 &:= - \left( \frac{g_A m_\pi}{2f_\pi} \right)^2, \end{aligned} \quad (3.3.1)$$

where in the last lines we remember the values those constants will take if the potential had been calculated at LO in  $\chi$ PT. The hat and the VS subscript will be dropped in the following.

Let us define:

$$\mathcal{A}(\mathbf{k}') \delta^{ij} := \int^\Lambda \frac{d^3 k''}{(2\pi)^3} \frac{T^{ij}(\mathbf{k}'', \mathbf{k}')}{E - \frac{\mathbf{k}''^2}{M} + i\eta}. \quad (3.3.2)$$

Then (3.3.1) reads:

$$T^{ij}(\mathbf{k}, \mathbf{k}') = c_0(1 + \mathcal{A}(\mathbf{k}')) \delta^{ij} + \frac{c_2 \delta^{ij}}{(\mathbf{k} - \mathbf{k}')^2 + m_\pi^2} + \int^\Lambda \frac{d^3 k''}{(2\pi)^3} \frac{c_2}{(\mathbf{k} - \mathbf{k}'')^2 + m_\pi^2} \frac{T^{ij}(\mathbf{k}'', \mathbf{k}')}{E - \frac{\mathbf{k}''^2}{M} + i\eta} \quad (3.3.3)$$

and can be rewritten after solving:

$$T_2(\mathbf{k}, \mathbf{k}') = \frac{1}{(\mathbf{k} - \mathbf{k}')^2 + m_\pi^2} + \int^\Lambda \frac{d^3 k''}{(2\pi)^3} \frac{c_2}{(\mathbf{k} - \mathbf{k}'')^2 + m_\pi^2} \frac{T_2(\mathbf{k}'', \mathbf{k}')}{E - \frac{\mathbf{k}''^2}{M} + i\eta}, \quad (3.3.4)$$

in the form:

$$T(\mathbf{k}, \mathbf{k}') = c_2 T_2(\mathbf{k}, \mathbf{k}') + c_0(1 + \mathcal{A}(\mathbf{k}')) \left[ 1 + c_2 \int^\Lambda \frac{d^3 k''}{(2\pi)^3} \frac{T_2(\mathbf{k}, \mathbf{k}'')}{E - \frac{\mathbf{k}''^2}{M} + i\eta} \right], \quad (3.3.5)$$

where we have dropped the  $\delta^{ij}$  structure. If  $\mathcal{A}(\mathbf{k}')$  was a fixed function, the equation above would be well defined and could already be solved with no need to regularize it. However  $\mathcal{A}(\mathbf{k}')$  is a functional of  $T$  and a second equation which relates them must be introduced. This is achieved by multiplying eq.(3.3.5) by  $1/(E - \frac{\mathbf{k}^2}{M} + i\eta)$  and integrating over  $\mathbf{k}$ . We obtain:

$$c_0(1 + \mathcal{A}(\mathbf{k}')) = \frac{1 + c_2 \int^\Lambda \frac{d^3 k}{(2\pi)^3} \frac{T_2(\mathbf{k}, \mathbf{k}')}{E - \frac{\mathbf{k}^2}{M} + i\eta}}{\frac{1}{c_0} - \left[ \mathcal{I}_0 + c_2 \int^\Lambda \frac{d^3 k}{(2\pi)^3} \int^\Lambda \frac{d^3 k''}{(2\pi)^3} \frac{1}{E - \frac{\mathbf{k}^2}{M} + i\eta} T_2(\mathbf{k}, \mathbf{k}'') \frac{1}{E - \frac{\mathbf{k}''^2}{M} + i\eta} \right]},$$

$$\mathcal{I}_0 := \int^\Lambda \frac{d^3 k}{(2\pi)^3} \frac{1}{E - \frac{\mathbf{k}^2}{M} + i\eta}. \quad (3.3.6)$$

Substituting iteratively  $T_2$  in (3.3.4) in the rhs of (3.3.6) we see that only the first iteration produces further divergent expressions when  $\Lambda \rightarrow \infty$ . We can then write (3.3.6) as:

$$c_0(1 + \mathcal{A}(\mathbf{k}')) = \frac{1 + c_2 \mathcal{F}(\mathbf{k}')}{\frac{1}{c_0} - [\mathcal{I}_0 + c_2 \mathcal{L} + c_2 \mathcal{F}']}, \quad (3.3.7)$$

where  $\mathcal{I}_0$  and  $\mathcal{L}$  contain linearly and logarithmically divergent terms respectively, whereas  $\mathcal{F}$  ( $\mathcal{F}'$ ) just denote finite functions:

$$\begin{aligned} \mathcal{L} &:= \int^\Lambda \frac{d^3 k}{(2\pi)^3} \int^\Lambda \frac{d^3 k''}{(2\pi)^3} \frac{1}{E - \frac{\mathbf{k}^2}{M} + i\eta} \frac{1}{(\mathbf{k} - \mathbf{k}'')^2 + m_\pi^2} \frac{1}{E - \frac{\mathbf{k}''^2}{M} + i\eta}, \\ \mathcal{F}(\mathbf{k}') &:= \int^\Lambda \frac{d^3 k}{(2\pi)^3} \frac{T_2(\mathbf{k}, \mathbf{k}')}{E - \frac{\mathbf{k}^2}{M} + i\eta}, \\ \mathcal{F}' &:= \int^\Lambda \frac{d^3 k}{(2\pi)^3} \int^\Lambda \frac{d^3 k''}{(2\pi)^3} \int^\Lambda \frac{d^3 k'''}{(2\pi)^3} \frac{1}{E - \frac{\mathbf{k}^2}{M} + i\eta} \frac{c_2}{(\mathbf{k} - \mathbf{k}'')^2 + m_\pi^2} \frac{T_2(\mathbf{k}'', \mathbf{k}''')}{E - \frac{\mathbf{k}''^2}{M} + i\eta} \frac{1}{E - \frac{\mathbf{k}'''^2}{M} + i\eta} \end{aligned} \quad (3.3.8)$$

It is clear that the expression (3.3.7) can be renormalized by a redefinition of  $c_0$ . In dimensional regularization, ( $D=3+2\epsilon$ ), we obtain:

$$\begin{aligned} \frac{1}{c_0} &= -\frac{M^2 c_2}{4(4\pi)^2} \left( \frac{1}{\epsilon} + \chi_{sch} \right) + \frac{1}{c_0^r(\mu)}, \\ \chi_{MS} &= 0, \\ \chi_{\overline{MS}} &= \gamma_E - \text{Log}(4\pi), \end{aligned} \quad (3.3.9)$$

which is in agreement with [63], as was anticipated after (3.1.1.21), and for a hard cutoff:

$$\frac{1}{c_0} = -\frac{M\Lambda}{2\pi^2} + \frac{M^2 c_2}{32\pi^2} \text{Log} \left( \frac{\Lambda^2}{\mu^2} \right) + \frac{1}{c_0^r(\mu)}. \quad (3.3.10)$$

If we now wish to solve numerically the LS equation, we should proceed as usual and introduce a hard cutoff. However  $c_0$  is not to be fitted to the experimental data but substituted by (3.3.10) and the cutoff made as large as possible (in practice it should be enough if  $\sqrt{EM}/\Lambda$  is of the order of neglected subleading contributions from the NLO potential. What we have just proved is that the result will be cutoff independent up to corrections  $\sqrt{EM}/\Lambda$ .  $\mu$  must be fixed at the relevant momentum scale  $\mu \sim (\sqrt{EM}, m_\pi)$  and  $c_0^r(\mu)$  tuned to fit the experimental data.

Although we have no prediction for  $c_0^r(\mu)$  we can try to understand from (3.3.10) how large scattering lengths may arise. Since  $c_0^r(\mu)$  evolves according to a non-perturbative renormalization group (RG) equation it might take very different values depending on the scale it is evaluated at. After solving it:

$$c_0^r(\mu) = \frac{c_0^r(\mu_0)}{1 + \frac{M^2 c_2 c_0^r(\mu_0)}{16\pi^2} \text{Log} \frac{\mu}{\mu_0}}. \quad (3.3.11)$$

if we input the value  $c_0^r(m_\pi) = -(\frac{1}{79 \text{ MeV}})^2$  (3.1.1.21), we obtain  $c_0^r(M) = -(\frac{1}{125 \text{ MeV}})^2$ , which is not quite at the natural scale ( $\sim M$ ). Hence, the non-perturbative low energy dynamics does not seem to be enough to fill the gap between the natural scales and the large scattering lengths. In spite of that, the variation of  $c_0^r(\mu)$  from  $m_\pi$  to  $M$  is large enough as to justify a non-perturbative treatment of the OPE in this channel.

### 3.4 The isosinglet-vector channel

The LS equation for this channel reads:

$$\widehat{T}_{SV}^{ij}(\mathbf{k}, \mathbf{k}') = V_{SV}^{ij}(\mathbf{k}, \mathbf{k}') + \int^\Lambda \frac{d^3 k''}{(2\pi)^3} V_{SV}^{ik}(\mathbf{k}, \mathbf{k}'') \frac{1}{E - \frac{\mathbf{k}''^2}{M} + i\eta} \widehat{T}_{SV}^{kj}(\mathbf{k}'', \mathbf{k}'),$$

where

$$V_{SV}^{ij}(\mathbf{k}, \mathbf{k}') = \left\{ c_0 + \frac{c_2}{(\mathbf{k} - \mathbf{k}')^2 + m_\pi^2} \right\} \delta^{ij} + c_1 \frac{(\mathbf{k} - \mathbf{k}')^i (\mathbf{k} - \mathbf{k}')^j}{(\mathbf{k} - \mathbf{k}')^2 + m_\pi^2},$$

$$c_0 := C_S + C_T + 3 \left( \frac{g_A}{2f_\pi} \right)^2,$$



$$\begin{aligned}
c_1 &:= -6 \left( \frac{g_A}{2f_\pi} \right)^2, \\
c_2 &:= -3 \left( \frac{g_A m_\pi}{2f_\pi} \right)^2,
\end{aligned} \tag{3.4.1}$$

where we show also the LO values of the coupling constants. We shall drop the subscript  $SV$  and the hat in the following. We call the term proportional to  $c_1$  above spin symmetry breaking (SSB) term. This term breaks orbital angular momentum conservation and makes the analysis of this channel qualitatively different from the previous one. In order to illustrate it, let us take  $\mathbf{k}' = \mathbf{0}$  for simplicity. As we regulate (3.4.1), the possible divergences arising when the regulator is removed depend on the high momentum behaviour of  $T^{ij}(\mathbf{k})$ . If  $T^{ij}(\mathbf{k}) \sim |\mathbf{k}|^\alpha$ , the usual power counting arguments imply that, due to the SSB term, the integral on the rhs will rise this power by one. Hence, the high momentum behaviour of the lhs of the equation will not match the one of its rhs unless:

1.  $\alpha = -1$  and the high momentum contribution of the potential cancels out the one arising from the integral;
2.  $\alpha = 0$  and the bare coupling constant  $c_1$  goes to zero as the cutoff goes to infinity, which removes the  $|\mathbf{k}|^{\alpha+1}$  term on the rhs.

We prove in the Appendix E that the case 1. in fact reduces to 2.

So in next subsection we will proceed keeping in mind that  $c_1 \rightarrow 0$  in some, at the moment undetermined, way. After having explored the consequences this flow has on the amplitude, we will examine in subsection 3.4.2 the alternative of treating SSB as a perturbation. In such a case we find that  $c_1$  is not required to depend on the cutoff.

### 3.4.1 Non-perturbative treatment of the SSB term

Let us then return to equation (3.4.1). It has the following structure:

$$\begin{aligned}
T^{ij}(\mathbf{k}, \mathbf{k}') &= c_0(\delta^{ij} + \mathcal{A}^{ij}(\mathbf{k}')) + c_1 \left[ \frac{(\mathbf{k} - \mathbf{k}')^i (\mathbf{k} - \mathbf{k}')^j}{(\mathbf{k} - \mathbf{k}')^2 + m_\pi^2} + \mathcal{B}^{ij}(\mathbf{k}, \mathbf{k}') \right] + \\
&\quad + c_2 \frac{\delta^{ij}}{(\mathbf{k} - \mathbf{k}')^2 + m_\pi^2} + c_2 \int^\Lambda \frac{d^3 k''}{(2\pi)^3} \frac{1}{(\mathbf{k} - \mathbf{k}'')^2 + m_\pi^2} \frac{T^{ij}(\mathbf{k}'', \mathbf{k}')}{E - \frac{\mathbf{k}''^2}{M} + i\eta}, \\
\mathcal{A}^{ij}(\mathbf{k}') &= \int^\Lambda \frac{d^3 k}{(2\pi)^3} \frac{T^{ij}(\mathbf{k}, \mathbf{k}')}{E - \frac{\mathbf{k}^2}{M} + i\eta},
\end{aligned}$$

$$\mathcal{B}^{ij}(\mathbf{k}, \mathbf{k}') = \int^\Lambda \frac{d^3 k''}{(2\pi)^3} \frac{(\mathbf{k} - \mathbf{k}'')^i (\mathbf{k} - \mathbf{k}'')^k}{(\mathbf{k} - \mathbf{k}'')^2 + m_\pi^2} \frac{T^{kj}(\mathbf{k}'', \mathbf{k}')}{E - \frac{\mathbf{k}''^2}{M} + i\eta}. \quad (3.4.1.1)$$

Let us define:

$$\begin{aligned} T^{ij}(\mathbf{k}, \mathbf{k}') &:= c_0(\delta^{ij} + \mathcal{A}^{ij}(\mathbf{k}')) T_0(\mathbf{k}) + c_1 T_1^{ij}(\mathbf{k}, \mathbf{k}') + c_2 T_2(\mathbf{k}, \mathbf{k}') \delta^{ij}, \\ T_0(\mathbf{k}) &= 1 + c_2 \int^\Lambda \frac{d^3 k''}{(2\pi)^3} \frac{1}{(\mathbf{k} - \mathbf{k}'')^2 + m_\pi^2} \frac{T_0(\mathbf{k}'')}{E - \frac{\mathbf{k}''^2}{M} + i\eta}, \\ T_1^{ij}(\mathbf{k}, \mathbf{k}') &= \frac{(\mathbf{k} - \mathbf{k}')^i (\mathbf{k} - \mathbf{k}')^j}{(\mathbf{k} - \mathbf{k}')^2 + m_\pi^2} + \mathcal{B}^{ij}(\mathbf{k}, \mathbf{k}') + c_2 \int^\Lambda \frac{d^3 k''}{(2\pi)^3} \frac{1}{(\mathbf{k} - \mathbf{k}'')^2 + m_\pi^2} \frac{T_1^{ij}(\mathbf{k}'', \mathbf{k}')}{E - \frac{\mathbf{k}''^2}{M} + i\eta}, \\ T_2(\mathbf{k}, \mathbf{k}') &= \frac{1}{(\mathbf{k} - \mathbf{k}')^2 + m_\pi^2} + c_2 \int^\Lambda \frac{d^3 k''}{(2\pi)^3} \frac{1}{(\mathbf{k} - \mathbf{k}'')^2 + m_\pi^2} \frac{T_2(\mathbf{k}'', \mathbf{k}')}{E - \frac{\mathbf{k}''^2}{M} + i\eta}, \end{aligned} \quad (3.4.1.2)$$

which allows us to isolate in  $T_1^{ij}(\mathbf{k}, \mathbf{k}')$  and  $c_0(\delta^{ij} + \mathcal{A}^{ij}(\mathbf{k}'))$  all sources of divergent behaviour, since  $T_0(\mathbf{k})$  and  $T_2(\mathbf{k}, \mathbf{k}')$  are perfectly well defined.

Using the expressions of  $\mathcal{B}^{ij}(\mathbf{k}, \mathbf{k}')$  in (3.4.1.1) and  $T^{ij}(\mathbf{k}, \mathbf{k}')$  in (3.4.1.2),  $T_1^{ij}(\mathbf{k}, \mathbf{k}')$  can be recasted in the form:

$$\begin{aligned} T_1^{ij}(\mathbf{k}, \mathbf{k}') &= c_0(\delta^{kj} + \mathcal{A}^{kj}(\mathbf{k}')) T_{10}^{ik}(\mathbf{k}) + T_{11}^{ij}(\mathbf{k}, \mathbf{k}') + c_2 T_{12}^{ij}(\mathbf{k}, \mathbf{k}'), \\ T_{10}^{ij}(\mathbf{k}) &= \int^\Lambda \frac{d^3 k''}{(2\pi)^3} \frac{(\mathbf{k} - \mathbf{k}'')^i (\mathbf{k} - \mathbf{k}'')^j}{(\mathbf{k} - \mathbf{k}'')^2 + m_\pi^2} \frac{T_0(\mathbf{k}'')}{E - \frac{\mathbf{k}''^2}{M} + i\eta} + \\ &\quad + \int^\Lambda \frac{d^3 k''}{(2\pi)^3} \frac{c_1 (\mathbf{k} - \mathbf{k}'')^i (\mathbf{k} - \mathbf{k}'')^k + c_2 \delta^{ik}}{(\mathbf{k} - \mathbf{k}'')^2 + m_\pi^2} \frac{T_{10}^{kj}(\mathbf{k}'')}{E - \frac{\mathbf{k}''^2}{M} + i\eta}, \\ T_{11}^{ij}(\mathbf{k}, \mathbf{k}') &= \frac{(\mathbf{k} - \mathbf{k}')^i (\mathbf{k} - \mathbf{k}')^j}{(\mathbf{k} - \mathbf{k}')^2 + m_\pi^2} + \int^\Lambda \frac{d^3 k''}{(2\pi)^3} \frac{c_1 (\mathbf{k} - \mathbf{k}'')^i (\mathbf{k} - \mathbf{k}'')^k + c_2 \delta^{ik}}{(\mathbf{k} - \mathbf{k}'')^2 + m_\pi^2} \frac{T_{11}^{kj}(\mathbf{k}'', \mathbf{k}')}{E - \frac{\mathbf{k}''^2}{M} + i\eta}, \\ T_{12}^{ij}(\mathbf{k}, \mathbf{k}') &= \int^\Lambda \frac{d^3 k''}{(2\pi)^3} \frac{(\mathbf{k} - \mathbf{k}'')^i (\mathbf{k} - \mathbf{k}'')^j}{(\mathbf{k} - \mathbf{k}'')^2 + m_\pi^2} \frac{T_2(\mathbf{k}'', \mathbf{k}')}{E - \frac{\mathbf{k}''^2}{M} + i\eta} + \\ &\quad + \int^\Lambda \frac{d^3 k''}{(2\pi)^3} \frac{c_1 (\mathbf{k} - \mathbf{k}'')^i (\mathbf{k} - \mathbf{k}'')^k + c_2 \delta^{ik}}{(\mathbf{k} - \mathbf{k}'')^2 + m_\pi^2} \frac{T_{12}^{kj}(\mathbf{k}'', \mathbf{k}')}{E - \frac{\mathbf{k}''^2}{M} + i\eta}. \end{aligned} \quad (3.4.1.3)$$

This decomposition enables us to compute  $c_0(\delta^{ij} + \mathcal{A}^{ij}(\mathbf{k}'))$ , and hence the full amplitude  $T^{ij}(\mathbf{k}, \mathbf{k}')$ , in terms of  $T_0(\mathbf{k})$ ,  $T_{1n}^{ij}(\mathbf{k}, \mathbf{k}')$  ( $n = 0, 1, 2$ ) and  $T_2(\mathbf{k}, \mathbf{k}')$  through the equation:

$$\begin{aligned} &\left[ \frac{\delta^{ik}}{c_0} - \int^\Lambda \frac{d^3 k}{(2\pi)^3} \frac{T_0(\mathbf{k}) \delta^{ik}}{E - \frac{\mathbf{k}^2}{M} + i\eta} - c_1 \int^\Lambda \frac{d^3 k}{(2\pi)^3} \frac{T_{10}^{ik}(\mathbf{k})}{E - \frac{\mathbf{k}^2}{M} + i\eta} \right] c_0(\delta^{kj} + \mathcal{A}^{kj}(\mathbf{k}')) = \\ &= \delta^{ij} + c_1 \int^\Lambda \frac{d^3 k}{(2\pi)^3} \frac{T_{11}^{ij}(\mathbf{k}, \mathbf{k}')}{E - \frac{\mathbf{k}^2}{M} + i\eta} + c_2 \int^\Lambda \frac{d^3 k}{(2\pi)^3} \frac{T_2(\mathbf{k}, \mathbf{k}') \delta^{ij}}{E - \frac{\mathbf{k}^2}{M} + i\eta}. \end{aligned} \quad (3.4.1.4)$$

As we have already mentioned  $T_0(\mathbf{k})$  and  $T_2(\mathbf{k}, \mathbf{k}')$  are finite when the cutoff is removed. If we solve  $T_{1n}^{ij}(\mathbf{k}, \mathbf{k}')$ ,  $n = 0, 1, 2$  iteratively, the most divergent pieces in the  $n$ -th iteration are  $T_{10} \sim (c_1 \Lambda)^n \Lambda$ ,  $T_{11} \sim (c_1 \Lambda)^n$  and  $T_{12} \sim (c_1 \Lambda)^{n-1} c_1$ . These series are expected to have a finite radius of convergence. The radius of convergence is in any case non-zero because they are bounded by geometric series (or derivatives of them). If  $c_1$  does not go to zero as  $1/\Lambda$  or stronger (in particular, if  $c_1$  is not allowed to flow), each series will separately diverge. In that case, a finite result can only be obtained if non-trivial cancellations occur for all  $n$ , which we do not see how they could actually happen. If, on the contrary,

$$c_1(\Lambda) = \frac{\bar{c}_1}{\Lambda} + \dots \quad (3.4.1.5)$$

and  $\bar{c}_1$  is small enough, the series will converge. For the T-matrix, such a strong cutoff dependence implies that the terms:

$$\begin{aligned} c_1 T_{10}^{ij}(\mathbf{k}) &\longrightarrow t_{10}^{(0)} \delta^{ij} + \frac{t_{10}^{ij}(\mathbf{k})}{\Lambda} + \dots, \\ c_1 T_{11}^{ij}(\mathbf{k}, \mathbf{k}') &\longrightarrow \frac{t_{11}^{ij}(\mathbf{k}, \mathbf{k}')}{\Lambda} + \dots, \\ c_1 T_{12}^{ij}(\mathbf{k}, \mathbf{k}') &\longrightarrow \frac{t_{12}^{ij}(\mathbf{k}, \mathbf{k}')}{\Lambda} + \dots, \end{aligned} \quad (3.4.1.6)$$

where  $t_{10}^{(0)}$  is simply a finite constant and, as we see, all  $\mathbf{k}, \mathbf{k}'$ -encoded information will be washed out from the amplitude.

That is to say:

$$\begin{aligned} T^{ij}(\mathbf{k}, \mathbf{k}') &= \lim_{\Lambda \rightarrow \infty} c_0 (\delta^{kj} + \mathcal{A}^{kj}(\mathbf{k}')) \left( T_0(\mathbf{k}) \delta^{ik} + c_1 T_{10}^{ik}(\mathbf{k}) \right) + c_1 T_{11}^{ij}(\mathbf{k}, \mathbf{k}') + c_2 \left( T_2(\mathbf{k}, \mathbf{k}') \delta^{ij} + \right. \\ &\quad \left. + c_1 T_{12}^{ij}(\mathbf{k}, \mathbf{k}') \right) = c_0 (\delta^{ij} + \mathcal{A}^{ij}(\mathbf{k}')) \left( T_0(\mathbf{k}) + c_1 t_{10}^{(0)} \right) + c_2 T_2(\mathbf{k}, \mathbf{k}') \delta^{ij}, \end{aligned} \quad (3.4.1.7)$$

which is finite provided  $c_0 (\delta^{ij} + \mathcal{A}^{ij}(\mathbf{k}'))$  is finite. In order to prove the latter we borrow from section 3 the following results:

$$\begin{aligned} \int^\Lambda \frac{d^3 k}{(2\pi)^3} \frac{T_0(\mathbf{k})}{E - \frac{k^2}{M} + i\eta} &= -\frac{M\Lambda}{2\pi^2} + \frac{M^2 c_2}{32\pi^2} \text{Log} \left( \frac{\Lambda^2}{\mu^2} \right) + \mathcal{O}(1), \\ \int^\Lambda \frac{d^3 k}{(2\pi)^3} \frac{T_2(\mathbf{k}, \mathbf{k}')}{E - \frac{k^2}{M} + i\eta} &= \mathcal{O}(1), \end{aligned} \quad (3.4.1.8)$$

and find in Appendix F:

$$\begin{aligned}
c_1 \int^\Lambda \frac{d^3k}{(2\pi)^3} \frac{T_{10}^{ii}(\mathbf{k})}{E - \frac{k^2}{M} + i\eta} &= a_0\Lambda + ib_0\sqrt{EM} + d_0 \text{Log} \left( \frac{\Lambda}{m_\pi} \right) + \mathcal{O} \left( \frac{1}{\Lambda} \right), \\
c_1 \int^\Lambda \frac{d^3k}{(2\pi)^3} \frac{T_{11}^{ii}(\mathbf{k}, \mathbf{k}')}{E - \frac{k^2}{M} + i\eta} &= \mathcal{O}(1), \\
c_1 \int^\Lambda \frac{d^3k}{(2\pi)^3} \frac{T_{12}^{ii}(\mathbf{k}, \mathbf{k}')}{E - \frac{k^2}{M} + i\eta} &= \mathcal{O} \left( \frac{1}{\Lambda} \right),
\end{aligned} \tag{3.4.1.9}$$

where  $a_0, b_0, d_0$  are cutoff independent constants related to  $\bar{c}_1$ . Then the flow:

$$\frac{1}{c_0} = -\frac{M\Lambda}{2\pi^2} + \frac{a_0\Lambda}{3} + \frac{M^2 c_2}{32\pi^2} \text{Log} \left( \frac{\Lambda^2}{\mu^2} \right) + \frac{d_0}{6} \text{Log} \left( \frac{\Lambda^2}{\mu^2} \right) + \frac{1}{c_0^{\bar{c}}(\mu)}, \tag{3.4.1.10}$$

makes  $c_0(\delta^{ij} + \mathcal{A}^{ij}(\mathbf{k}'))$  finite and hence does (3.4.1.7). We have then proved that the flows (3.4.1.5) and (3.4.1.10) renormalize the triplet channel.

It is not difficult to see that the various series above involving divergent terms are bounded by geometric series or derivatives of them. This ensures that our flows provide actually finite expressions for the amplitude if  $\bar{c}_1$  is small enough. However, this amplitude appears to be diagonal in spin space and hence orbital angular momentum is conserved. Although, the observed  ${}^3S_1$ - ${}^3D_1$  mixing, which is small, might be attributed to a higher order effect, it is clear from ref. [62] that it is due to the OPE to a large extend. In order to preclude the conservation of orbital angular momentum, we can foresee two ways out:

1. a SSB term may survive in the renormalized amplitude if  $\bar{c}_1$  is tuned infinitely close to the radius of convergence of the series, so that our bounds do not hold anymore, and
2. the SSB term from OPE must be treated as a perturbation and renormalized as such.

The possibility 1. is examined in Appendix G where we show it unlikely to be realized. In the following subsection we explore 2. and prove that if a suitable SSB term is treated as a perturbation, the amplitude is renormalizable at first order and the mixing survives.

### 3.4.2 Treating the SSB term perturbatively

Let us split the potential as:

$$V^{ij}(\mathbf{k}, \mathbf{k}') = V^{(0)ij}(\mathbf{k}, \mathbf{k}') + V^{(1)ij}(\mathbf{k}, \mathbf{k}'),$$

$$\begin{aligned}
V^{(0)ij}(\mathbf{k}, \mathbf{k}') &= \left\{ \tilde{c}_0 + \frac{\tilde{c}_2}{(\mathbf{k} - \mathbf{k}')^2 + m_\pi^2} \right\} \delta^{ij}, \\
V^{(1)ij}(\mathbf{k}, \mathbf{k}') &= \tilde{c}_1 \frac{(\mathbf{k} - \mathbf{k}')^i (\mathbf{k} - \mathbf{k}')^j - \frac{(\mathbf{k} - \mathbf{k}')^2}{3} \delta^{ij}}{(\mathbf{k} - \mathbf{k}')^2 + m_\pi^2}, \\
\tilde{c}_0 &:= C_S + C_T + \left( \frac{g_A}{2f_\pi} \right)^2, \\
\tilde{c}_1 &:= -6 \left( \frac{g_A}{2f_\pi} \right)^2, \\
\tilde{c}_2 &:= - \left( \frac{g_A m_\pi}{2f_\pi} \right)^2,
\end{aligned} \tag{3.4.2.1}$$

with LO values for the coupling constants indicated. In the following we drop the SV-channel subindexes.

The amplitude will be written as:

$$T^{ij}(\mathbf{k}, \mathbf{k}') = T^{(0)ij}(\mathbf{k}, \mathbf{k}') + T^{(1)ij}(\mathbf{k}, \mathbf{k}'), \tag{3.4.2.2}$$

where  $T^{(0)ij}(\mathbf{k}, \mathbf{k}')$  fulfills:

$$T^{(0)ij}(\mathbf{k}, \mathbf{k}') = V^{(0)ij}(\mathbf{k}, \mathbf{k}') + \int^\Lambda \frac{d^3 k''}{(2\pi)^3} V^{(0)ik}(\mathbf{k}, \mathbf{k}'') \frac{1}{E - \frac{\mathbf{k}''^2}{M} + i\eta} T^{(0)kj}(\mathbf{k}'', \mathbf{k}'). \tag{3.4.2.3}$$

The renormalized solution to this equation is given by  $T^{(0)ij}(\mathbf{k}, \mathbf{k}') = T(\mathbf{k}, \mathbf{k}') \delta^{ij}$  in section

3.3. At first order in perturbation theory  $T^{(1)ij}(\mathbf{k}, \mathbf{k}')$  verifies:

$$\begin{aligned}
T^{(1)ij}(\mathbf{k}, \mathbf{k}') &= V^{(1)ij}(\mathbf{k}, \mathbf{k}') + \int^\Lambda \frac{d^3 k''}{(2\pi)^3} V^{(1)ik}(\mathbf{k}, \mathbf{k}'') \frac{1}{E - \frac{\mathbf{k}''^2}{M} + i\eta} T^{(0)kj}(\mathbf{k}'', \mathbf{k}') + \\
&+ \int^\Lambda \frac{d^3 k''}{(2\pi)^3} V^{(0)ik}(\mathbf{k}, \mathbf{k}'') \frac{1}{E - \frac{\mathbf{k}''^2}{M} + i\eta} T^{(1)kj}(\mathbf{k}'', \mathbf{k}').
\end{aligned} \tag{3.4.2.4}$$

Using (3.3.4) and (3.3.5) we can see that the second term above is finite. We can then gather the first and second terms into a new, energy dependent, potential defined as:

$$\tilde{V}^{(1)ij}(\mathbf{k}, \mathbf{k}'') := V^{(1)ij}(\mathbf{k}, \mathbf{k}') + \int^\Lambda \frac{d^3 k''}{(2\pi)^3} V^{(1)ik}(\mathbf{k}, \mathbf{k}'') \frac{1}{E - \frac{\mathbf{k}''^2}{M} + i\eta} T^{(0)kj}(\mathbf{k}'', \mathbf{k}'). \tag{3.4.2.5}$$

Therefore, the integral equation reduces to:

$$\begin{aligned}
T^{(1)ij}(\mathbf{k}, \mathbf{k}') &= \tilde{V}^{(1)ij}(\mathbf{k}, \mathbf{k}'') + \tilde{c}_0 \mathcal{R}^{ij}(\mathbf{k}') + \int^\Lambda \frac{d^3 k''}{(2\pi)^3} \frac{\tilde{c}_2}{(\mathbf{k} - \mathbf{k}'')^2 + m_\pi^2} \frac{T^{(1)ij}(\mathbf{k}'', \mathbf{k}')}{E - \frac{\mathbf{k}''^2}{M} + i\eta}, \\
\mathcal{R}^{ij}(\mathbf{k}') &:= \int^\Lambda \frac{d^3 k''}{(2\pi)^3} \frac{T^{(1)ij}(\mathbf{k}'', \mathbf{k}')}{E - \frac{\mathbf{k}''^2}{M} + i\eta}.
\end{aligned} \tag{3.4.2.6}$$

In order to prove it finite we decompose:

$$T^{(1)ij}(\mathbf{k}, \mathbf{k}') = \tilde{c}_0 \mathcal{R}^{kj}(\mathbf{k}') T_0^{ik}(\mathbf{k}) + \tilde{T}_1^{ij}(\mathbf{k}, \mathbf{k}'), \quad (3.4.2.7)$$

with  $T_0^{ij}(\mathbf{k})$  defined in (3.4.1.2) and  $\tilde{T}_1^{ij}(\mathbf{k}, \mathbf{k}')$  given by:

$$\tilde{T}_1^{ij}(\mathbf{k}, \mathbf{k}') := \tilde{V}^{(1)ij}(\mathbf{k}, \mathbf{k}') + \int^\Lambda \frac{d^3 k''}{(2\pi)^3} \frac{\tilde{c}_2}{(\mathbf{k} - \mathbf{k}'')^2 + m_\pi^2} \frac{\tilde{T}_1^{ij}(\mathbf{k}'', \mathbf{k}')}{E - \frac{\mathbf{k}''^2}{M} + i\eta}. \quad (3.4.2.8)$$

Both  $T_0^{ij}(\mathbf{k})$  and  $\tilde{T}_1^{ij}(\mathbf{k}, \mathbf{k}')$  are well defined (the tensor structure is crucial for the latter to be so). Divergences can only arise in  $\tilde{c}_0 \mathcal{R}^{ij}(\mathbf{k}')$ , which reads:

$$\tilde{c}_0 \mathcal{R}^{ij}(\mathbf{k}') = \frac{\int^\Lambda \frac{d^3 k}{(2\pi)^3} \frac{\tilde{T}_1^{ij}(\mathbf{k}, \mathbf{k}')}{E - \frac{\mathbf{k}^2}{M} + i\eta}}{\tilde{c}_0^{-1} - \frac{1}{3} \int^\Lambda \frac{d^3 k}{(2\pi)^3} \frac{T_0^{ii}(\mathbf{k})}{E - \frac{\mathbf{k}^2}{M} + i\eta}}. \quad (3.4.2.9)$$

The numerator is well defined (for that the tensor structure is again crucial) and the divergences in the denominator have exactly the same structure as in the denominator of (3.3.7). Hence they are renormalized by the same  $c_0$  flows. We have then proved that if we treat the SSB term as a perturbation, the amplitude is renormalizable at first order in perturbation theory and no extra counterterm needs to be introduced.

### 3.5 Isovector-vector channel

If we use (3.2.6)-(3.2.7) in order to obtain  $T_{VV}(\mathbf{k}, \mathbf{k}')$ , the calculation of  $\hat{T}_{VV}(\mathbf{k}, \mathbf{k}')$  would reduce to that of the previous section. However, as mentioned in section 3.2, the UV behaviour is smoother in terms of (3.2.5), as it happens in the SS channel, although here we still need to introduce a regularization. The LS equation, dropping de isospin delta, reads:

$$T_{VV}^{ij}(\mathbf{k}, \mathbf{k}') = V_{VV}^{A,ij}(\mathbf{k}, \mathbf{k}') + \int^\Lambda \frac{d^3 k''}{(2\pi)^3} V_{VV}^{A,ik}(\mathbf{k}, \mathbf{k}'') \frac{1}{E - \frac{\mathbf{k}''^2}{M} + i\eta} T_{VV}^{kj}(\mathbf{k}'', \mathbf{k}'), \quad (3.5.1)$$

where:

$$V_{VV}^{A,ij}(\mathbf{k}, \mathbf{k}') = \frac{1}{2} \left( V_{VV}^{ij}(\mathbf{k}, \mathbf{k}') - V_{VV}^{ij}(-\mathbf{k}, \mathbf{k}') \right) = \frac{c_1}{2} \left( \frac{(\mathbf{k} - \mathbf{k}')^i (\mathbf{k} - \mathbf{k}')^j}{(\mathbf{k} - \mathbf{k}')^2 + m_\pi^2} - \frac{(\mathbf{k} + \mathbf{k}')^i (\mathbf{k} + \mathbf{k}')^j}{(\mathbf{k} + \mathbf{k}')^2 + m_\pi^2} \right) + \frac{c_2}{2} \left( \frac{\delta^{ij}}{(\mathbf{k} - \mathbf{k}')^2 + m_\pi^2} - \frac{\delta^{ij}}{(\mathbf{k} + \mathbf{k}')^2 + m_\pi^2} \right), \quad (3.5.2)$$

where those constants calculated at first in  $\chi$ PT take the values:

$$\begin{aligned} c_1 &:= 2 \left( \frac{g_A}{2f_\pi} \right)^2, \\ c_2 &:= \left( \frac{g_A m_\pi}{2f_\pi} \right)^2. \end{aligned} \quad (3.5.3)$$

We have not analyzed the possible existence of non-trivial flows which may renormalize the above equation. The fact that the SSB term must be treated perturbatively in the SV channel, indicates that also here we should proceed according to the same philosophy. The potential (3.5.2) in the zeroth order approximation reads:

$$V_{VV}^{(0),ij}(\mathbf{k}, \mathbf{k}') = \frac{c_2}{2} \left( \frac{\delta^{ij}}{(\mathbf{k} - \mathbf{k}')^2 + m_\pi^2} - \frac{\delta^{ij}}{(\mathbf{k} + \mathbf{k}')^2 + m_\pi^2} \right), \quad (3.5.4)$$

which leads to a well defined LS equation. At first order in perturbation theory we will have:

$$\begin{aligned} T_{VV}^{ij}(\mathbf{k}, \mathbf{k}') &= T_{VV}^{(0)ij}(\mathbf{k}, \mathbf{k}') + T_{VV}^{(1)ij}(\mathbf{k}, \mathbf{k}'), \\ T_{VV}^{(1)ij}(\mathbf{k}, \mathbf{k}') &= V_{VV}^{(1)ij}(\mathbf{k}, \mathbf{k}') + \int^\Lambda \frac{d^3 k''}{(2\pi)^3} V_{VV}^{(1)ik}(\mathbf{k}, \mathbf{k}'') \frac{T_{VV}^{(0)kj}(\mathbf{k}'', \mathbf{k}')}{E - \frac{\mathbf{k}''^2}{M} + i\eta} + \\ &\quad + \int^\Lambda \frac{d^3 k''}{(2\pi)^3} V_{VV}^{(0)ik}(\mathbf{k}, \mathbf{k}'') \frac{T_{VV}^{(1)kj}(\mathbf{k}'', \mathbf{k}')}{E - \frac{\mathbf{k}''^2}{M} + i\eta}, \end{aligned} \quad (3.5.5)$$

which is also well defined. We expect the divergences arising at higher order to be absorbed by local counterterms.

### 3.6 Discussion

We have addressed the renormalization of the LS equation for the LO potentials (in the  $\chi$ PT counting) of the NN system in all channels. In addition, for each channel we have been able to carry out our analysis for all partial waves (including partial wave mixing) at once. The isoscalar scalar channel does not require regularization. For the isovector scalar channel we recover the flows of ref. [63]. The remaining two channels have deserved a more detailed study.

The first non-trivial result is that the renormalization of the isoscalar vector channel requires a strong flow of the coupling constant of a non-local potential, the SSB one, or, in other words, if only the coupling constants of the local potentials are allowed to flow, the isoscalar vector channel is not renormalizable. Several comments are in order.

First of all, the flow (3.4.1.5) of the coupling constant of the SSB term is not such a big surprise. Notice that at high momentum this term tends to a (direction dependent) constant, which is the same behaviour (except for the direction dependence) as the  $\delta$ -function term both in the singlet and the triplet channel, the coupling constants of which also show similar flows. The main difference is that the leading behaviour for  $c_0$  is fixed and the subleading contains the free parameter ( $c_0^r(\mu)$ ). For  $c_1$  instead, the leading behaviour contains the free parameter ( $\bar{c}_1$ ) and the subleading behaviour is not observable.

The flow (3.4.1.5), however, has undesirable consequences: the renormalized T-matrix conserves orbital angular momentum, even if the bare interaction does not (see Appendix G)<sup>5</sup>. Since the results of [62] indicate that it is precisely the OPE the main responsible for the mixing of higher partial waves, we would like it to keep doing this job for us. We are then forced to exclude the SSB term from the (low energy) LO potential, and to treat it as a perturbation. This also appears to be reasonable from the phenomenological point of view since the observed mixings are small[62].

We have developed this line in sections 4.2 and 5. We have proved that at first order the vector channels remain renormalizable (at zeroth order the problem reduces to the one in the singlet channels, which are renormalizable). The picture which emerges is half way between [64], where the pions are treated perturbatively, and [61, 74] where the whole potential is treated non-perturbatively. The (low energy) LO potential is the part of the LO potential in the  $\chi$ PT counting which conserves orbital angular momentum. We are tempted to propose the following counting. The  $\mathcal{O}(Q^n)$  ( $n = 0, 1, \dots$ ) contribution to the NN potential in the  $\chi$ PT counting must be divided into two pieces: the one which conserves orbital angular momentum (SS) and the one which does not (SSB). The SSB terms keep their  $\chi$ PT counting but the SS ones are enhanced and must be counted as  $\mathcal{O}(Q^{n-1})$ . Only the LO potential  $\mathcal{O}(Q^{-1})$  must be treated (and renormalized) non-perturbatively. We have seen here that this proposal is theoretically consistent at next to leading order, and, in addition, it does not require any coupling constant of a non-local potential to flow anymore. It remains to be seen if it is still so beyond that order and, of course, whether it is phenomenologically successful.

Let us finally comment on recent work on the subject [67, 68]. The authors in both references try to renormalize the triplet channel by adjusting the coupling constant of the  $\delta$ -potential only. Hence,

---

<sup>5</sup>We have also checked perturbatively in  $\bar{c}_1$  and  $c_2$  up to order  $\bar{c}_1 c_2$  that the effective range depends on  $\bar{c}_1$  only through the scattering length. Since the latter can be adjusted by tuning  $c_0^r(\mu)$ , up to this order both the scattering length and the effective range are blind to  $\bar{c}_1$ . We have not looked at what happens to the rest of the amplitude or to higher orders but we suspect that they are also insensitive to  $\bar{c}_1$ .



according to our results both works should show a remnant cutoff dependence when the cutoff is large enough. Note also that it is only in the large cutoff limit when a meaningful comparison is possible, since the regularizations used in the three works are different.

The authors of ref. [67], who use a subtracted ( $\mu$ -dependent) LS equation, argue that a reasonable boundary condition is that for large  $\mu$  the T-matrix coincides with the potential, and check numerically whether, once the scattering lengths are fixed, the remaining observables are independent of  $\mu$  for large  $\mu$ . They find that for laboratory energies up to 100 MeV. the  ${}^3S_1$  and  ${}^3D_1$  phase shifts are remarkably independent of  $\mu$  for  $\mu \geq 0.8$  GeV. but the mixing angle shows a strong  $\mu$ -dependence for  $6 \text{ GeV} \geq \mu \geq 0.8 \text{ GeV}$ . and only for  $\mu \geq 6 \text{ GeV}$ . the  $\mu$ -dependence smooths and the results may appear to converge. We interpret this stronger  $\mu$ -dependence of the mixing angle as an indication of the remnant cutoff dependence mentioned above.

The authors of ref. [68] obtain the flows by analyzing the short distance behaviour of the Schrödinger equation (see also [73]). For the  ${}^1S_0$  channel they are in qualitative agreement with ours. For the triplet one they present analytic flow equations which are argued to coincide with those of the chiral limit. The flow of the  $\delta$ -function term is given implicitly by their equation (18). They assume that their  $\alpha_\pi$ , which is proportional to our  $c_1$ , does not flow<sup>6</sup> and find a multibranch structure for the flow of their  $V_0 R^3$ , which is proportional to our  $c_0$  ( $R \rightarrow 0$ ,  $R$  playing the role of an inverse cutoff). It is interesting to note that if they allowed  $\alpha_\pi$  flow like our  $c_1$  in section 4.1, namely  $\alpha_\pi \sim R$ , and  $V_0 R^3$  like our  $c_0$ , namely  $V_0 \sim 1/R^2$ , their eq. (18) becomes cutoff independent. Hence our flow (4.1.5) is a solution in the  $R \rightarrow 0$  limit to the flow equation (18) of ref. [68]. Recall, however that, if  $\alpha_\pi$  is not allowed to flow, the strict limit  $R \rightarrow 0$  cannot be taken. More precisely, it is not difficult to prove that there is no continuous solution to this equation for  $R \rightarrow 0$  (see Appendix H). Hence eq. (18) of [68] does not produce any acceptable flow for  $V_0$  and, therefore, it cannot be used to properly renormalize<sup>7</sup> the triplet channel.

Furthermore, we would like to remark that leaving the cutoff finite and checking that the finite cutoff effects are higher order in the EFT expansion is a procedure which unavoidably will lead to problems in this case. If we wish to improve the accuracy of our EFT calculation, we will have to

<sup>6</sup>Whereas the combination  $\alpha_\pi m_\pi^2$  that appears in the singlet channel is equivalent to our  $c_2$  and, accordingly, remains fixed.

<sup>7</sup>We use here the standard meaning of *renormalization* in quantum field theory, namely that the cutoff can be taken arbitrarily large (like, for instance, in refs. [63, 64, 67, 69]).

calculate at higher orders. Even if we insist in keeping  $R$  finite, we will have to choose it smaller and smaller for the LO terms not to jeopardize the accuracy of the higher order calculation. Then, at some point,  $R$  will hit the region where no continuous solution exists and we will lose all predictive power (if we give up continuity, an infinite number of inequivalent solutions exists).

## Chapter 4

# New predictions for inclusive heavy-quarkonium P-wave decays

### 4.1 Motivation

Inclusive P-wave decays to light hadrons have proved to be an optimal testing ground of our understanding of heavy quarkonia. The underlying assumption was that in such systems, the annihilation of the heavy quark and antiquark is a short distance process. Set by the scale of the heavy quark mass  $M$ , it provides with some Wilson coefficients which, because of the asymptotic freedom of QCD, can be computed in perturbation theory. Whereas, the bound state dynamics is factorized and accurately described by means of a lower energy EFT, originally NRQCD[76, 77]. This is a non-relativistic field theory for the heavy quark and antiquark that is coupled to the usual relativistic field theory for light quarks and gluons. The theory is made equivalent to full QCD through the addition of local interactions that incorporate relativistic corrections to any order in the heavy-quark velocity  $v \ll 1$ . The Lagrangian for NRQCD is:

$$\mathcal{L} = \mathcal{L}_{light} + \mathcal{L}_{heavy} + \delta\mathcal{L},$$

$$\mathcal{L}_{light} = -\frac{1}{2}\text{Tr} G_{\mu\nu}G^{\mu\nu} + \sum \bar{q} i \not{D} q + \mathcal{O}\left(\frac{1}{M^2}\right), \quad (4.1.1)$$

$$\mathcal{L}_{heavy} = \psi^\dagger \left( iD_t + \frac{\mathbf{D}^2}{2M} \right) \psi + \chi^\dagger \left( iD_t - \frac{\mathbf{D}^2}{2M} \right) \chi, \quad (4.1.2)$$

$\mathbf{n}^{2\mathbf{S}+1}\mathbf{L}_J$	$\mathbf{J}^{\mathbf{PC}}$	$\mathbf{c}\bar{\mathbf{c}}$	$\mathbf{b}\bar{\mathbf{b}}$
$1^1S_0$	$0^{-+}$	$\eta_c$	$\eta_b$
$1^3S_1$	$1^{--}$	$J/\psi$	$\Upsilon$
$2^3S_1$	$1^{--}$	$\psi(2S)$	$\Upsilon(2S)$
$1^1P_1$	$1^{+-}$	$h_c$	$h_b$
$1^3P_0$	$0^{++}$	$\chi_{c0}$	$\chi_{b0}$
$1^3P_1$	$1^{++}$	$\chi_{c1}$	$\chi_{b1}$
$1^3P_2$	$2^{++}$	$\chi_{c2}$	$\chi_{b2}$

**Table IX:** Classification of charmonium and bottomonium states.

$$\begin{aligned}
\delta\mathcal{L}_{bilinear} = & \frac{c_1}{8M^3} \left( \psi^\dagger (\mathbf{D}^2)^2 \psi - \chi^\dagger (\mathbf{D}^2)^2 \chi \right) + \\
& + \frac{c_2}{8M^2} \left( \psi^\dagger (\mathbf{D} \cdot g\mathbf{E} - g\mathbf{E} \cdot \mathbf{D}) \psi + \chi^\dagger (\mathbf{D} \cdot g\mathbf{E} - g\mathbf{E} \cdot \mathbf{D}) \chi \right) + \\
& + \frac{c_3}{8M^2} \left( \psi^\dagger (i\mathbf{D} \times g\mathbf{E} - g\mathbf{E} \times \mathbf{D}) \cdot \sigma_1 \psi + \chi^\dagger (i\mathbf{D} \times g\mathbf{E} - g\mathbf{E} \times \mathbf{D}) \cdot \sigma_2 \chi \right) + \\
& + \frac{c_4}{2M} \left( \psi^\dagger (g\mathbf{B} \cdot \sigma_1) \psi - \chi^\dagger (g\mathbf{B} \cdot \sigma_2) \chi \right) + \mathcal{O} \left( \frac{1}{M^3} \right), \tag{4.1.3}
\end{aligned}$$

where the gauge covariant derivative is  $D^\mu = \partial^\mu + igA^\mu$ ,  $\psi$  is the Pauli spinor field that annihilates a heavy quark,  $\chi$  is the field that creates a heavy antiquark and  $\mathbf{E}$  and  $\mathbf{B}$  are the electric and magnetic components of the gluon field strength tensor  $G^{\mu\nu}$ . The coefficients  $c_i$  in (4.1.1) are determined, to any given precision in  $v$ , the relative velocity of the heavy quark, and  $\alpha_s(M)$ , by matching low-energy scattering amplitudes to their corresponding counterparts in full QCD, so that physical observables are the same.

Therefore, in NRQCD, non perturbative effects acquired the form of expectation values of some 4-heavy-quark operators at a quantum-field level, and were taken care of in a systematic way. The main advantage offered by the EFT over QCD in this context is that in the former, beyond the usual expansion in  $\alpha_s(M)$ , it is easier to separate contributions of different order in  $v$ .

Power-counting rules, based on the equations of motion, and symmetries – e.g. total angular momentum  $J$ , parity  $P$  and charge conjugation  $C$  are exactly conserved quantum numbers in NRQCD,

while there is an approximate heavy-quark spin symmetry—, allowed for a recognition of those terms that contributed to a given process. Take a heavy meson  $|H\rangle$ , whose dominant component is a pure quark-antiquark state  $|Q\bar{Q}\rangle$ . There, the Fock state which contains a dynamical gluon,  $|Q\bar{Q}g\rangle$ , is suppressed by a power of  $v^2$ . Its angular momentum state can be denoted by the spectroscopic notation  $^{2S+1}L_J$ , which means it has parity  $P = (-1)^{L+1}$  and, if it is in a colour-singlet state, charge-conjugation number  $C = (-1)^{L+S}$ . Conservation of  $J^{PC}$  means that mixing is allowed only between the angular-momentum states  $^3(J-1)_J$  and  $^3(J+1)_J$ . However, such mixing is suppressed because operators that change orbital angular momentum must contain at least one power of  $v^2$ .

As was stated by the authors of [76], in contrast to the S-wave states, Fock states containing dynamical gluons may play an important role in P-wave annihilation decays. The argument went like this: the  $1^{+-}$  state  $|h_c\rangle$  consists predominantly of the Fock state  $|Q\bar{Q}\rangle$ , with the  $Q\bar{Q}$  pair in a colour-singlet  $^1P_1$  state but it has a probability of order  $v^2$  for the Fock state  $|Q\bar{Q}g\rangle$ , with the  $Q\bar{Q}$  pair in a colour-octet  $^1S_0$  or  $^1D_2$  state. As the Fock state  $|Q\bar{Q}\rangle$  is created and annihilated by the dimension-8 operator  $\mathcal{O}_1(^1P_1) = \psi^\dagger\left(-\frac{i}{2}\mathbf{D}\right)\chi \cdot \chi^\dagger\left(-\frac{i}{2}\mathbf{D}\right)\chi$ , the Fock state  $|Q\bar{Q}g\rangle$ , with the  $Q\bar{Q}$  in a colour-octet  $^1S_0$  state, also contributes to the decay at the same order in  $v$  through the operator  $\mathcal{O}_8(^1S_0) = \psi^\dagger T^a \chi \chi^\dagger T^a \psi$ . The resulting expression for the decay rates were said to be of the form:

$$\begin{aligned} \Gamma(h_c \rightarrow LH) &= 2\frac{\text{Im}f_1(^1P_1)}{M^4}\langle h_c|\mathcal{O}_1(^1P_1)|h_c\rangle + 2\frac{\text{Im}f_8(^1S_0)}{M^2}\langle h_c|\mathcal{O}_8(^1S_0)|h_c\rangle + \mathcal{O}(v^2\Gamma), \\ \Gamma(\chi_{cJ} \rightarrow LH) &= 2\frac{\text{Im}f_1(^3P_J)}{M^4}\langle \chi_{cJ}|\mathcal{O}_1(^3P_J)|\chi_{cJ}\rangle + 2\frac{\text{Im}f_8(^3S_1)}{M^2}\langle \chi_{cJ}|\mathcal{O}_8(^3S_1)|\chi_{cJ}\rangle + \mathcal{O}(v^2\Gamma) \end{aligned} \quad (4.1.4)$$

Furthermore, singlet matrix elements could be easily understood in terms of the non-relativistic Coulomb-gauge radial wavefunctions. Defined as:

$$R_{\eta_c}(r)\frac{1}{\sqrt{4\pi}} \equiv \frac{1}{\sqrt{2N_c}}\langle 0|\chi^\dagger\left(-\frac{\mathbf{r}}{2}\right)\psi\left(+\frac{\mathbf{r}}{2}\right)|\eta_c\rangle_{Coulomb}, \quad (4.1.5)$$

and so on, use could be made of relations such as:

$$\begin{aligned} \langle \eta_c|\mathcal{O}_1(^1S_0)|\eta_c\rangle &= \frac{N_c}{2\pi}|\bar{R}_{\eta_c}|^2\left(1 + \mathcal{O}(v^2)\right), \\ \langle \psi|\mathcal{O}_1(^3S_1)|\psi\rangle &= \frac{N_c}{2\pi}|\bar{R}_\psi|^2\left(1 + \mathcal{O}(v^2)\right), \\ \langle \eta_c|\mathcal{P}_1(^1S_0)|\eta_c\rangle &= -\frac{N_c}{2\pi}\text{Re}(\bar{R}_S^*\bar{\nabla}^2 R_S)\left(1 + \mathcal{O}(v^2)\right), \\ \langle \psi|\mathcal{P}_1(^3S_1)|\psi\rangle &= -\frac{N_c}{2\pi}\text{Re}(\bar{R}_S^*\bar{\nabla}^2 R_S)\left(1 + \mathcal{O}(v^2)\right), \end{aligned}$$

$$\begin{aligned}
\langle h_c | \mathcal{O}_1(^1P_1) | h_c \rangle &= \frac{3N_c}{2\pi} |\overline{R}_P'|^2 (1 + \mathcal{O}(v^2)), \\
\langle \chi_{cJ} | \mathcal{O}_1(^3P_J) | \chi_{cJ} \rangle &= \frac{3N_c}{2\pi} |\overline{R}_P'|^2 (1 + \mathcal{O}(v^2)),
\end{aligned} \tag{4.1.6}$$

which require from the use of the vacuum-saturation approximation and where some wave functions have been replaced by their weighted average  $\overline{R}_S$ , without any loss of accuracy.

Nevertheless, besides the so-called colour-singlet operators, for which their expectation values could be related to wave functions in an intuitive way, there were also colour-octet operators. The latter were decisive in solving the infrared sensitivity of earlier calculations[78]<sup>1</sup>. It was thought that these colour-octet expectation values could not be related with a Schrödinger-like formulation in any way. In the following it will be shown that it is not so. For certain states, those in which a potential description applies, the expectation values of colour-octet operators can also be written in terms of wave functions and additional bound-state-independent non-perturbative parameters. We shall focus on the operators relevant to P-wave decays into light hadrons, but it should become apparent that this is a general feature[79].

The line of developments that led us to this result is the following. It was pointed out in ref.[75] that NRQCD still contains dynamical scales, which are not relevant to the kinematical situation of the lower-lying states in heavy quarkonium, whose energy scale is ultrasoft ( $\sim Mv^2$ ). Hence, further simplifications occur if we integrate them out. We call pNRQCD the resulting effective field theory[40, 41]. When the typical scale of non-perturbative physics, say  $\Lambda_{\text{QCD}}$ , is smaller than the soft scale  $mv$ , and larger than the ultrasoft scale  $mv^2$ , the soft scale can be integrated out perturbatively. This leads to an intermediate EFT that contains, besides the singlet, also octet fields and ultrasoft gluons as dynamical degrees of freedom [45, 75]. These are eventually integrated out by the (non-perturbative) matching to pNRQCD [45]. When  $\Lambda_{\text{QCD}}$  is of the order of the soft scale, the (non-perturbative) matching to pNRQCD has to be done in one single step. This framework has been developed in a systematic way in refs. [40, 41].

---

<sup>1</sup>That is, the infrared logs encountered in those coefficients accompanying the colour-singlet terms, are cancelled by the ultraviolet behaviour of colour-octet operators.

## 4.2 Computation

Then, we will compute the inclusive P-wave decay widths into light hadrons at leading order for  $\Lambda_{\text{QCD}} \gg mv^2$  by using pNRQCD. In this situation the singlet is the only dynamical field in pNRQCD (Goldstone bosons are also present, but they play a negligible role in the present analysis and will be ignored), if hybrids and other degrees of freedom associated with heavy–light meson pair threshold production develop a mass gap of  $\mathcal{O}(\Lambda_{\text{QCD}})$ , as we will assume in what follows[45, 40], or if they play a minor role in the heavy-quarkonium dynamics. Therefore, the pNRQCD Lagrangian reads[45, 40]:

$$\mathcal{L}_{\text{pNRQCD}} = \text{Tr} \left\{ \mathbf{S}^\dagger (i\partial_0 - h) \mathbf{S} \right\}, \quad (4.2.1)$$

where  $h$  is the pNRQCD Hamiltonian, to be determined by matching the EFT to NRQCD. The total decay width of the singlet heavy-quarkonium state is then given by:

$$\Gamma = -2 \text{Im} \langle n, L, S, J | h | n, L, S, J \rangle, \quad (4.2.2)$$

where  $|n, L, S, J\rangle$  are the eigenstates of the Hamiltonian  $h$ . The imaginary parts are inherited from the 4-heavy-fermion NRQCD Wilson coefficients and, for P-wave decays, first appear as local (delta-like)  $\mathcal{O}(1/m^4)$  potentials in the pNRQCD Lagrangian. The relevant structure reads (we shall concentrate on potentials, which inherit imaginary parts from the NRQCD operators and which contribute to P-wave states at first order in quantum-mechanical perturbation theory (QMPT)):

$$-2 \text{Im} h \Big|_{\text{P-wave}} = F_{SJ} \mathcal{T}_{SJ}^{ij} \frac{\nabla_{\mathbf{r}}^i \delta^{(3)}(\mathbf{r}) \nabla_{\mathbf{r}}^j}{m^4}, \quad (4.2.3)$$

where  $\mathcal{T}_{SJ}^{ij}$  corresponds to the spin and total angular momentum wave-function projector. What is now left is to compute  $F_{SJ}$ , i.e. to perform the matching between NRQCD and pNRQCD. The situation A): when  $mv \gg \Lambda_{\text{QCD}} \gg mv^2$ , will be displayed in full detail in the following pages, in addition to being easily reproduced by taking the results of [45]. For the more general situation B): when  $mv \gtrsim \Lambda_{\text{QCD}}$ , one should use the formalism of refs. [40]. In both situations we get:

$$F_{SJ} = -2N_c \text{Im} f_1(2S+1\text{P}_J) - \frac{4T_F}{9N_c} \mathcal{E} \text{Im} f_8(2S+1\text{S}_S), \quad (4.2.4)$$

where  $f_1(2S+1\text{L}_J)$  and  $f_8(2S+1\text{L}_J)$  are the short distance Wilson coefficients of NRQCD as defined in ref. [77] and

$$\mathcal{E} = T_F \int_0^\infty d\tau \tau^3 \langle g\mathbf{E}^a(\tau, \mathbf{0}) \Phi_{ab}(\tau, 0; \mathbf{0}) g\mathbf{E}^b(\tau, \mathbf{0}) \rangle. \quad (4.2.5)$$

**A) P-wave potentials for  $mv \gg \Lambda_{\text{QCD}} \gg mv^2$ .**

In this case the matching from NRQCD to pNRQCD at the scale  $\Lambda_{\text{QCD}}$  can be done in two steps. In the first step, which can be done perturbatively, we integrate out the scale  $mv$  and end up with an EFT, which contains singlet (S) and octet (O) fields as dynamical degrees of freedom. At the next-to-leading order in the multipole expansion the Lagrangian reads[45, 75]:

$$\begin{aligned} \mathcal{L} = & \text{Tr} \left\{ S^\dagger (i\partial_0 - h_s) S + O^\dagger (iD_0 - h_o) O \right\} + \\ & + \text{Tr} \left\{ O^\dagger \mathbf{r} \cdot g\mathbf{E} S + \text{h.c.} + \frac{O^\dagger \mathbf{r} \cdot g\mathbf{E} O}{2} + \frac{O^\dagger O \mathbf{r} \cdot g\mathbf{E}}{2} \right\} - \\ & - \frac{1}{4} F_{\mu\nu}^a F^{\mu\nu a}, \end{aligned} \quad (4.2.6)$$

where  $h_s$  and  $h_o$  have to be determined by matching to NRQCD. They read as follows:

$$\begin{aligned} h_s = & -\frac{\nabla_{\mathbf{r}}^2}{m} + V_s(r) + \dots + N_c f_1(2S+1P_J) \mathcal{T}_{SJ}^{ij} \frac{\nabla_{\mathbf{r}}^i \delta^{(3)}(\mathbf{r}) \nabla_{\mathbf{r}}^j}{m^4} + \dots, \\ h_o = & -\frac{\nabla_{\mathbf{r}}^2}{m} + V_o(r) + \dots + T_F f_8(2S+1S_S) \mathcal{T}_S \frac{\delta^{(3)}(\mathbf{r})}{m^2} + \dots, \end{aligned} \quad (4.2.7)$$

neglecting centre-of-mass recoil terms.  $\mathcal{T}_S$  corresponds to the total spin projector:

$$\begin{aligned} \mathcal{T}_0 &= \mathbf{1} \otimes \mathbf{1}, \\ \mathcal{T}_1 &= \sigma^i \otimes \sigma^i, \\ \mathcal{T}_{01}^{ij} &= \delta^{ij} \mathbf{1} \otimes \mathbf{1}, \\ \mathcal{T}_{10}^{ij} &= \frac{1}{3} \sigma^i \otimes \sigma^j, \\ \mathcal{T}_{11}^{ij} &= \frac{1}{2} \varepsilon^{ikl} \varepsilon^{jml} \sigma_k \otimes \sigma_m, \\ \mathcal{T}_{12}^{ij} &= \left( \frac{\delta_k^i \sigma_l + \delta_l^j \sigma_k}{2} - \frac{\sigma^i \delta_{lk}}{3} \right) \otimes \left( \frac{\delta^{jk} \sigma^l + \delta^{jl} \sigma^k}{2} - \frac{\sigma^j \delta^{lk}}{3} \right), \end{aligned} \quad (4.2.8)$$

and the corresponding Feynman rules for the propagators and vertices defined by the Lagrangian (4.2.6) are shown in fig. 1.

Beyond  $\mathcal{O}(1/m)^0$  we have only displayed the terms that are relevant to our calculation. In the second step we integrate out (non-perturbatively) the gluons and the octet field as shown in fig. 2, ending up with the pNRQCD Lagrangian (4.2.1). The Hamiltonian  $h$  has to be determined by matching the two




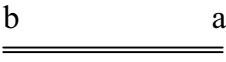
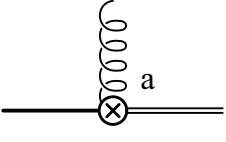
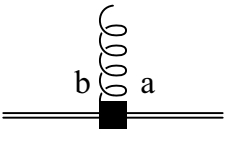
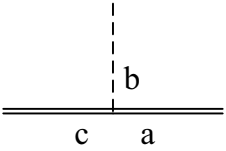
	$= \theta(T) e^{-ih_s T}$	singlet propagator
	$= \theta(T) \left( e^{-ih_o T} e^{-ig \int_{-T/2}^{T/2} dt A_0^{\text{adj}}} \right)_{ab}$	octet propagator
	$= ig \sqrt{\frac{T_F}{N_c}} \mathbf{r} \cdot \mathbf{E}^a$	singlet–octet vertex
	$= \frac{ig}{2} d^{abc} \mathbf{r} \cdot \mathbf{E}^c$	octet–octet vertex
	$= gf^{abc}$	Coulomb octet–octet vertex

Figure 1: Propagators and vertices of the pNRQCD Lagrangian (4.2.6). In perturbative calculations the octet propagator is understood without the gluonic string, using instead the Coulomb octet–octet vertex. Also the singlet–octet and the octet–octet vertices produce three diagrams each in perturbative calculations with the Coulomb gauge: one with a longitudinal gluon line, one with a transverse gluon line, and one with both a longitudinal and a transverse gluon line.

effective field theories. It reads  $h = h_s + \delta h_s$ , with (at leading non-vanishing order in the multipole expansion):

$$\delta h_s = -i \frac{T_F}{N_c} \int_0^\infty d\tau e^{ih_s \frac{\tau}{2}} \left\langle \mathbf{r} \cdot g \mathbf{E}^a(\tau, \mathbf{0}) e^{-ih_o \tau} \Phi_{ab}(\tau, 0; \mathbf{0}) g \mathbf{E}^b(0, \mathbf{0}) \cdot \mathbf{r} \right\rangle e^{ih_s \frac{\tau}{2}}, \quad (4.2.9)$$

where consistency with  $\Lambda_{\text{QCD}} \gg mv^2$  requires an expansion of the exponentials of  $h_o$  and  $h_s$ . Care must be taken at this point, as the above expression still contains wave function renormalization corrections. To get rid of them in a systematic way, one only needs to substitute  $h_s$  by  $E$  (the on-shell energy of the external legs) and regroup together  $h_o$  and  $E$  in a unique  $e^{-i(h_o - E)\tau}$  term. Next we write  $h_o$  as  $-\frac{\nabla_{\mathbf{r}}^2}{m} + V_o(r)$ . Any  $V_o(r)$  insertion renders a genuine correction, whereas the  $E + \frac{\nabla_{\mathbf{r}}^2}{m}$  ones con-

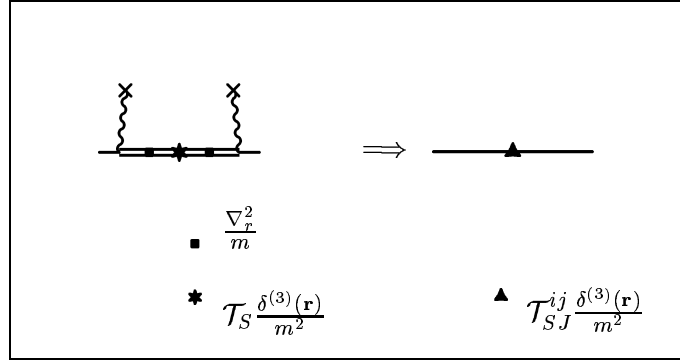


Figure 2: Non-perturbative integration of the octet degrees of freedom.

tribute through their commutator with the external vertices, and leave an extra  $V_s(r)$  coming from the exchanged term. It can easily be seen that the latter do not generate any contribution to the imaginary ( $\delta^{(3)}(\mathbf{r})$ -like)  $\delta h_s$  of P-wave states at leading order.

Taking into account that we are interested in P-wave states, only the perturbation that puts one  $V_o$  S-wave potential in the middle of two  $\left[-\frac{\nabla_{\mathbf{r}}^2}{m}, \mathbf{r}\right]$  terms survives at leading order. The final result reads:

$$\text{Im } \delta h_s \Big|_{\text{P-wave}} = \frac{2T_F}{9N_c} \mathcal{E} \frac{\nabla_{\mathbf{r}} \delta^{(3)}(\mathbf{r}) \nabla_{\mathbf{r}}}{m^4} \mathcal{T}_S \text{Im} f_8^{(2S+1)S_S}, \quad (4.2.10)$$

which plugged into eq. (4.2.3) gives eq. (4.2.4). This shows how a colour-octet operator in NRQCD becomes a colour-octet potential in the EFT of eq. (4.2.6) and, eventually, contributes to a colour-singlet potential in pNRQCD, which is one of our main points.

### B) P-wave potentials for $mv \gtrsim \Lambda_{\text{QCD}}$ .

In the case  $mv \gtrsim \Lambda_{\text{QCD}}$  the matching from NRQCD to pNRQCD at the scale  $\Lambda_{\text{QCD}}$  has to be done directly, since no other relevant scales are supposed to lie between  $m$  and  $mv$ . The only dynamical degree of freedom of pNRQCD is the heavy-quarkonium singlet field  $S$ . The Lagrangian has been written in (4.2.1). The Hamiltonian  $h$  is obtained by matching (non-perturbatively) to NRQCD, order by order in  $1/m$ , within a Hamiltonian formalism [40]. We will only sketch the main steps of the derivation. In short, we can formally expand the NRQCD Hamiltonian in  $1/m$ :

$$H_{\text{NRQCD}} = H_{\text{NRQCD}}^{(0)} + \frac{1}{m} H_{\text{NRQCD}}^{(1)} + \dots \quad (4.2.11)$$

The eigenstates of the heavy-quark-antiquark sector can be labelled as:

$$|\underline{g}; \mathbf{x}_1, \mathbf{x}_2\rangle = |\underline{g}; \mathbf{x}_1, \mathbf{x}_2\rangle^{(0)} + \frac{1}{m} |\underline{g}; \mathbf{x}_1, \mathbf{x}_2\rangle^{(1)} + \dots,$$

where  $\underline{g}$  labels the colour-related degrees of freedom (spin labels are not explicitly displayed for simplicity). Assuming a mass gap of  $\mathcal{O}(\Lambda_{\text{QCD}})$  much larger than  $mv^2$ , all the excitations ( $\underline{g} \neq \underline{0}$ ) decouple and the ground state ( $\underline{g} = \underline{0}$ ) corresponds to the singlet state. Therefore, the matching condition reads:

$$\langle \underline{0}; \mathbf{x}_1, \mathbf{x}_2 | H | \underline{0}; \mathbf{x}'_1, \mathbf{x}'_2 \rangle = h(\mathbf{x}_1, \mathbf{x}_2, \nabla_{\mathbf{x}_1}, \nabla_{\mathbf{x}_2}) \delta^{(3)}(\mathbf{x}_1 - \mathbf{x}'_1) \delta^{(3)}(\mathbf{x}_2 - \mathbf{x}'_2). \quad (4.2.12)$$

Up to  $\mathcal{O}(1/m^4)$  the imaginary contributions are only carried by the Wilson coefficients of the dimension 6 and 8 four-heavy-fermion operators in NRQCD. Since we are only interested in eq. (4.2.3) a huge simplification occurs and only two contributions survive. From the dimension 8 operators we obtain:

$$\begin{aligned} \text{Im } \delta h \delta^{(3)}(\mathbf{x}_1 - \mathbf{x}'_1) \delta^{(3)}(\mathbf{x}_2 - \mathbf{x}'_2) &= \frac{1}{m^4} \text{Im} \langle \underline{0}; \mathbf{x}_1, \mathbf{x}_2 | H_{\text{NRQCD}}^{(4)} | \underline{0}; \mathbf{x}'_1, \mathbf{x}'_2 \rangle^{(0)} \Big|_{\text{P-wave}} = (4.2.13) \\ &= N_c \mathcal{T}_{SJ}^{ij} \text{Im } f_1(2S+1P_J) \frac{\nabla_{\mathbf{r}}^i \delta^{(3)}(\mathbf{r}) \nabla_{\mathbf{r}}^j}{m^4} \delta^{(3)}(\mathbf{x}_1 - \mathbf{x}'_1) \delta^{(3)}(\mathbf{x}_2 - \mathbf{x}'_2). \end{aligned}$$

On the other hand, we also have contributions from the iteration of lower-order  $1/m$  corrections to the NRQCD Hamiltonian with the dimension 6 four-heavy-fermion operators. The only term that contributes to eq. (4.2.3) is:

$$\text{Im } \delta h \delta^{(3)}(\mathbf{x}_1 - \mathbf{x}'_1) \delta^{(3)}(\mathbf{x}_2 - \mathbf{x}'_2) = \frac{1}{m^4} \text{Im} \langle \underline{0}; \mathbf{x}_1, \mathbf{x}_2 | H_{\text{NRQCD}}^{(2)} | \underline{0}; \mathbf{x}'_1, \mathbf{x}'_2 \rangle^{(1)} \Big|_{\text{P-wave}}. \quad (4.2.14)$$

The explicit computation of the right-hand side of eq. (4.2.14) gives (as far as the P-wave contribution is concerned) eq. (4.2.7). Therefore, the sum of the contributions from eqs. (4.2.13) and (4.2.14) coincides with eq. (4.2.3), after the replacements (4.2.4) and (4.2.5).

We can now obtain the decay widths by using eq. (4.2.3). At first order in QMPT, we obtain:

$$\Gamma(\chi_{QJ}^S(nP) \rightarrow \text{LH}) = \left[ \frac{3N_c}{\pi} \text{Im } f_1(2S+1P_J) + \frac{2T_F}{3\pi N_c} \text{Im } f_8(2S+1S_S) \mathcal{E} \right] \frac{|R'_{Qn1}(0)|^2}{m^4}, \quad (4.2.15)$$

where:  $\chi_{QJ}^1(nP) := \chi_{QJ}(nP)$ ,  $\chi_{QJ}^0(nP) := h_Q(nP)$  ( $Q = b, c$ ),  $n$  is the principal quantum number, and  $R_{Qn1}(r)$  the radial wave function at leading order. Comparing with the standard NRQCD formula, where spin symmetry has already been used, we have:

$$\langle h_Q(nP) | \mathcal{O}_8(^1S_0) | h_Q(nP) \rangle(\mu) = \frac{|R'_{Qn1}(0)|^2}{3\pi N_c m^2} T_F \mathcal{E}(\mu). \quad (4.2.16)$$

The information gained with this formula is that all non-perturbative flavour and principal quantum number dependence is encoded in the wave function, as in the colour-singlet operators. The additional non-perturbative parameter  $\mathcal{E}(\mu)$  is universal: it only depends on the light degrees of freedom of QCD. This implies that the following relation between decay widths is also universal:

$$\mathcal{E}(\mu) = -\frac{9N_c^2 \operatorname{Im} f_1(2^{S+1}P_J) \cdot \Gamma(\chi_{QJ}^{S'}(nP) \rightarrow \text{LH}) - \operatorname{Im} f_1(2^{S'+1}P_{J'}) \cdot \Gamma(\chi_{QJ}^S(nP) \rightarrow \text{LH})}{2T_F \operatorname{Im} f_8(2^{S+1}S_S) \cdot \Gamma(\chi_{QJ}^{S'}(nP) \rightarrow \text{LH}) - \operatorname{Im} f_8(2^{S'+1}S_{S'}) \cdot \Gamma(\chi_{QJ}^S(nP) \rightarrow \text{LH})}. \quad (4.2.17)$$

It is interesting to notice that the UV behaviour of  $\mathcal{E}$  has the logarithmic divergence:

$$\mathcal{E}(\mu) \simeq 12 N_c C_F \frac{\alpha_s}{\pi} \ln \mu, \quad (4.2.18)$$

which matches exactly the IR log of the  $\mathcal{O}(\alpha_s)$  correction of  $\operatorname{Im} f_1(2^{S+1}P_J)$ , and hence the cancellation originally observed in [76] is fulfilled. Then one could consider the LL RG improvement of  $\mathcal{E}$  by using the results of ref. [77] for the running of the octet-matrix element. One obtains ( $\beta_0 = 11 \frac{C_A}{3} - 4n_f \frac{T_F}{3}$ ):

$$\mathcal{E}(\mu) = \mathcal{E}(\mu') + \frac{24N_c C_F}{\beta_0} \ln \frac{\alpha_s(\mu')}{\alpha_s(\mu)}. \quad (4.2.19)$$

### 4.3 Applications

Let us apply the above results to actual quarkonium, under the assumption that our framework, discussed in the paragraph before eq. (4.2.1), provides a reasonable description for the P-wave states observed in nature. The numerical extraction of  $\mathcal{E}$  is a delicate task, since several of the Wilson coefficients (see Ref. [80] for a full list of them) have large next-to-leading order contributions, which may spoil the convergence of the perturbative series. This problem is not specific of our formalism, but belongs to the standard formulation of NRQCD. Here, in order to give an estimate, it is only used those data that provide more stable results in going from the leading to the next-to-leading order, more precisely the average of eq. (4.2.17) for  $(J, S) = (1, 1)$ ,  $(J', S') = (0, 1)$ , and  $(J, S) = (1, 1)$ ,  $(J', S') = (2, 1)$ . The experimental data have been taken from [81] and updated accordingly to [82, 83]. The final value reads:

$$\mathcal{E}(1 \text{ GeV}) = 5.3_{-2.2}^{+3.5}(\text{exp}), \quad (4.3.1)$$

where we have used the NLO results for the Wilson coefficients with a LL improvement. The errors only refer to the experimental uncertainties on the decay widths. Theoretical uncertainties mainly come

from subleading operators in the power counting ( $\mathcal{O}(v)$  suppressed) and subleading terms in the perturbative expansion of the Wilson coefficients ( $\mathcal{O}(\alpha_s)$  suppressed), whose bad convergence may affect considerably the figure of eq. (4.3.1). We feel, therefore, that further studies, maybe along the lines of refs. [84], are needed before a complete numerical analysis, including theoretical uncertainties, can be done. In any case, the above figure is compatible with the values that are usually assigned to the NRQCD octet and singlet matrix elements (e.g. from the fit of [85] one gets  $\mathcal{E}(1 \text{ GeV}) = 3.6_{-2.9}^{+3.6}(\text{exp})$ ). The above figure is also compatible with the charmonium (quenched) lattice data of [86], whereas, if the running (4.2.19) is taken into account, bottomonium lattice data, quenched [86] and unquenched [87], appear to give a lower value. Note that, in the language of refs. [86, 87], eq. (4.2.16) reads  $\mathcal{E}(\mu) = 81 m_{b,c}^2 \mathcal{H}_8(\mu)/\mathcal{H}_1|_{b,c}$ , which implies  $\mathcal{H}_8(\mu)/\mathcal{H}_1|_b \times \mathcal{H}_1/\mathcal{H}_8(\mu)|_c = m_c^2/m_b^2$ . For all quarkonium states that satisfy our assumptions this equality must be fulfilled by lattice results for any number of light fermions and for any value of the heavy-quark masses.

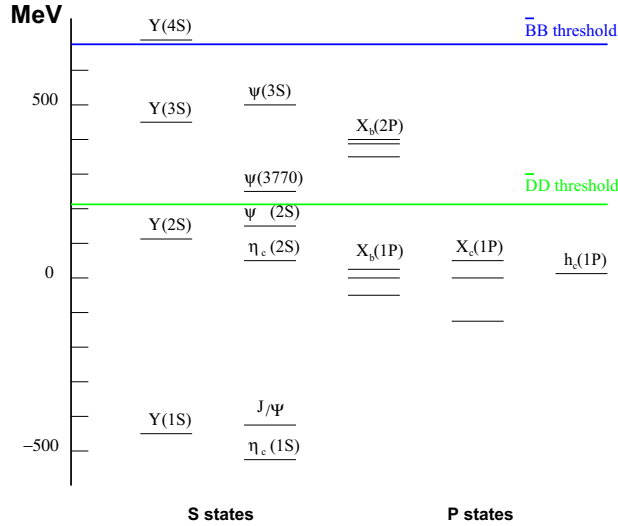


Figure 3: The experimental heavy meson spectrum ( $b\bar{b}$  and  $c\bar{c}$ ) relative to the spin-average of the  $\chi_b(1P)$  and  $\chi_c(1P)$  states.

By using the estimate (4.3.1), we can also predict the branching ratios for the  $n = 1, 2$  P-wave bottomonium states. It is obtained:

$$\frac{\Gamma(\chi_{b1}^1(1P))}{\Gamma(\chi_{b2}^1(1P))} = \frac{\Gamma(\chi_{b1}^1(2P))}{\Gamma(\chi_{b2}^1(2P))} = 0.50_{-0.04}^{+0.06}, \quad (4.3.2)$$

where only the errors inherited from eq. (4.3.1) have been included. For what concerns theoretical

uncertainties, the comments after eq. (4.3.1) apply also here (with a better behaviour of the perturbative series). Note that the first equality holds independently from eq. (4.3.1) and from the use of charmonium data and, hence, provides a more robust prediction. The remaining branching ratios can be obtained using spin symmetry. Notice also that, although no model-independent predictions can be made for the decay widths (they depend on the wave function at the origin, which is flavour and state dependent), our results allow any model that gives a definite value to  $R'_{Qn1}(0)$  to make definite predictions.

In conclusion, we have exploited the fact that NRQCD still contains irrelevant degrees of freedom for certain heavy quarkonium states, which can be integrated out in order to constrain the form of the matrix elements of colour-octet operators. We have focused on the operators relevant to P-wave decays, which allowed us to produce concrete, new, rigorous results. However, it should be clear from the structure of the pNRQCD Lagrangian itself, that similar results can be obtained for matrix elements of any colour-octet operator.

# Conclusion

In the previous pages we have offered a brief account on some facets of non-relativistic effective field theories, as seen through present concern calculations. From the accurate computation of ponium's lifetime, a low energy observable sensitive to a high energy QCD parameter such as the quark condensate, to P-wave quarkonia hadronic decays, going through the display of analytic expressions for the corrections induced by light fermion finite mass effects, or the problem of renormalizing the nucleon-nucleon interaction, every chapter constitutes a well-defined problem whose solution goes, inextricably, tied up to a NREFT of its own. So, while in the first chapter, we were compelled to derive a low energy version of the Chiral Lagrangian( $\chi\mathcal{L}$ ), well-suited to tackle with ponium, the second chapter introduced the non-relativistic offsprings of QED and QCD and, in the third one, pions were integrated from the two nucleon sector of the  $\chi\mathcal{L}$ .

All results extracted can be quickly summarized in the following lines:

- Concerning ponium's lifetime calculation, we performed a step-by-step construction of the different Lagrangians that appear all the way down from the  $\chi\mathcal{L}$  to our  $pNR\chi\mathcal{L}$ , that is the right theory to address the problem at hand. We kept track of all the terms that are needed in order to achieve the expected accuracy aimed by the DIRAC's experiment (10%) and our final formula (1.7.3) is exhibited in the most convenient form. That is, all corrections coming from the quantum mechanical calculation are shown explicitly, whereas the ones that enter through the matching with Chiral Perturbation Theory ( $\chi PT$ ) are resummed in the  $\Delta_{\chi PT}$  term. That provides a very general (and pedagogical) framework where the power and simplicity of non-relativistic techniques is best grasped. It is worth emphasizing that only such a computation is capable of delivering a result where systematicity allows for a straightforward implementation and accuracy

is always under control.

- In the chapter devoted to light fermion finite mass effects the results (2.2.1) and (2.3.1) constitute analytical expressions that apply to a large range of different systems among which we find hadronic atoms (see Tables II and III), as well as quarkonia (see Table IV). Given their importance, those corrections are of current interest, as we learn from the section on **Related works**.
- The third chapter, which starts with a fairly large historical introduction to the subject of renormalization in the context of nucleon-nucleon interaction, offers a rigorous approach to the problem from a purely theoretical point of view. That allows us to draw very definite conclusions on the nature of the solution, besides signalling those lines that should be pursued in order to define a consistent effective field theory out of such a nuclear issue. So, what we get is that the traditional OPEP (One Pion Exchange Potential) in the  ${}^3S_1$ - ${}^3D_1$  channel, which is iterated through a Lippmann-Schwinger equation, cannot be renormalized unless we allow the constant accompanying a non local potential (the tensor term) to flow. What is worst, in this case the amplitude lacks from partial wave mixing. So, we expect that this tensor interaction should be treated perturbatively. We show that, up to first order in perturbation theory, that defines a renormalizable potential and get the flows that prove this (see eqs. (3.4.1.5), (3.4.1.10), (3.4.2.9) and (3.3.11)).
- The last part of the work concerns the inclusive hadronic decay of P-wave quarkonia. After realising that NRQCD is still a too general theory for actual states, we integrate the potential one in both the perturbative ( $mv^2 \ll \Lambda_{QCD} \ll mv$ ) and non perturbative ( $\Lambda_{QCD} \lesssim mv$ ) situations. What we get, expressions (4.2.3) and (4.2.4), is that the former colour-octet matrix elements in NRQCD, can be rewritten in terms of the derivative of the singlet P-wave wavefunction at the origin and additional universal constants (4.2.5). The latter also absorb infrared divergences encountered in the singlet coefficients. In all, we are able to produce new relations (4.2.17) and give some predictions (4.3.1) that relate the branching ratios of hadronic decays of systems with different heavy flavour and different principal quantum number.



# Resumen

## Sistemas no relativistas

En esta tesis hemos tratado fundamentalmente de transmitir parte del espíritu que anima a las teorías efectivas no relativistas (NREFTs). Mediante una serie de cálculos recientes y variados, basados en su filosofía, se ha demostrado que existe un gran campo de aplicabilidad de su potencial entre aquellos sistemas ligados cuya velocidad relativa  $v$  constituye un adecuado parámetro de expansión. A través de los diferentes capítulos, que tratan a la vez de enfatizar los aspectos teóricos más destacables en el desarrollo del cálculo, distintos átomos hadrónicos regidos por la jerarquía  $M \gg Mv \gg Mv^2$  han merecido nuestra atención.

De hecho en la naturaleza existen varios sistemas de partículas ligados para los que se verifica esta condición. Ejemplos típicos en el dominio de las interacciones electromagnéticas son el positronium ( $e^+e^-$ ) y el muonium ( $e^-\mu^+$ ). Sus análogos en el mundo de las interacciones fuertes son los estados de *heavy quarkonia* ( $t\bar{t}$ ,  $b\bar{b}$ ,  $b\bar{c}$ ,  $c\bar{c}$ ). Entre unos y otros encontramos a sistemas tales como los átomos hidrogenoides y el pionium ( $\pi^+\pi^-$ ). En su tratamiento se dan problemas técnicos comunes a cualquier cálculo de un estado ligado no relativista, aun y cuando nos hallemos en una situación puramente perturbativa. Complicaciones adicionales surgen en el contexto de una teoría fuertemente acoplada, como es el caso de QCD.

Tradicionalmente se habían empleado ecuaciones de Bethe-Salpeter (relativistas) en la resolución del espectro de estados ligados. No obstante, este procedimiento, que resulta en todo adecuado para el cálculo de amplitudes de *scattering*, no es eficaz a la hora de hallar energías de ligadura. La razón estriba en el hecho de que las funciones de onda iniciales y finales son, en este último caso, las

interactuantes y, por lo tanto, no resulta trivial la selección del conjunto de diagramas que intervienen a un orden determinado en la constante de acoplamiento. Esto es, la contribución de cada diagrama no se deriva directamente del número de vértices de éste. Por ejemplo, es bien sabido que en el positronium es preciso resumir la infinita serie de fotones potenciales, ya que todos ellos intervienen al mismo orden en  $\alpha$ .

El problema es, en su raíz, que se está obviando la naturaleza inherentemente no relativista del problema, y la consiguiente existencia de tres escalas físicas vinculadas:  $M$ , la masa de las partículas;  $p \sim Mv$ , que es el momento relativo del estado; y  $E \sim Mv^2$  o energía de ligadura. Todas ellas aparecen enlazadas en cualquier diagrama de Feynman.

Otras maneras de atacar el problema de estos estados ligados, reducciones no relativistas esencialmente, carecen de sistematicidad y de un mecanismo de control sobre las correcciones relativistas. Problemas emergentes como la incorporación de los efectos no potenciales, la cancelación de las divergencias ultravioletas en el cálculo mecánico-cuántico o la carencia de criterios para incluir los distintos términos, ya sea perturbativa o no perturbativamente, se vieron solventados tras la aparición de las NREFTs.

Éstas establecieron un puente de conexión entre la teoría de campos y la mecánica cuántica. Como toda teoría efectiva, su punto de partida es la construcción, a partir de una teoría más general (física de altas energías), de una serie de técnicas que permitan abordar cálculos referidos a una escala más restringida (experimentos a baja energía). El nexo común a todas ellas es, pues, el hacer del momento relativo del estado ligado, una de estas escalas de baja energía cuya dinámica se pretende describir, e integrar la información procedente de aquellos modos que no podemos excitar,  $\sim M$ , en unos pocos coeficientes ordenados en potencias crecientes de  $\frac{1}{M}$ .

Los ingredientes básicos para construir una EFT son:

- Las **simetrías** que debe obedecer la teoría de bajas energías. Nos permitirán construir un Lagrangiano cuyos operadores se hallarán acordemente organizados en base al análisis dimensional específico de nuestro problema. Como la **precisión** con que se desea describir la física de bajas energías es conocida de antemano, la expansión de Lagrangiano en la/s escala/s de alta energía se truncará siempre al orden que nos interese.
- Este mismo **análisis dimensional** nos permite prefiar si un determinado operador es irrelevante,

relevante o marginal para nuestra física.

- El **matching** permite relacionar los parámetros de ambas teorías. Éste consiste en imponer que diferentes funciones de Green off shell sean equivalentes a aquéllas calculadas en la teoría de altas energías. Procedimientos análogos son la integración de los grados de libertad irrelevantes o las transformaciones de Foldy-Wouthysen para la eliminación de antipartículas.
- Un procedimiento de **regularización** de las divergencias que surgen al calcular las correcciones cuánticas, así como un esquema de **renormalización**.

El hecho de que nos reframamos en el primer punto al análisis particular de nuestro sistema ligado, viene dado por el hecho que, atendiendo a los valores de las masas y al número de fermiones pesados de que éste conste, nos hallaremos en distintas situaciones y, por lo tanto, precisaremos de diferentes NREFTs. Esto es:

- **Un partícula pesada y otras ligeras (relativistas).** La masa de la partícula pesada ( $M$ ) es mucho mayor que las escalas típicas de las ligeras, y su inverso constituye el parámetro de expansión de la teoría efectiva. Como éstas últimas son relativistas, obedecen una relación de dispersión lineal ( $|\mathbf{p}| \sim E$ ). En definitiva, se verifica:

$$M \gg |\mathbf{p}| \sim E. \quad (.1)$$

En el caso de QCD, estas dos últimas escalas son, además  $\sim \Lambda_{QCD}$ . La teoría efectiva diseñada a su propósito es HQET (*heavy quark effective theory*). En ella, la integración de la escala  $M$ , puede ser realizada perturbativamente en  $\alpha_s(M)$ . A bajas energías rige una simetría aproximada de *spin-flavour* que le presta poder predictivo. Por todo ello, los cálculos aparecen organizados en una doble expansión en  $\alpha_s(M)$  y  $\frac{\Lambda_{QCD}}{M}$ . Para evaluar el tamaño de un término dado del Lagrangiano se asigna, pues, la escala  $\Lambda_{QCD}$  a cada potencia con dimensiones de energía.

- **Dos partículas pesadas.** En este caso tenemos:

$$M_a, M_b \gg |\mathbf{p}| \gg E. \quad (.2)$$

La escala  $\sim M_a, M_b$  se denomina *hard*, la escala  $|\mathbf{p}|$  recibe el nombre de *soft* y  $E$  constituye la escala *ultrasoft*. Dentro de este apartado se puede distinguir entre:

- $M_a \gg M_b$ . Es el caso de los átomos hidrogenoides o del sistema  $B_c$ , aunque en este último caso de manera ya no tan clara. La partícula más pesada se toma como estática (negligiéndose su término cinético) y la otra como no relativista.
- $M_a \sim M_b$ . En esta situación se encuentran el positronium, muonium,  $Q\bar{Q}$ , entre otros. Ambas partículas deben ser consideradas como no relativistas.

Respecto a QCD, la primera NREFT creada fue NRQCD (*non-relativistic QCD*). Factorizaba la escala  $M$  sin preocuparse por la jerarquía adicional  $Mv \gg Mv^2$ . Con la presencia adicional de  $\Lambda_{QCD}$ , tres escalas permanecían indeterminadas, con lo consiguiente falta de un conteo unívoco más allá de primer orden. Su problema radica, por lo tanto, en que no resulta explícito en modo alguno la dominancia del régimen potencial de la interacción (esto es, del potencial Coulombiano estático en la situación perturbativa). pNRQCD (*potential NRQCD*) es la teoría que se ocupa de ello. Proviene de integrar en NRQCD los grados de libertad *soft*. Ello fija dos *cutoff* ultravioleta:  $\Lambda_1$  y  $\Lambda_2$ . El primero satisface  $Mv^2 \ll \Lambda_1 \ll Mv$  y es el *cutoff* de la energía de los quarks y de la energía y momento de los gluones. El segundo verifica  $Mv \ll \Lambda_2 \ll M$  y es el *cutoff* del momento relativo del sistema ligado.

Mientras que el *matching* entre QCD y NRQCD es perturbativo en  $\alpha_s(M)$ , el *matching* entre NRQCD y pNRQCD puede ( $Mv \gg \Lambda_{QCD}$ ) o no ( $Mv \sim \Lambda_{QCD}$ ) serlo, en función del sistema que nos ocupe. En cualquier caso, la integración de la escala  $Mv$  produce, como coeficientes de *matching* en pNRQCD, términos potenciales. En general éstos dependerán de la escala de *matching*. Esta funcionalidad es cancelada en el espectro por la contribución de los gluones *ultrasoft*.

## Aspectos tratados

Empezamos por el pionium, sistema formado por  $\pi^+$  y  $\pi^-$ , ligado electromagnéticamente y que decae por interacción fuerte, para dedicar al cálculo de su vida media el primer capítulo. Éste nos sirvió como perfecto ejemplo de cómo la integración de diferentes escalas de momento/energía no dinámicas, mediante la técnica de *matching*, nos conduce de una teoría efectiva de baja energía a otra subyacente y simplificada, en la que la información de más altas energías relevante para acometer el

problema que nos ocupa queda condensada en unos pocos parámetros. En este ejemplo en concreto se requería que estas constantes fueran calculadas explícitamente, estableciendo la equivalencia entre amplitudes de *scattering* calculadas en una teoría a energías intermedias, tal como *Chiral Perturbation Theory* ( $\chi$ PT) y nuestra teoría efectiva no relativista cuyo único grado de libertad era el estado ligado. Pero sólo porque únicamente así podíamos aislar uno de estos coeficientes, el llamado condensado de quarks, responsable de la rotura de la simetría quiral de QCD, y cuyo valor, pobremente determinado, nos interesaba. No obstante, tal como se desarrolló el cálculo, esta necesidad queda relegada a las últimas secciones, con lo que se pretende dar relevancia al hecho de que cuánto se está haciendo es reflejo de un procedimiento totalmente general y que, por lo que respecta a la vida media del estado, bien se podría dejar estos coeficientes como parámetros a determinar, ya sea por simulación, ya experimentalmente. Otros puntos sobre los que se debatió fueron el papel fundamental de las simetrías obedecidas por la teoría de bajas energías a la hora de construir el correspondiente Lagrangiano, la invariancia Lorentz, la posibilidad de reparametrizar los campos, cómo la observancia del *power counting* selecciona únicamente los términos que serán precisos posteriormente en vistas a ofrecer resultados consistentes, de error acotado y prefijado, ...

Por lo que atañe a la parte más técnica, hemos desarrollado un método que permite obtener el propagador Coulombiano  $G_c(\mathbf{0}, \mathbf{0}; E)$  en Regularización Dimensional (DR). Dado que los coeficientes de nuestra última teoría de bajas energías se derivan de  $\chi$ PT, dónde los cálculos son realizados en DR, es imprescindible que todas las expresiones sean ofrecidas en este esquema, para mayor eficacia.

El segundo capítulo constituyó también un ejemplo de cálculo estándar dentro de una teoría efectiva no relativista. Hablamos de los efectos de masa finita de los grados de libertad ligeros, a través de la corrección por polarización del vacío, sobre la energía de ligadura y la función de onda en el origen de estados débilmente ligados. Las correspondientes NREFTs aportan los conceptos precisos para entender porqué éstos no pueden ser negligidos (importancia relativa de las escalas integradas), nos fijan cómo deben tratarse escalas de similar magnitud que desean ser integradas, y flexibilizan que un mismo cálculo sea susceptible de aplicación a multitud de sistemas, cuya dinámica es, o puede ser, en gran medida diferente. Así pues, nuestras Tablas II, III y IV se refieren, respectivamente, a átomos hadrónicos y *heavy quarkonia*. Todas estas correcciones han sido halladas aplicando las expresiones analíticas (2.2.1) y (2.3.1), que ofrecemos por vez primera en la literatura.

Se ha querido cerrar el capítulo con una breve exposición acerca de dos trabajos ajenos relativos a los efectos de la masa del *charm* en la determinación de la masa del quark *bottom*, así como en el espectro de bottomonium. Ello ha de servir para contextualizar nuestro propio trabajo, al mismo tiempo que permite referir, aunque sea de forma muy parcial, algunas cuestiones interesantes acerca de las ambigüedades que causan los renormalones en la masa *pole* del *bottom*, cómo se circunvala este problema adoptando en los observables otros parámetros de expansión menos sensibles al infrarrojo, y cómo ello da cuenta, en gran medida, de los efectos no perturbativos en el espectro de estados ligados de bottomonium.

El tercer capítulo lo ocupa el acercamiento a uno de los problemas recientes en el mundo de las NREFTs que han exigido mayor esfuerzo y que, no obstante, han redundado en una de las menos gratificantes recompensas. Nos referimos al desafío que representa el campo de las interacciones nucleares para los teóricos del área. En concreto, la comprensión y formulación clara de cómo se debería organizar un cálculo sistemático para tratar la interacción nucleón-nucleón parece escapárenos todavía. Se combinan en este caso la dificultad inherente a su naturaleza no perturbativa, con la exigua separación entre las distintas escalas implicadas a integrar (masas del nucleón y de los mesones vectoriales, *splittings* de resonancias nucleares, masa del pión, *scattering lengths* en los canales  $^1S_0$  y  $^3S_1$ - $^3D_1$ , ...), y con la arbitrariedad con que, tradicionalmente, se han renormalizado las divergencias surgidas al iterar la interacción *leading* mediante la inabordable ecuación de Lippmann-Schwinger. En nuestro caso, hemos decidido atacar el problema desde una vertiente puramente teórica y preguntarnos bajo qué circunstancias es renormalizable, en su sentido estricto, el tradicional OPEP (One Pion Exchange Potential). Entre nuestros resultados, para el canal del deuterón, se implica que, o bien la constante asociada a un potencial no local depende de la escala de normalización y el *mixing* entre ondas *S* y *D* desaparece, o bien este término tensorial debe tratarse como una perturbación. En este último caso demostramos también renormalizabilidad a primer orden en teoría de perturbaciones. Todos estos resultados quedan resumidos en las fórmulas (3.4.1.5), (3.4.1.10), (3.4.2.9) y (3.3.11).

Paralelamente, y como presentación a este trabajo, el capítulo viene precedido de un breve *tour* histórico por los trabajos originales que resultan, desde mi punto de vista, más interesantes o novedosos. Empezando por la teoría efectiva (puramente local) de más bajas energías, en que el pión ha sido integrado[59]; para seguir con el trabajo de Lepage[60], que formula una propuesta de renormalización para atacar los problemas de materia nuclear en términos más prácticos; y continuar con la teoría con piones vista

a través de distintos *power countings*[63, 64], donde queda perfectamente ilustrada la inextricabilidad entre el problema de conteo y la renormalizabilidad; acabamos esbozando algunos acercamientos alternativos más recientes[67, 68] de los cuales pormenorizamos las dificultades existentes en la Discusión del capítulo y en el Apéndice H.

Finalmente, el último capítulo ha sido dedicado a analizar los decaimientos hadrónicos de los estados en onda P de quarkonium. Se ha visto que, siempre que se puede integrar en NRQCD la escala soft  $Mv$ , se alcanza una nueva teoría, que contiene únicamente grados de libertad *ultrasoft* y que es más restrictiva. Ello, a la vez que da lugar a nuevas relaciones entre procesos en que decaen sistemas con diferente *flavour*, nos permite escribir aquellos pretéritos elementos de matriz de NRQCD que eran octetes de color, en términos de derivadas de la función de onda en el origen del estado singlete observable, y de constantes universales adicionales que son susceptibles de ser calculadas en el *lattice*. Los cálculos han sido realizados tanto en la situación perturbativa, esto es  $mv^2 \ll \Lambda_{QCD} \ll mv$ , como en la no perturbativa,  $\Lambda_{QCD} \lesssim mv$ . Las nuevas relaciones y predicciones se resumen en las expresiones (4.2.17) y (4.3.1).

# Appendix A

## The DIRAC experiment

DIRAC (Dimeson Relativistic Atom Complex) experiment[88], aimed to determine the difference of scattering lengths  $|a_0^0 - a_0^2|$  with 5% accuracy by measuring the lifetime of ponium[88], will provide us, as discussed in Chapter 1, with evidence in favour or against the existence of a large quark-antiquark condensate in QCD's vacuum. Last available experimental data[89] for the isospin zero scattering length,  $a_0^0 = .26 \pm .05$ , is certainly poorly determined for such a purpose.

### A.1 Experimental method

To form atomic  $\pi^+\pi^-$  bound states, pions must have a small relative momentum in the center of mass (CM) rest frame ( $\approx 1$  MeV.) and must be found closer than the Bohr radius (387 fm.). Such pions originate from short-living sources, such as the  $\rho$  and  $\omega$  mesons or the  $\Delta$  baryon resonances, and not from the long-living ones ( $\nu$  and  $K_s^0$ ). So, ponium production is proportional to the double inclusive cross section  $\frac{d\sigma_s^0}{d\mathbf{p}_1 d\mathbf{p}_2}$  of  $\pi^+$  and  $\pi^-$  pairs from short-living sources without Coulomb interaction in the final state, and to the squared atomic wave function of  $nS$ -states at the origin  $|\Psi_n(\mathbf{0})|^2$ :

$$\frac{d\sigma_n^A}{d\mathbf{p}_A} = (2\pi)^3 \frac{E_A}{M_A} |\Psi_n(\mathbf{0})|^2 \frac{d\sigma_s^0}{d\mathbf{p}_1 d\mathbf{p}_2} \Big|_{\mathbf{p}_1 = \mathbf{p}_2 = \frac{\mathbf{p}_A}{2}}, \quad (\text{A.1.1})$$

where  $\mathbf{p}_A$ ,  $E_A$  and  $M_A$  are momentum, energy and mass of the ponium atom in the laboratory system.

After being produced by hadronic interaction, relativistic ponium atoms ( $2 \text{ GeV.} < p_A < 6 \text{ GeV.}$ ) move in the target. Then, they decay or, due to the electromagnetic interaction with the target material, get excited or ionized. The break-up process is easy to track, as it creates characteristic



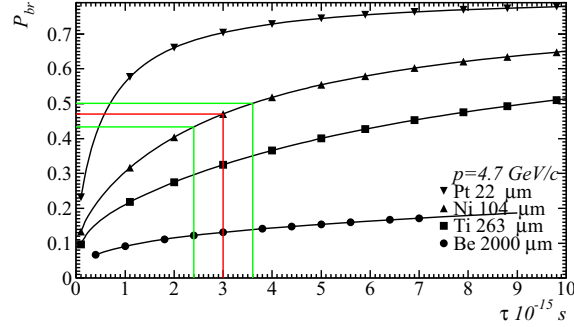


Figure 1: Probability of pionium break-up in the target.

$\pi^+\pi^-$  atomic pairs with small CM relative momentum ( $< 3$  MeV.), small opening angle ( $\theta_{\pm} \approx .35$  mrad. for  $p_A=4.7$  GeV.) and nearly identical energies in the laboratory system ( $E_+ = E_-$  at .3 % level). Using atomic interaction cross sections, for a given material and thickness, one can calculate the break-up probability for arbitrary values of pionium momentum and lifetime. In fig. 1 we show those dependencies for the pionium momentum  $p=4.7$  GeV.

Comparison of the measured break-up probability  $P_{br} = \frac{n_A}{N_A}$  (ratio of broken-ups  $n_A$  over  $N_A$  produced pionium atoms) with the calculated dependence of  $P_{br}$  on  $\tau$  gives the value of the lifetime.

The measurement of broken-up  $n_A$  pionium atoms is performed through the analysis of the experimental distribution in relative momenta ( $Q$ ) of  $\pi^+\pi^-$  pairs. The free pion pair distribution can be written as the sum of the non-Coulomb (nC) and the Coulomb (C) pair distributions:

$$\frac{dN^{free}}{dQ} = \frac{dN^{nC}}{dQ} + \frac{dN^C}{dQ},$$

$$\frac{dN^{nC}}{dQ} \sim \frac{dN_{acc}^{exp}}{dQ} \equiv \Sigma(Q) \quad ; \quad \frac{dN^C}{dQ} \sim \Sigma(Q) A_c(Q) (1 + aQ), \quad (A.1.2)$$

where  $A_c(Q)$  is the Coulomb and  $(1 + aQ)$  the strong correlation factors. Here it is assumed that the non-Coulomb distribution of  $\pi^+\pi^-$  pairs can be extracted from the experimental distribution of accidental pairs  $\Sigma(Q)$ . Then the free pion pair distribution is given by:

$$\frac{dN^{free}}{dQ} = \frac{dN^{nC}}{dQ} + \frac{dN^C}{dQ} = N_0 \Sigma(Q) [f + A_c(Q)(1 + aQ)], \quad (A.1.3)$$

where  $N_0$ ,  $f$  and  $a$  are free parameters. In the region  $Q > 3$  MeV. there are mainly free pairs. After fitting this part of the distribution with the function (A.1.3), the extrapolation of the function to the

region  $Q < 2$  MeV. yields the number of free pairs in this region. Hence:

$$n_A = \int_{Q < 2} \left( \frac{dN^{exp}}{dQ} - \frac{dN^{free}}{dQ} \right) dQ. \quad (A.1.4)$$

## A.2 Experimental setup

The experimental setup has been designed to detect pion pairs and to select atomic pairs at low relative momentum with a resolution better than 1 MeV. it was installed and commissioned in 1998 at the ZT8 beam area of the PS East Hall at CERN. After a calibration run in 1998, DIRAC has been collecting data since summer 1999.

The 24 GeV. proton beam extracted from PS is focused on the target. The secondary particle channel, with an aperture of 1.2 msr., has the reaction plane tilted upwards at  $5.7^\circ$  relative to the horizontal plane. It consists of the following components: 4 planes of Micro Strip Gas Chambers (MSGC) with  $4 \times 512$  channels; 2 planes Scintillation Fiber Detector (SciFi) with  $2 \times 240$  channels; 2 planes Ionization Hodoscope (IH) with  $2 \times 16$  channels; and 1 Spectrometer Magnet of 2.3 Tm. bending power. Downstream to the magnet the setup splits into two arms placed at  $\pm 19^\circ$ , relative to the central axis. Each arm is equipped with a set of identical detectors: 4 Drift Chambers (DC), the first one common to both arms, with 6 planes and 800 channels, while the other DC's have altogether 8 planes per arm and 608 channels; 1 Vertical scintillation Hodoscope (VH) plane with 18 channels; 1 Horizontal scintillation Hodoscope (HH) plane with 16 channels; 1 Cherenkov detector (Ch) with 10 channels; 1 Preshower scintillation detector (PSh) plane with 8 channels; and 1 Muon counter (Mu) plane with (28+8) channels.

For suppressing the large background rate, a multilevel trigger was designed to select atomic pion pairs. The trigger levels are defined as follows:  $T_0 = (VH \cdot PSh)_1 \cdot (VH \cdot PSh)_2 \cdot IH$ , fast zero level trigger;  $T_1 = (VH \cdot HH \cdot \bar{Ch} \cdot PSh)_1 \cdot (VH \cdot HH \cdot \bar{Ch} \cdot PSh)_2$ , first level trigger from the downstream detectors;  $T_2 = T_0 \cdot (IH \cdot SciFi)$ , second level trigger from the upstream detectors, which selects particle pairs with small relative distance; and  $T_3$  is a logical trigger which applies a cut to the relative momentum of particle pairs. It handles the patterns of VH and IH detectors.  $T_3$  did not trigger so far the DAQ system, but its decisions were recorded.

An incoming flux of  $\sim 10^{11}$  protons/s. would produce a rate of secondaries of about  $3 \times 10^6$  /s. in the upstream detectors and  $1.5 \times 10^6$  /s. in the downstream detectors. At the trigger level this rate is

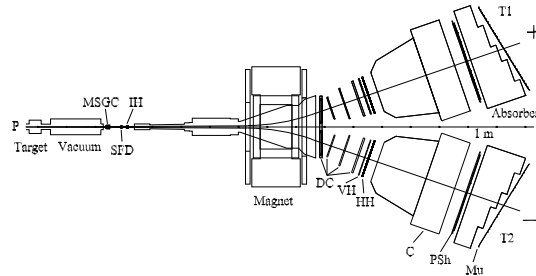


Figure 2: Experimental setup

reduced to about  $2 \times 10^3/s.$ , with an average event size of about .75 Kbytes.

With the  $95 \mu\text{m.}$  thin Ni target, the expected average ponium yield, within the setup acceptance, is  $\sim .7 \times 10^{-3}/s.$ , equivalent to a total number of  $\sim 10^{13}$  protons on target in order to produce one ponium atom.

### A.3 First experimental results

The data taking has been done mainly with  $\pi^+\pi^-$  and  $p\pi^-$  pairs and also  $e^+e^-$  pairs for detector calibration. For the first data analysis only the most simple events were selected and processed, that is, those with a single track in each arm and signals in DC, VH and HH. The tracks in the DC's were extrapolated to the target plane crossing point of the proton beam. A cut was applied along X and Y distances between the extrapolated track and the hit fiber of the SciFi planes (18 mm. divided by the particle momentum in GeV., to take into account the multiple scattering effect). Finally, these events were interpreted as  $\pi^+\pi^-$  or  $p\pi^-$  pairs produced in the target.

The difference in the time-of-flight  $\Delta t$  between the positive particle (left arm) and negative particle (right arm) of the pair at the level of VH is presented in fig. 3.

The first interval  $-20 < \Delta t < -.5 \text{ ns.}$  corresponds to accidental hadron pairs (mainly  $\pi^+\pi^-$ ). In the second interval  $-.5 < \Delta t < .5 \text{ ns.}$  one observes the peak of coincidence hits associated to correlated hadron pairs over the background of accidental pairs. The width of the correlated pair peak yields the time resolution of the VH ( $\sigma_t \approx 250 \text{ ps.}$ ). The asymmetry on the right side of the peak is due to the

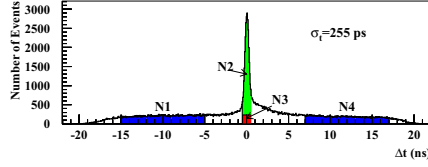


Figure 3: VH time-of-flight difference distribution for pair events

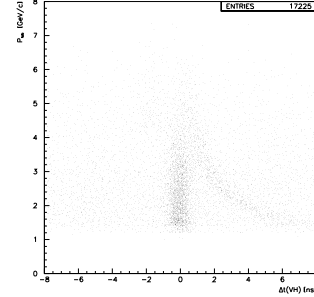


Figure 4: Positive particle momentum versus VH time-of-flight difference for particle pairs

admixture of protons in the  $\pi^+$  sample, that is,  $p\pi^-$  events. Hence the third interval  $.5 < \Delta t < 20$  ns. contains both accidental pairs and  $p\pi^-$  events.

This time-of-flight discrimination between  $\pi^+\pi^-$  and  $p\pi^-$  events is effective for momenta of positive particles below 4.5 GeV. This is demonstrated in fig. 4, where the scatter plot of positive particle momentum versus difference in time-of-flight  $\Delta t$  in VH is shown. The single particle momentum interval accepted by the spectrometer is  $1.3 \div 7$  GeV.

For correlated  $\pi^+\pi^-$  pairs, Coulomb interaction in the final state has to be considered, because it increases noticeably the yield of  $\pi^+\pi^-$  pairs with low relative momentum in CM ( $Q < 5$  MeV.). For accidental pairs this enhancement is absent.

Fig. 5 shows the distribution of the longitudinal components  $Q_L$  (the projection of  $Q$  along the total momentum of the pair) for correlated pairs. There are plotted pair events with positive particle momentum  $p_{lab} < 4.5$  GeV., occurring within the correlated  $\Delta t$  peak and with transversal component  $Q_T < 4$  MeV. to increase the fraction of low relative momentum pairs.

In the region  $|Q_L| \leq 10$  MeV. there is a noticeable enhancement of correlated  $\pi^+\pi^-$  pairs due to Coulomb attraction in the final state.

The most important parameter for data analysis is the resolution in  $Q_L$  and  $Q_T$ . This has been measured by the reconstruction of the invariant mass of  $p\pi^-$  pairs. The distribution of  $p\pi^-$  invariant mass is presented in fig. 6. Positive particles are restricted to momenta larger than 3 GeV., and the time-

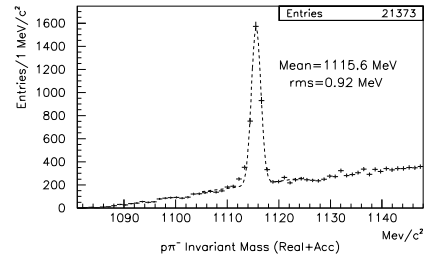
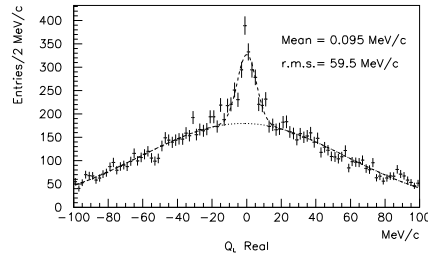


Figure 5: Correlated  $\pi^+\pi^-$  pairs with positive particle momenta  $p_{lab} < 4.5 \text{ GeV}/c$  and  $Q_T < 4 \text{ MeV}/c$ . Figure 6:  $p\pi^-$  invariant mass for proton momenta  $p_{lab} > 3 \text{ GeV}$ .

of-flight must lie in  $.5 < \Delta t < 18 \text{ ns}$ . A clear peak at the  $\Lambda$  mass  $m_\Lambda = 1115.6 \text{ MeV}$ .<sup>2</sup> with a standard deviation  $\sigma = 0.92 \text{ MeV}$ .<sup>2</sup> can be seen. These mass parameter values show a good detector calibration and coordinate detector alignment, with an accuracy in momentum reconstruction better than 0.5 % in the kinematic range of  $\Lambda$  decay products. This gives for the relative momentum resolution  $\sigma_Q \sim 2.7 \text{ MeV}$ . For  $\pi^+\pi^-$  pairs a better resolution can be obtained, due to the different kinematics.

The following table displays the breakup probability results so obtained until now:

Run	Status	$n^A$	$N^C$	$\frac{n^A}{N^C}$	$P_{br} \text{ Exp.}$	$P \text{ Th.}$
<b>Pt-99</b> (21 days)	analysed	$150 \pm 35$	$250 \pm 30$	$0.58 \pm 0.16$	$0.81 \pm 0.24$	$0.68 \pm 0.01$
<b>Ni-00</b> (89 days)	analysed	$1470 \pm 140$	$4730 \pm 130$	$0.31 \pm 0.04$	$0.43 \pm 0.05$	
<b>Ti-00</b> (31 days)	analysed	$710 \pm 100$	$2010 \pm 85$	$0.29 \pm 0.04$	$0.49 \pm 0.09$	
<b>Ti-01</b> (46 days)	analysed	$1120 \pm 130$	$3820 \pm 120$	-	$0.36 \pm 0.05$	
<b>Ni-01</b> (72 days)	progress	$2120 \pm 170$	$6630 \pm 150$	-	$\pm 0.04$	
<b>Ni-01</b> (45 days)	expected	$1330 \pm 140$	$4150 \pm 120$	-	$\pm 0.04$	
<b>Ni-00/01</b> (206 days)	all	$4920 \pm 140$	$15510 \pm 230$	-	$\pm 0.025$	$0.436 \pm 0.022$
<b>Ti-00/01</b> (77 days)	all	$1830 \pm 160$	$5830 \pm 150$	-	$0.39 \pm 0.04$	$0.304 \pm 0.017$

**Table X:** Breakup probability results. The last two rows provide an an accuracy of  $\frac{\Delta\tau}{\tau} = 10\%$ .

As for the lifetime value this means:

	Lifetime ( $\cdot 10^{-15}$ s.)	Statistical errors
$\tau(Ni \text{ 2000})$	$2.8^{+1.1}_{-0.8}$	$\pm 34 \%$
$\tau(Ti \text{ 2000/1})$	$5.4^{+1.5}_{-1.3}$	$\pm 26 \%$
$\tau(Ni + Ti)$	$3.6^{+0.9}_{-0.7}$	$\pm 22 \%$

Note that the current error estimate is purely statistical. So far no systematic errors have been proposed, in spite of the fact that they are expected to be quite significant.

## Appendix B

# Reparametrization invariance

Consider  $\phi(x)$  a relativistic spin zero field and its partition function:

$$Z(J) = \int D\phi e^{i(S(\phi) + \int d^4x J(x)\phi(x))}. \quad (\text{B.1})$$

If  $S$  is Lorentz invariant then:

$$Z(J) = Z(J') \quad , \quad J'(x) = J(\Lambda^{-1}x). \quad (\text{B.2})$$

In the non-relativistic regime we only need a subset of  $J$ s which generate Green functions with the external legs almost on shell. These may be chosen as:

$$J(x) = \sqrt{2m} ( e^{-imx^0} J_h(x) + e^{imx^0} J_h^\dagger(x) ), \quad (\text{B.3})$$

where  $m$  is the mass of  $\phi$  and  $J_h(x)$  is slowly varying (i.e. contains energy and momentum much smaller than  $m$ ). From (B.2) and (B.3) one easily finds that for Lorentz transformations close to the identity:

$$J_h(x) \longrightarrow J'_h(x) = e^{-im(\Lambda^{-1}-1)_\mu^0 x^\mu} J_h(\Lambda^{-1}x). \quad (\text{B.4})$$

In the non-relativistic regime  $Z(J)$  can be approximated to the desired order of accuracy by:

$$Z(J) \sim Z_{NR}(J_h, J_h^\dagger) = \int Dh Dh^\dagger e^{i(S_{NR}(h, h^\dagger) + \int d^4x (h^\dagger(x)J_h(x) + J_h^\dagger(x)h(x)))}. \quad (\text{B.5})$$

Then  $Z_{NR}(J_h, J_h^\dagger)$  must be invariant under the transformation (B.4). Invariance of the terms coupled to the sources implies the following transformations for  $h(x)$ :

$$h(x) \longrightarrow h'(x) = e^{-im(\Lambda^{-1}-1)_\mu^0 x^\mu} h(\Lambda^{-1}x). \quad (\text{B.6})$$

Hence  $S_{NR}(h, h^\dagger)$  must be constructed in such a way that it is invariant under (B.6). In order to do so, notice first of all that  $\partial_\mu h(x)$  does not transform in a way similar to  $h(x)$ . We would like to introduce a kind of covariant derivative. The following operator appears to be a successful candidate:

$$D = i\partial_0 - \frac{\partial_\mu \partial^\mu}{2m}. \quad (\text{B.7})$$

We have under Lorentz transformations:

$$Dh(x) \longrightarrow e^{-im(\Lambda^{-1}-1)_\mu^0 x^\mu} (D + i(\Lambda^{-1} - 1)_\mu^0 \partial^\mu) h(\Lambda^{-1}x), \quad (\text{B.8})$$

which upon the change  $x \rightarrow \Lambda x$  becomes:

$$Dh(x) \longrightarrow e^{-im(1-\Lambda)_\mu^0 x^\mu} Dh(x). \quad (\text{B.9})$$

Analogously, if we have  $C_w(x) = (h^\dagger(x))^m (h(x))^n$ ,  $w = n - m$ , we may define for  $w \neq 0$  a generalization of (B.7):

$$D = i\partial_0 - \frac{\partial_\mu \partial^\mu}{2wm}. \quad (\text{B.10})$$

Then  $D^k C_w(x)$  has the same transformation properties as  $C_w(x)$ . We call  $w$  the weight of the composite field  $C_w(x)$ . If  $w = 0$  then  $\partial_\mu C_0(x)$  transforms as a usual Lorentz vector.

From the discussion above the following rules can be inferred in order to build a Lorentz invariant non-relativistic effective theory for spin zero particles:

1. Write down all possible terms in the particle sector we are interested in with weight zero and no derivatives up to the desired order.
2. For each term, which is not already of the higher relevant order, insert  $D$ s or  $\partial_\mu$ s in all possible ways. All  $\mu$  indices coming from the  $\partial_\mu$  must be contracted in a Lorentz invariant way.

Applying the rules above we obtain the Lagrangians (1.3.3) and (1.3.4). Recall also that, for the particular case we are interested in, the (minimal) suppression of  $D$  is  $\Delta m/m$  whereas the (minimal) suppression of  $\partial_\mu$  is  $\sqrt{\Delta m/m}$ .

Finally, let us mention that for practical purposes the rules that we have obtained are identical to those derived from the so called reparametrization invariance [90] (see also [91]). Hence, it should



be clear that reparametrization invariance is nothing but a way to implement Lorentz symmetry in a non-relativistic theory. We believe that this point is important and has not been sufficiently stressed in the literature[92].

## Appendix C

### $F_2$ and $F_3$

$F_2(x)$  in (2.3.2) can be expressed in terms of Clausen integrals. We get:

$$F_2(x) = \begin{cases} 2Cl_2(\arcsin x) - \frac{1}{2}Cl_2(2 \arcsin x) & \text{if } x < 1 \\ 2 \sum_{k=0}^{\infty} \frac{(-1)^k}{(2k+1)^2} \sim 1.831932 & \text{if } x = 1 \\ \begin{aligned} & -i Li_2(-x - \sqrt{x^2 - 1}) + i Li_2(i(-x + \sqrt{x^2 - 1})) - \\ & -i Li_2(-x + \sqrt{x^2 - 1}) + i Li_2(-i(x + \sqrt{x^2 - 1})) + \\ & + \frac{\pi}{8} \left( i\pi + 4\text{Log}(2x) - 4\text{Log}(1 + ix - i\sqrt{x^2 - 1}) - 4\text{Log}(1 + ix + i\sqrt{x^2 - 1}) \right) + \\ & + 2 \left( \frac{\pi}{2} - i\text{Log} \left( \sqrt{\frac{x+1}{2}} - \sqrt{\frac{x-1}{2}} \right) \right) \left( -2i \arctan \left( \frac{x-1}{\sqrt{x^2-1}} \right) + \right. \\ & \left. + \text{Log}(1 + x - \sqrt{x^2 - 1}) - \text{Log}(1 + ix - i\sqrt{x^2 - 1}) + \right. \\ & \left. + \text{Log}(1 + ix + i\sqrt{x^2 - 1}) - \text{Log}(1 + x + \sqrt{x^2 - 1}) \right) \end{aligned} & \text{if } x > 1. \end{cases} \quad (\text{C.1})$$

Recall that the Clausen integral is defined as:

$$Cl_2(x) := - \int_0^x d\theta \text{Log} \left( 2 \sin \frac{\theta}{2} \right) = i \frac{\pi^2}{6} - \frac{i}{4} x^2 - x \text{Log}(ie^{-i\frac{x}{2}}) - i Li_2(e^{ix}). \quad (\text{C.2})$$

$F_3(x)$  in (2.3.2) can be expressed in terms of dilogarithms. We get:

$$F_3(x) = \frac{1}{\sqrt{1-x^2}} \left[ Li_2 \left( -\frac{(1+a+b)}{2b} \right) - Li_2 \left( -\frac{(1+a-b)}{2b} \right) + Li_2 \left( -\frac{2b}{(1+a+b)} \right) - \right. \\ \left. - Li_2 \left( \frac{2b}{(1+a+b)} \right) - Li_2 \left( -\frac{(a+b)}{2b} \right) + Li_2 \left( -\frac{(a-b)}{2b} \right) - Li_2 \left( -\frac{2b}{(a+b)} \right) + \right.$$

$$\begin{aligned}
 &+Li_2\left(\frac{2b}{(a+b)}\right) + Li_2\left(\frac{(a+b)}{(1+a+b)}\right) - Li_2\left(\frac{(a-b)}{(1+a-b)}\right) + \\
 &+ \text{Log}(bx) \text{Log}\left(\frac{(1+a+b)}{(1+a-b)}\right) \Big] \qquad \text{if } x < 1,
 \end{aligned}$$

where  $a := x^{-1}$  and  $b := \frac{\sqrt{1-x^2}}{x}$ .

$$F_3(1) = 2 - \text{Log}2$$

$$\begin{aligned}
 F_3(x) = & \frac{1}{i\sqrt{x^2-1}} \left[ Li_2\left(-\frac{(1+a+ib)}{2ib}\right) - Li_2\left(-\frac{(1+a-ib)}{2ib}\right) + Li_2\left(-\frac{2ib}{(1+a+ib)}\right) - \right. \\
 & - Li_2\left(\frac{2ib}{(1+a+ib)}\right) - Li_2\left(-\frac{(a+ib)}{2ib}\right) + Li_2\left(-\frac{(a-ib)}{2ib}\right) - Li_2\left(-\frac{2ib}{(a+ib)}\right) + \\
 & + Li_2\left(\frac{2ib}{(a+ib)}\right) + Li_2\left(\frac{(a+ib)}{(1+a+ib)}\right) - Li_2\left(\frac{(a-ib)}{(1+a-ib)}\right) + \\
 & \left. + 2 \arctan\left(\frac{b}{1+a}\right) \left(i\text{Log}(bx) - \frac{\pi}{2}\right) \right] \qquad \text{if } x > 1, \text{ (C.3)}
 \end{aligned}$$

where  $a := x^{-1}$  and  $b := \frac{\sqrt{x^2-1}}{x}$ .

In order to make contact with the expressions found in the literature for the massless limit of (2.2.1) the following formula is useful:

$$\psi(2n) - \frac{(n+l)!(n-l-1)!}{(2n-1)!} \sum_{k=0}^{n-l-2} \frac{(2(n-l-1-k)-1)!(2(k+l)+1)!}{(n-l-k-1)!^2(2l+1+k)!k!} = \psi(n+l+1) \quad \text{(C.4)}$$

## Appendix D

# Energy Shift and Wave Function correction

We sketch here the main steps which lead to our analytic formulas. For the energy shift we have to calculate ( $v = \sqrt{1 - x^2}$ ):

$$\delta E_{nl} = \langle nl | V_{vpc} | nl \rangle = \frac{2\alpha E_n}{3\pi} \frac{(n+l)!}{(n-l-1)!(2l+1)!} \xi^{2n-2l-2} \int_0^1 dx \frac{x^{2l+1}}{(x+\xi)^{2n}} \sqrt{1-x^2} (2+x^2) F(-n-l-1, -n-l-1, 2l+2; \frac{x^2}{\xi^2}). \quad (D.1)$$

Since  $l < n$  the hypergeometric function above reduces to a polynomial:

$$F(-n-l-1, -n-l-1, 2l+2; z) = \sum_{j=0}^{n-l-1} \frac{(2l+1)!(n-l-1)!^2}{(n-l-1-j)!^2(j+2l+1)!j!} z^j. \quad (D.2)$$

Hence:

$$\delta E_{nl} = \frac{2\alpha E_n}{3\pi} \sum_{j=0}^{n-l-1} \binom{n-l-1}{j} \binom{n+l}{n-l-j-1} \xi^{2n-2l-2j-2} \times \int_0^1 dx \frac{x^{2l+2j+1}}{(\xi+x)^{2n}} \sqrt{1-x^2} (2+x^2), \quad (D.3)$$

and upon writing:

$$\left( \frac{1}{\xi+x} \right)^{2n} = -\frac{d^{2n-1}}{d\xi^{2n-1}} \frac{1}{\xi+x}, \quad (D.4)$$

and making the change  $x \rightarrow \sin \theta$  we obtain (2.1.1).

For the wave function at the origin we have to calculate:

$$\delta\Psi_{n0}(\mathbf{0})\Psi_{n0}(\mathbf{0}) = \lim_{E \rightarrow E_n} \langle n0 | \delta(\mathbf{x}) \left( \frac{1}{E-H} - \frac{|n0\rangle\langle n0|}{E-E_n} \right) V_{vpc} | n0 \rangle . \quad (\text{D.5})$$

Upon using the following representation for the Coulomb propagator[25]:

$$\langle \mathbf{x} | \frac{1}{E-H} | \mathbf{y} \rangle = \sum_{l=0}^{\infty} G_l(x, y, E) \sum_{m=-l}^l Y_l^m \left( \frac{\mathbf{x}}{x} \right) Y_l^{*m} \left( \frac{\mathbf{y}}{y} \right) , \quad (\text{D.6})$$

$$G_l(x, y, E) = -4k\mu(2kx)^l(2ky)^l e^{-k(x+y)} \sum_{n'=1}^{\infty} \frac{L_{n'-1}^{2l+1}(2kx)L_{n'-1}^{2l+1}(2ky)\Gamma(n')}{(n'+l-\frac{\mu\alpha}{k})\Gamma(n'+2l+1)} , \quad (\text{D.7})$$

where  $k^2 = -2\mu E$ , (D.5) can be split into three pieces:

$$\delta\Psi_{n0}(\mathbf{0}) = \delta_{ps}\Psi_{n0}(\mathbf{0}) + \delta_{zph}\Psi_{n0}(\mathbf{0}) + \delta_{mph}\Psi_{n0}(\mathbf{0}) . \quad (\text{D.8})$$

The first piece (pole subtraction) corresponds to the term  $n' = n$  in the sum (D.7) and it can be calculated using the formulas given above. The remaining pieces read:

$$\begin{aligned} \delta_{zph}\Psi_{n0}(\mathbf{0}) + \delta_{mph}\Psi_{n0}(\mathbf{0}) &= \frac{\alpha}{\pi}\Psi_{n0}(\mathbf{0}) \int_0^1 dv \frac{v^2 \left(1 - \frac{v^2}{3}\right) \xi^{n-1}}{(\xi + \sqrt{1-v^2})^{n+1}} \sum_{n'=1, n' \neq n}^{\infty} \frac{n'n}{n'-n} \\ &\quad \left( \frac{\xi}{\xi + \sqrt{1-v^2}} \right)^{n'-1} F \left( -(n-1), -(n'-1); 2; \frac{1-v^2}{\xi^2} \right) . \end{aligned} \quad (\text{D.9})$$

Again the hypergeometric function above reduces to a polynomial. For  $n = 1$  it reduces in fact to 1 and the sum over  $n'$  can be carried out explicitly. We obtain:

$$\delta_{zph}\Psi_{10}(\mathbf{0}) + \delta_{mph}\Psi_{10}(\mathbf{0}) = \frac{\alpha}{\pi}\Psi_{10}(\mathbf{0}) \int_0^1 dv \frac{v^2 \left(1 - \frac{v^2}{3}\right)}{(\xi + \sqrt{1-v^2})^2} \left\{ \frac{\xi}{\sqrt{1-v^2}} + \text{Log} \left( \frac{\xi + \sqrt{1-v^2}}{\sqrt{1-v^2}} \right) \right\} , \quad (\text{D.10})$$

where the first term corresponds to the zero photon exchange and the second one to the multiphoton exchange. Again the change of variable  $v \rightarrow \cos \theta$  and a number of manipulations allow us to obtain (2.3.1) from the above.

## Appendix E

### The case $\alpha = -1$

The more general decomposition of the high momentum behaviour of  $T^{ij}(\mathbf{k})$  for  $\alpha = -1$  reads:

$$T^{ij}(\mathbf{k}) = \mathcal{B}_{-1} \frac{\delta^{ij}}{|\mathbf{k}|} + \tilde{\mathcal{B}}_{-1} \frac{\mathbf{k}^i \mathbf{k}^j}{|\mathbf{k}|^3} + \mathcal{P}^{ij}(\mathbf{k}), \quad (\text{E.1})$$

where  $\lim_{\mathbf{k} \rightarrow \infty} \mathcal{P}^{ij}(\mathbf{k}) \sim \frac{1}{\mathbf{k}^2}$ . Notice then that the integral in (3.4.1) at most diverges logarithmically and, furthermore, the divergent term must be proportional to the  $\delta^{ij}$  tensor. By calculating the high energy behaviour of the integral in the rhs of (3.4.1) we obtain:

$$\begin{aligned} T^{ij}(\mathbf{k}) \sim & c_0 \delta^{ij} + c_1 \frac{\mathbf{k}^i \mathbf{k}^j}{\mathbf{k}^2} - \frac{M c_0}{2\pi^2} \left[ \mathcal{B}_{-1} + \frac{\tilde{\mathcal{B}}_{-1}}{3} \right] \text{Log} \left( \frac{\Lambda^2}{-EM} \right) \delta^{ij} + \frac{M c_1}{4\pi^2} \frac{\mathcal{B}_{-1} + \tilde{\mathcal{B}}_{-1}}{3} \cdot \\ & \cdot \left[ \text{Log} \left( \frac{\mathbf{k}^2}{\Lambda^2} \right) + f_1 \right] \delta^{ij} - \frac{M c_1}{4\pi^2} \left[ \mathcal{B}_{-1} + \frac{\tilde{\mathcal{B}}_{-1}}{3} \right] \left[ \text{Log} \left( \frac{\mathbf{k}^2}{-EM} \right) + f_2 \right] \frac{\mathbf{k}^i \mathbf{k}^j}{\mathbf{k}^2}, \quad (\text{E.2}) \end{aligned}$$

with  $f_1$  and  $f_2$  two finite, constant terms. Observe that, although the cutoff dependence can be removed by a suitable redefinition of  $c_0$ , the non-analytic terms  $\sim \text{Log}|\mathbf{k}|$  cannot be compensated by the potential. Self-consistency of (E.1) and (E.2) force  $c_1 \rightarrow 0$  again.

## Appendix F

### Proof of (3.4.1.9)

Let us define:

$$\mathcal{H}_\alpha(EM) := c_1 \int^\Lambda \frac{d^3 k}{(2\pi)^3} \frac{T_{1\alpha}^{ii}(\mathbf{k})}{E - \frac{\mathbf{k}^2}{M} + i\eta} \quad \alpha = 0, 1, 2, \quad (\text{F.1})$$

and concentrate on  $\mathcal{H}_0(EM)$  (the analysis for  $\mathcal{H}_1(EM)$  is identical). We have:

$$\begin{aligned} \mathcal{H}_0(EM) &= \int^\Lambda \frac{d^3 k}{(2\pi)^3} \int^\Lambda \frac{d^3 k''}{(2\pi)^3} \frac{c_1}{E - \frac{\mathbf{k}^2}{M} + i\eta} \frac{(\mathbf{k} - \mathbf{k}'')^i (\mathbf{k} - \mathbf{k}'')^j}{(\mathbf{k} - \mathbf{k}'')^2 + m_\pi^2} \frac{T_0(\mathbf{k}'')}{E - \frac{\mathbf{k}^2}{M} + i\eta} \\ &+ \int^\Lambda \frac{d^3 k}{(2\pi)^3} \int^\Lambda \frac{d^3 k''}{(2\pi)^3} \frac{c_1}{E - \frac{\mathbf{k}^2}{M} + i\eta} \frac{c_1 (\mathbf{k} - \mathbf{k}'')^i (\mathbf{k} - \mathbf{k}'')^k + c_2 \delta^{ik}}{(\mathbf{k} - \mathbf{k}'')^2 + m_\pi^2} \frac{T_{10}^{kj}(\mathbf{k}'')}{E - \frac{\mathbf{k}^2}{M} + i\eta}. \end{aligned} \quad (\text{F.2})$$

If we solve the equation above iteratively using (3.4.1.2) for  $T_0(\mathbf{k})$  and (3.4.1.3) for  $T_{10}^{ij}(\mathbf{k})$ , the most divergent term in the  $n$ -th. iteration is (superindexes  $j$  and  $k$  are contracted with unwritten momenta):

$$\begin{aligned} c_1^{n+1} &\left\{ \prod_{l=1}^{n+2} \int^\Lambda \frac{d^3 k_l}{(2\pi)^3} \right\} \frac{1}{E - \frac{\mathbf{k}_1^2}{M} + i\eta} \frac{(\mathbf{k}_1 - \mathbf{k}_2)^i (\mathbf{k}_1 - \mathbf{k}_2)^j}{(\mathbf{k}_1 - \mathbf{k}_2)^2 + m_\pi^2} \frac{1}{E - \frac{\mathbf{k}_2^2}{M} + i\eta} \dots \\ &\dots \frac{1}{E - \frac{\mathbf{k}_{n+1}^2}{M} + i\eta} \frac{(\mathbf{k}_{n+1} - \mathbf{k}_{n+2})^k (\mathbf{k}_{n+1} - \mathbf{k}_{n+2})^i}{(\mathbf{k}_{n+1} - \mathbf{k}_{n+2})^2 + m_\pi^2} \frac{1}{E - \frac{\mathbf{k}_{n+2}^2}{M} + i\eta}. \end{aligned} \quad (\text{F.3})$$

Taking into account that the limits  $E \rightarrow 0$  and  $m_\pi^2 \rightarrow 0$  exist and the flow (3.4.1.5), the leading behaviour in  $\Lambda$  reads:

$$(-M)^{n+2} c_1^{n+1} \left\{ \prod_{l=1}^{n+2} \int^\Lambda \frac{d^3 k_l}{(2\pi)^3} \frac{1}{k_l^2} \right\} \frac{(\mathbf{k}_1 - \mathbf{k}_2)^i (\mathbf{k}_1 - \mathbf{k}_2)^j}{(\mathbf{k}_1 - \mathbf{k}_2)^2} \dots \frac{(\mathbf{k}_{n+1} - \mathbf{k}_{n+2})^k (\mathbf{k}_{n+1} - \mathbf{k}_{n+2})^i}{(\mathbf{k}_{n+1} - \mathbf{k}_{n+2})^2} \sim \bar{c}_1^{n+1} \Lambda, \quad (\text{F.4})$$

which proves that  $a_0$  is a ( $\bar{c}_1$ -dependent) constant. Notice also that the integral in (F.4) is bound by  $(\int^\Lambda d^3\mathbf{k}/\mathbf{k}^2)^{n+2}$ . Let us next identify the subleading behaviour. Consider first  $E = 0$ . The derivative of (F.3) with respect to  $m_\pi^2$  at  $m_\pi^2 = 0$  has at most a logarithmic singularity which means that the next to leading behaviour in  $\Lambda$  is  $\sim c_1^{n+1}\Lambda^{n-1}m_\pi^2\text{Log}\Lambda$ , which gives rise to  $\mathcal{O}\left(\frac{1}{\Lambda}\right)$  contributions in (3.4.1.9). Terms contributing to  $d_0$  in the  $n$ th. iteration appear when: (i) the  $c_2$ -proportional term of  $T_0(\mathbf{k})$  is iterated through only  $c_1$  potential insertions coming from the second line in (F.2); (ii) the equal to 1 term of  $T_0(\mathbf{k})$  is iterated in such a way that a  $c_2$  potential from the last piece appears only once in the iteration. The relevant integral is obtained by substituting:

$$c_1 \frac{(\mathbf{k}_p - \mathbf{k}_{p+1})^i (\mathbf{k}_p - \mathbf{k}_{p+1})^j}{(\mathbf{k}_p - \mathbf{k}_{p+1})^2 + m_\pi^2} \rightarrow \frac{c_2 \delta^{ij}}{(\mathbf{k}_p - \mathbf{k}_{p+1})^2 + m_\pi^2} \quad (\text{F.5})$$

in (F.3). In order to get the leading behaviour in  $\Lambda$  of this integral we can set  $m_\pi^2 = 0$  in all but the substituted term above. We have (superindexes  $j, l, q$  and  $k$  are contracted with unwritten momenta):

$$\begin{aligned} & (-M)^{n+2} c_2 c_1^n \left\{ \prod_{l=1 \setminus \{p, p+1\}}^n \int^\Lambda \frac{d^3 k_l}{(2\pi)^3} \frac{1}{\mathbf{k}_l^2} \right\} \frac{(\mathbf{k}_1 - \mathbf{k}_2)^i (\mathbf{k}_1 - \mathbf{k}_2)^j}{(\mathbf{k}_1 - \mathbf{k}_2)^2} \dots \left[ \int^\Lambda \frac{d^3 k_p}{(2\pi)^3} \right. \\ & \left. \int^\Lambda \frac{d^3 k_{p+1}}{(2\pi)^3} \frac{(\mathbf{k}_{p-1} - \mathbf{k}_p)^l}{(\mathbf{k}_{p-1} - \mathbf{k}_p)^2} \frac{1}{\mathbf{k}_p^2} \frac{(\mathbf{k}_{p-1} - \mathbf{k}_p) \cdot (\mathbf{k}_{p+1} - \mathbf{k}_{p+2})}{(\mathbf{k}_p - \mathbf{k}_{p+1})^2 + m_\pi^2} \frac{1}{\mathbf{k}_{p+1}^2} \frac{(\mathbf{k}_{p+1} - \mathbf{k}_{p+2})^q}{(\mathbf{k}_{p+1} - \mathbf{k}_{p+2})^2} \right] \dots \\ & \dots \frac{(\mathbf{k}_{n-1} - \mathbf{k}_n)^k (\mathbf{k}_{n-1} - \mathbf{k}_n)^i}{(\mathbf{k}_{n-1} - \mathbf{k}_n)^2} \sim c_2 \bar{c}_1^n \text{Log}\Lambda, \end{aligned} \quad (\text{F.6})$$

which proves (with the flow (3.4.1.1)) that  $d_0$  is a constant.

Let us next address the energy dependent contribution to (F.1). Notice that any analytic contribution in  $EM$  would show up at  $\mathcal{O}(1/\Lambda)$ . Hence only non-analytic contributions (like the one in (F.6)) are relevant to us. Let us then look for non-analytic contributions in  $EM$  in the most divergent diagram in the  $n$ th. iteration (F.3). Since the  $m_\pi^2 \rightarrow 0$  limit exists we can take it and have:

$$\begin{aligned} & c_1^{n+1} \int^\Lambda \frac{dk_1}{(2\pi)^3} \frac{\mathbf{k}_1^2}{E - \frac{\mathbf{k}_1^2}{M} + i\eta} \dots \int^\Lambda \frac{dk_{n+2}}{(2\pi)^3} \frac{\mathbf{k}_{n+2}^2}{E - \frac{\mathbf{k}_{n+2}^2}{M} + i\eta} \\ & \int d\Omega_1 \dots \int d\Omega_{n+2} \frac{(\mathbf{k}_1 - \mathbf{k}_2)^i (\mathbf{k}_1 - \mathbf{k}_2)^j}{(\mathbf{k}_1 - \mathbf{k}_2)^2} \dots \frac{(\mathbf{k}_{n+1} - \mathbf{k}_{n+2})^k (\mathbf{k}_{n+1} - \mathbf{k}_{n+2})^i}{(\mathbf{k}_{n+1} - \mathbf{k}_{n+2})^2}. \end{aligned} \quad (\text{F.7})$$

where  $d\Omega_i$ ,  $i = 1, \dots, n+2$  stand for angular integrals. Since the most singular contribution comes from the region  $|\mathbf{k}_l| \sim \Lambda \forall l$ , the angular integral will give rise to a constant (which, furthermore, is bound by  $(4\pi)^{n+2}$ ), and the integrals over  $|\mathbf{k}_l|$  decouple. Hence the leading behaviour for small  $E$  turns



out to be the non-analytic contribution we are looking for ( $\alpha_0, \beta_0, \tilde{\alpha}_0$  and  $\tilde{\beta}_0$  are constants):

$$\begin{aligned} \sim c_1^{n+1} \left[ \int^\Lambda dk \frac{\mathbf{k}^2}{E - \frac{\mathbf{k}^2}{M} + i\eta} \right]^{n+2} &\sim c_1^{n+1} \left( \alpha_0 \Lambda + i\beta_0 \sqrt{EM} + \mathcal{O}\left(\frac{1}{\Lambda}\right) \right)^{n+2} \sim \\ &\sim \tilde{c}_1^{n+1} \left( \tilde{\alpha}_0 \Lambda + i\tilde{\beta}_0 \sqrt{EM} + \mathcal{O}\left(\frac{1}{\Lambda}\right) \right), \end{aligned} \quad (\text{F.8})$$

which proves, in addition, that  $b_0$  is a constant. Notice that a  $\text{Log}\Lambda$  dependence in this term would have been fatal for renormalization.

We have then proved the first formula in (3.4.1.9). The proof of the second formula is identical. The third formula is proved by simply noticing that all integrals involved are at most logarithmically divergent and, those which actually are, go multiplied by  $c_1 \sim \frac{1}{\Lambda}$ .

# Appendix G

## On $c_1$ tuning

In subsection 3.4.1, when we focused on proving that a certain behaviour of the bare constants of the potential as functions of the cutoff (namely,  $c_0, c_1 \sim \Lambda^{-1}$ ) would render a finite T-matrix, only  $c_0$  was conveniently fine-tuned. As a result the so-computed scattering amplitude lacked from partial wave mixing, which is expected due to the second rank tensorial term in the (bare) Hamiltonian. In order to obtain partial wave mixing two possibilities must be regarded. On the one hand, it could well happen that, indeed, mixing should not have been considered as LO, but as a NLO term to be treated perturbatively, the divergences it may cause being absorbed in the usual way by higher order local counterterms. This appears to be consistent with the fact that partial wave mixing in this channel amounts only to a few degrees. This treatment resums the  $\delta^{ij}$ -proportional part of OPE. Its SSB term, now eliminated by the strong suppression of  $c_1$ , is then recovered in a NLO analysis. We have shown how this works in subsection 3.4.2.

Nevertheless, another possibility remains unexamined. A proper tuning of  $c_1$  to a, let's say, non-trivial RG fixed point, could very well recover mixing at the leading order. So far, the existence of such a fixed point is anything but evident. Uncovering it or ruling it out requires detailed numerical work which is beyond the scope of this paper. However, in order to illustrate our point let us provide two approximations that exemplify how this tuning would emerge, how it would affect previous results and to which extent to achieve this goal we depend on the exact resolution of our actual system of integral equations.

Let's take in the following  $\mathbf{k}' = \mathbf{0}$  for simplicity. We will also apply the chiral limit ( $m_\pi, c_2 \rightarrow$

0) and work with  $\tilde{c}_0$  and  $\tilde{c}_1$  defined in section 3.4.2. After decomposing the T-matrix in:

$$T^{ij}(\mathbf{k}) = T_1(k) \delta^{ij} + \left[ \frac{\mathbf{k}^i \mathbf{k}^j - \frac{\mathbf{k}^2}{3} \delta^{ij}}{\mathbf{k}^2} \right] T_2(k), \quad (\text{G.1})$$

the following two angular integrals arise in the resolution of its LS equation

$$\begin{aligned} \tilde{c}_1 \int \frac{d\Omega''}{4\pi} \frac{(\mathbf{k} - \mathbf{k}'')^i (\mathbf{k} - \mathbf{k}'')^j - \frac{(\mathbf{k} - \mathbf{k}'')^2}{3} \delta^{ij}}{(\mathbf{k} - \mathbf{k}'')^2} &\longrightarrow \tilde{c}_1 \omega_1 \left( \frac{k}{k''} \right) \frac{\mathbf{k}^i \mathbf{k}^j - \frac{\mathbf{k}^2}{3} \delta^{ij}}{\mathbf{k}^2}, \\ \tilde{c}_1 \int \frac{d\Omega''}{4\pi} \frac{(\mathbf{k} - \mathbf{k}'')^i (\mathbf{k} - \mathbf{k}'')^k - \frac{(\mathbf{k} - \mathbf{k}'')^2}{3} \delta^{ik}}{(\mathbf{k} - \mathbf{k}'')^2} \left[ \frac{\mathbf{k}''^k \mathbf{k}''^j - \frac{\mathbf{k}''^2}{3} \delta^{kj}}{\mathbf{k}''^2} \right] &\longrightarrow \\ \longrightarrow \left[ \tilde{c}_1 \omega_2 \left( \frac{k}{k''} \right) \frac{\mathbf{k}^i \mathbf{k}^j - \frac{\mathbf{k}^2}{3} \delta^{ij}}{\mathbf{k}^2} + \tilde{c}_1 \omega_3 \left( \frac{k}{k''} \right) \delta^{ij} \right], & \quad (\text{G.2}) \end{aligned}$$

with  $\omega_i \left( \frac{k}{k''} \right)$ ,  $i = 1, 2, 3$ , as known functions ( $k = |\mathbf{k}|$ ,  $k'' = |\mathbf{k}''|$ ).

At this point we wish to introduce some reasonable approximation that allows us to transform the non-separable in  $k$  and  $k''$  functions  $\omega_i \left( \frac{k}{k''} \right)$  into separable ones. Once this is achieved we only need to solve a conventional system of equations and check whether, at least within this approximation, a non-trivial fixed point exists. Obviously our approximation should be as compatible as possible with what we know about the behaviour of the full  $d^3\mathbf{k}$ -integrals. For instance:

$$\int^\Lambda \frac{dk''}{2\pi^2} \frac{k''^2 \omega_i \left( \frac{k}{k''} \right)}{E - \frac{k''^2}{M} + i\eta} \sim k \quad i = 1, 2, \quad (\text{G.3})$$

that is, both are finite integrals proportional to  $k$  in the limit  $\Lambda \rightarrow \infty$ . Unfortunately, no separable  $\omega_i$  achieves this. We shall content ourselves with a simple but still reasonable starting point that enforces separability. Then, let us take  $\omega_3 \left( \frac{k}{k''} \right)$  as a constant ( $:= \alpha_3$ ) and substitute  $\omega_{1,2} \left( \frac{k}{k''} \right)$  by  $:= \alpha_{1,2} \frac{k}{k''}$  ( $\alpha_{1,2}$  also being constants). Although the latter introduces logarithmic divergences which do not exist in the actual function, it keeps the correct behaviour in  $k$  shown in (G.3).

The LS equation takes the form:

$$\begin{aligned} T^{ij}(\mathbf{k}) = \tilde{c}_0 (1 + T_1 \mathcal{I}_0) \delta^{ij} + \tilde{c}_1 \left[ \frac{\mathbf{k}^i \mathbf{k}^j - \frac{\mathbf{k}^2}{3} \delta^{ij}}{\mathbf{k}^2} \right] + \tilde{c}_1 \alpha_1 \left[ \frac{\mathbf{k}^i \mathbf{k}^j - \frac{\mathbf{k}^2}{3} \delta^{ij}}{\mathbf{k}^2} \right] k T_1 \mathcal{I}_{-1} + \\ + \tilde{c}_1 \alpha_2 \left[ \frac{\mathbf{k}^i \mathbf{k}^j - \frac{\mathbf{k}^2}{3} \delta^{ij}}{\mathbf{k}^2} \right] k \mathcal{C} + \tilde{c}_1 \alpha_3 \delta^{ij} \mathcal{B}, \end{aligned} \quad (\text{G.4})$$

where we have already used that  $T_1(k)$  becomes momentum independent, as it is easily verified through (G.4):

$$T_1 = \tilde{c}_0 (1 + T_1 \mathcal{I}_0) + \tilde{c}_1 \alpha_3 \mathcal{B},$$

$$T_2(k) = \tilde{c}_1(1 + \alpha_1 k T_1 \mathcal{I}_{-1} + \alpha_2 k \mathcal{C}). \quad (\text{G.5})$$

The following functions have been introduced:

$$\begin{aligned} \mathcal{I}_0 &:= \int^\Lambda \frac{dk}{2\pi^2} \frac{k^2}{E - \frac{k^2}{M} + i\eta}, \\ \mathcal{B} &:= \int^\Lambda \frac{dk}{2\pi^2} \frac{k^2 T_2(k)}{E - \frac{k^2}{M} + i\eta}, \\ \mathcal{I}_{-1} &= \int^\Lambda \frac{dk}{2\pi^2} \frac{k}{E - \frac{k^2}{M} + i\eta}, \\ \mathcal{C} &= \int^\Lambda \frac{dk}{2\pi^2} \frac{k T_2(k)}{E - \frac{k^2}{M} + i\eta}. \end{aligned} \quad (\text{G.6})$$

A few manipulations allow us to solve for  $T_1$  and the combination  $\alpha_1 T_1 \mathcal{I}_{-1} + \alpha_2 \mathcal{C}$ :

$$\begin{aligned} T_1 &= \frac{\tilde{c}_0 + \tilde{c}_1^2 \alpha_3 \mathcal{I}_0 + \tilde{c}_1^3 \alpha_1 \alpha_3 \frac{\mathcal{I}_1 \mathcal{I}_{-1}}{1 - \tilde{c}_1 \alpha_2 \mathcal{I}_0}}{1 - \tilde{c}_0 \mathcal{I}_0 - \tilde{c}_1^2 \alpha_1 \alpha_3 \frac{\mathcal{I}_1 \mathcal{I}_{-1}}{1 - \tilde{c}_1 \alpha_2 \mathcal{I}_0}}, \\ \alpha_1 T_1 \mathcal{I}_{-1} + \alpha_2 \mathcal{C} &= \left( \frac{\tilde{c}_1 \alpha_2 \mathcal{I}_{-1}}{1 - \tilde{c}_1 \alpha_2 \mathcal{I}_0} \right) \frac{(\tilde{c}_0 + \tilde{c}_1^2 \alpha_3 \mathcal{I}_0) \frac{\alpha_1}{\alpha_2} + \tilde{c}_1 (1 - \tilde{c}_0 \mathcal{I}_0)}{1 - \tilde{c}_0 \mathcal{I}_0 - \tilde{c}_1^2 \alpha_1 \alpha_3 \frac{\mathcal{I}_1 \mathcal{I}_{-1}}{1 - \tilde{c}_1 \alpha_2 \mathcal{I}_0}} \end{aligned} \quad (\text{G.7})$$

where a quadratic divergence:

$$\mathcal{I}_1 := \int^\Lambda \frac{dk}{2\pi^2} \frac{k^3}{E - \frac{k^2}{M} + i\eta}, \quad (\text{G.8})$$

enters.

It is not difficult to realize that little has been gained: the only way to get (G.7) finite is by an untuned  $\tilde{c}_1$ , ( $1 - \tilde{c}_1 \alpha_2 \mathcal{I}_0 \neq 0$ ), and a tuned  $\tilde{c}_0$ , which force  $T_2(k)$  to become trivial again. We have not been able to figure out any reasonable approximation which produces a non-trivial  $T_2(k)$ .

Anyway, in order to illustrate the kind of fixed point we are looking for, let us take another option which, unfortunately, is completely unrealistic. It consists of sending  $\omega_1 \left(\frac{k}{k^{\eta_1}}\right)$  and  $\omega_3 \left(\frac{k}{k^{\eta_3}}\right)$  to zero, keeping  $\omega_2 \left(\frac{k}{k^{\eta_2}}\right)$  as a mere constant ( $:= \alpha_2$ ). That presents the main advantage of producing decoupled equations for  $T_1$  and  $T_2$ :

$$\begin{aligned} T_1 &= \tilde{c}_0(1 + \mathcal{A}), \\ T_2 &= \tilde{c}_1(1 + \alpha_2 \mathcal{B}). \end{aligned} \quad (\text{G.9})$$

where  $\mathcal{A} := T_1 \mathcal{I}_0$  and  $\mathcal{B} = T_2 \mathcal{I}_0$ . Both are well defined provided  $\tilde{c}_0(1 + \mathcal{A})$  and  $\tilde{c}_1(1 + \alpha_2 \mathcal{B})$  are finite. We compute them multiplying above by  $1/(E - \frac{\mathbf{k}^2}{M} + i\eta)$  and integrating. This produces:

$$\begin{aligned}\tilde{c}_0(1 + \mathcal{A}) &= \frac{1}{\frac{1}{c_0} - \mathcal{I}_0}, \\ \tilde{c}_1(1 + \alpha_2 \mathcal{B}) &= \frac{1}{\frac{1}{c_1} - \alpha_2 \mathcal{I}_0}.\end{aligned}\tag{G.10}$$

It is obvious that divergences are absorbed if  $\tilde{c}_0, \tilde{c}_1$  behave like  $\Lambda^{-1}$  and non-trivial results ( $T_1, T_2 \neq 0$ ) require:

$$\begin{aligned}\frac{1}{\tilde{c}_0} &:= -\frac{M\Lambda}{2\pi^2} + \frac{1}{\tilde{c}_0^r(\mu)}, \\ \frac{1}{\tilde{c}_1} &:= -\frac{M\Lambda\alpha_2}{2\pi^2} + \frac{1}{\tilde{c}_1^r(\mu)}.\end{aligned}\tag{G.11}$$

Namely,  $\tilde{c}_1$  must be fine-tuned (to a non-trivial fixed point) as desired. Unfortunately, as mentioned before, the assumptions made for the  $\omega_i$  here are not realistic.

Summarizing, we are rather pessimistic about the possibility that a non-trivial RG fixed point for both  $\tilde{c}_0$  and  $\tilde{c}_1$  exists, which allows for partial wave mixing at leading order.

## Appendix H

### No continuous solutions of (3.1.1.37) when $R \rightarrow 0$

Consider eq.(3.1.1.37),

$$\sqrt{-MV_0}R \cot(\sqrt{-MV_0}R) = \frac{3}{4} + \sqrt{\frac{6M\alpha_\pi}{R}} \tan\left(2\sqrt{\frac{6M\alpha_\pi}{R}} + \phi_0\right), \quad (\text{H.1})$$

with  $V_0 < 0$ ,  $R > 0$ . We are interested in whether continuous solutions  $V_0 = V_0(R)$  exist when  $R \rightarrow 0$ .

Let us define:

$$y := \sqrt{-MV_0}R > 0, \quad x := 2\sqrt{\frac{6M\alpha_\pi}{R}} + \phi_0. \quad (\text{H.2})$$

In terms of these variables the question is recasted as the finding of a continuous  $y(x)$  when  $x \rightarrow \infty$ :

$$y \cot y = \frac{3}{4} + \frac{x - \phi_0}{2} \tan x. \quad (\text{H.3})$$

Having derived this equation once, one obtains:

$$\frac{\sin 2y - 2y}{2\sin^2 y} \frac{dy}{dx} = \frac{\sin 2x + 2(x - \phi_0)}{4\cos^2 x}, \quad (\text{H.4})$$

which proves that  $y(x)$  decreases when  $x$  increases. This holds everywhere except for the points  $x = \left(n + \frac{1}{2}\right)\pi$ ,  $y = m\pi$  ( $n, m = 0, 1, 2, \dots$ ). When  $x$  approaches  $\left(n + \frac{1}{2}\right)\pi$  for a given  $n$ ,  $y$  must necessarily approach  $m\pi$  for some  $m$  in order for eq.(H.3) to have a solution. If we write:

$$x = \left(n + \frac{1}{2}\right)\pi + \delta x, \quad y = m\pi + \delta y, \quad (\text{H.5})$$

we get, for  $m \neq 0$ ,

$$\delta y = -\frac{m}{n + \frac{1}{2}} \delta x + \mathcal{O}(\delta x^2). \quad (\text{H.6})$$

Hence, eq.(H.3) admits a continuous solution near the point  $x = \left(n + \frac{1}{2}\right) \pi$  provided that we choose  $m \neq 0$ . Notice also that  $y$  keeps decreasing when  $x$  increases in the neighbourhood of this point.

Now, if we increase  $x$  from  $\left(n + \frac{1}{2}\right) \pi$  to  $\left(n + \frac{3}{2}\right) \pi$ ,  $y$  must decrease from  $m\pi$  to  $(m - 1)\pi$ , if continuity is required. By iterating the argument, if we increase  $x$  till  $\left(n + m + \frac{1}{2}\right) \pi$ , continuity requires  $y$  to decrease till 0. So, for  $x = \left(n + m + \frac{1}{2}\right) \pi + \delta x$  and  $y = \delta y$ , eq.(H.3) does not have a solution anymore, since one obtains:

$$\mathcal{O}(1) \sim -\frac{\left(n + m + \frac{1}{2}\right) \pi}{\delta x}. \quad (\text{H.7})$$

In conclusion, no continuous solution  $y = y(x)$  of eq.(H.3) exists for  $x \rightarrow \infty$  ( $R \rightarrow 0$ ). In particular, the curves plotted in their fig. 4, which we show below, cannot be continuously extended below  $R \sim 0.25$  fm.,  $R \sim 0.13$  fm. and  $R \sim 0.09$  fm., respectively. Of course, if continuity is given up, an infinite number of solutions exist but none of them is relevant for renormalization purposes.

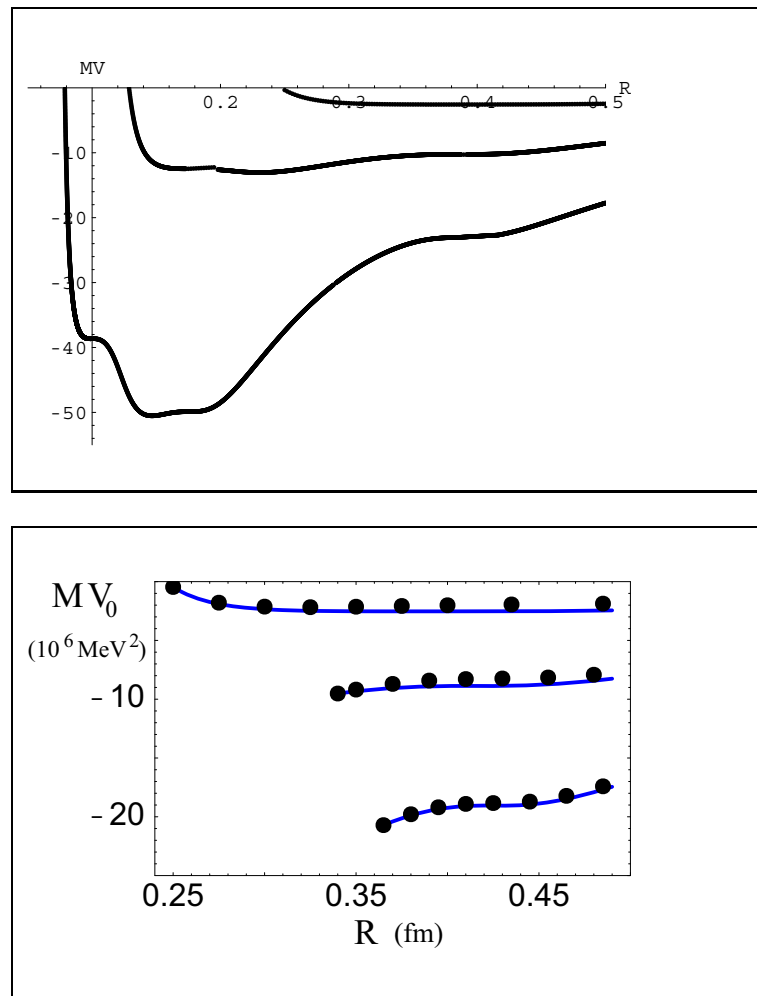


Figure 1: In the upper figure we show how the first three branches of the flow presented by the authors of [68], behave as one approaches the relevant limit  $R \rightarrow 0$ .



# Acknowledgments

A mi director de tesis, Joan Soto, por la oportunidad, la generosidad, la infinita paciencia. A mis padres por el apoyo y la libertad, por seguir perdonándome, por matizar mis días negros. A mis compañeros de tercer ciclo, por la alegría y la complicidad.

Gracias.



# Bibliography

- [1] H. Georgi, *Ann. Rev. Nucl. Sci.* **43** (1995) 209; D. B. Kaplan, *nucl-th/9506035*; A. V. Manohar, *hep-ph/9606222*; A. Pich, *hep-ph/9806303*; B.R. Holstein, *nucl-th/0010015*.
- [2] N. Brambilla, *hep-ph/0008279*; V. Antonelli et al., *Annals Phys.* **286** (2001) 108; G. S. Bali, *Phys. Rept.* **343** (2001) 1; A. Pineda, *Nucl. Phys. Proc. Suppl.* **93** (2001) 188.
- [3] W. E. Caswell and G. P. Lepage, *Phys. Lett.* **B 167** (1986) 437.
- [4] B. Adeva et al., *CERN-SPSLC-95-1*; J. Schacher, *hep-ph/9808407*; A. Lanaro,  *$\pi$ -N Newslett.* **15** (1999) 270; M. Pentic et al., *hep-ph/0001279*.
- [5] M. Knecht, B. Moussallam, J. Stern and N. H. Fuchs, *Nucl. Phys.* **B 457** (1995) 513; Erratum-*ibid.* **B 471** (1996) 445; L. Girlanda, M. Knecht, B. Moussallam and J. Stern, *Phys. Lett.* **B 409** (1997) 461.
- [6] S. Weinberg, *Physica A* **96** (1979) 327; J. Gasser and H. Leutwyler, *Ann. Phys. (N. Y.)* **158** (1984), 142 and *Nucl. Phys.* **B 250** (1985) 465.
- [7] I. I. Kogan, A. Kovner and M. A. Shifman, *Phys. Rev.* **D 59** (1999) 016001.
- [8] D. Weingarten, *Phys. Rev. Lett.* **51** (1983) 1830.
- [9] A. Dobado and J. R. Pelaez, *Acta Phys. Hung.* **8** (1998) 307.
- [10] K. P. Arnold et al., *Villigen Sin-Sin Newslett.* **20** (1988) 38.
- [11] L. L. Nemenov, *Sov. J. Nucl. Phys.* **41** (1985) 629.

- [12] T. L. Trueman, Nucl. Phys. **26** (1961) 57; U. Moor, G. Rasche and W. S. Woolcock, Nucl. Phys. **A 587**. (1995) 747; A. Gashi, G. C. Oades, G. Rasche and W. S. Woolcock, Nucl. Phys. **A 628** (1998) 101 and Nucl. Phys. **A 699** (2002) 732.
- [13] H. Jallouli and H. Sazdjian, Phys. Rev. **D 58** (1998) 014011; H. Sazdjian, *hep-ph/9809425* and Phys. Lett. **B 490** (2000) 203.
- [14] V. E. Lyubovitskij and A. G. Rusetsky, Phys. Lett. **B 389** (1996) 181; V. E. Lyubovitskij, E. Z. Lipartia and A. G. Rusetsky, JETP Lett. **66** (1997) 783; M. A. Ivanov, V. E. Lyubovitskij, E. Z. Lipartia and A. G. Rusetsky, Phys. Rev. **D 58** (1998) 094024.
- [15] X. Kong and F. Ravndal, Phys. Rev. **D 59** (1999) 014031 and Phys. Rev. **D 61** (2000) 077506; B. R. Holstein, Phys. Rev. **D 60** (1999) 114030.
- [16] A. Czarnecki, K. Melnikov and A. Yelkhovsky, Phys. Rev. **A 59** (1999) 4316.
- [17] J. Gasser, V. E. Lyubovitskij, A. Rusetsky and A. Gall, Phys. Rev. **D 64** (2001) 016008.
- [18] D. Eiras and J. Soto, Phys. Rev. **D 61** (2000) 114027 and  $\pi$ N Newslett. **15** (1999) 181.
- [19] S. Deser, M. L. Goldberger, K. Baumann and W. Thirring, Phys. Rev. **96** (1954) 774.
- [20] A.V. Manohar, Phys. Rev. **D 56** (1997) 230; A. Pineda and J. Soto, Phys. Rev. **D 58** (1998) 114011.
- [21] H. B. O'Connell, K. Maltman, A. W. Thomas and A. G. Williams, *hep-ph/9707404*.
- [22] J. Bijnens, G. Colangelo, G. Ecker, J. Gasser and M. E. Sainio, Nucl. Phys. **B 508** (1997) 263; Erratum-ibid. **B 517** (1998) 639; Phys. Lett. **B 374** (1996) 210.
- [23] M. Knecht and R. Urech, Nucl. Phys. **B 519** (1998) 329.
- [24] A. Pineda and J. Soto, Phys. Lett. **B 420** (1998) 391 and Phys.Rev. **D 59** (1999) 016005.
- [25] M. B. Voloshin, Sov. J. Nucl. Phys. **36** (1982) 143; A. Pineda, Nucl. Phys. **B 494** (1997) 213.
- [26] H. Bateman, Higher Transcendental Functions **Vol. I** (1953) McGraw-Hill.
- [27] P. Labelle and K. Buckley *hep-ph/9804201*.

- [28] R. Baur and R. Urech, Nucl. Phys. **B 499** (1997) 319.
- [29] J. Bijnens and J. Prades, Nucl. Phys. **B 490** (1997) 239; B. Moussallam, Nucl. Phys. **B 504** (1997) 381.
- [30] A. Gashi, G. Rasche, G. C. Oades and W. S. Woolcock, Nucl. Phys. **A 628** (1998) 101.
- [31] J. Gasser and H. Leutwyler, Phys. Lett. **B 125** (1983) 325.
- [32] J. Bijnens, G. Colangelo, G. Ecker, J. Gasser and M. E. Sainio, Phys. Lett. **B 374** (1996) 210.
- [33] G. Colangelo, J. Gasser and H. Leutwyler, Nucl. Phys. **B 603** (2001) 125.
- [34] M. M. Nagels et al., Nucl. Phys. **B 147** (1979) 189.
- [35] J. Bijnens et al., Phys. Lett. **B 374** (1996) 210.
- [36] A. Di Giacomo, Nucl. Phys. **B 11** (1969) 411.
- [37] A. Billoire, Phys. Lett. **B 92** (1980) 343.
- [38] M. B. Voloshin, Nucl. Phys. **B 154** (1979) 365; H. Leutwyler, Phys. Lett. **B 98** (1981) 447; A. Pineda, Nucl. Phys. **B 494** (1997) 213.
- [39] A. H. Hoang, *hep-ph/0008102*.
- [40] N. Brambilla, A. Pineda, J. Soto and A. Vairo, Phys. Rev. **D 63** (2001) 014023.
- [41] A. Pineda and A. Vairo, Phys. Rev. **D 63** (2001) 054007; Erratum-ibid. **D 64** (2001) 039902.
- [42] N. Brambilla, Y. Sumino and A. Vairo, Phys. Lett. **B 513** (2001) 381 and Phys. Rev. **D 65** (2002) 034001.
- [43] A. H. Hoang, A. V. Manohar, I. W. Stewart and T. Teubner, Phys. Rev. **D 65** (2002) 014014.
- [44] B. A. Kniehl, A. A. Penin, V. A. Smirnov and M. Steinhauser, *hep-ph/0203166*.
- [45] N. Brambilla, A. Pineda, J. Soto, A. Vairo, Nucl. Phys. **B 566** (2000) 275.
- [46] S. Titard, F. J. Ynduráin, Phys. Rev. **D 49** (1994) 6007.

- [47] G. E. Pustovalov, JETP **5** (1957) 1234.
- [48] U. D. Jentschura, G. Soff, V.G. Ivanov, S. G. Karshenboim, Phys. Rev. **A 56** (1997) 4483.
- [49] S. G. Karshenboim, U. D. Jentschura, V.G. Ivanov, G. Soff, Eur. Phys. J. **D 2** (1998) 209.
- [50] R. D. Ball, Phys. Rept. **182** (1989) 1.
- [51] K. Melnikov, A. Yelkhovsky, Phys. Rev. **D 59** (1999) 114009.
- [52] S. G. Karshenboim, Can. J. Phys. **76** (1998) 169.
- [53] A. Pineda, F. J. Ynduráin, Phys. Rev. **D 58** (1998) 094022 and **D 61** (2000) 077505.
- [54] A. H. Hoang, A.V. Manohar, Phys. Lett. **B 483** (2000) 94.
- [55] A. H. Hoang et al., Eur. Phys. J. direct **C 3** (2000) 1.
- [56] M. Beneke et al., *hep-ph/0003033*.
- [57] N. Gray, D. J. Broadhurst, W. Grafe and K. Schilcher, Z. Phys. **C 48** (1990) 673.
- [58] S. Weinberg, Phys. Lett. **B 251** (1990) 288; Nucl. Phys. **B 363** (1991) 3; Phys. Lett. **B 295** (1992) 114.
- [59] D. R. Phillips, S. R. Beane and T. D. Cohen, Annals Phys. **263** (1998) 255; D. R. Phillips, S. R. Beane and M. C. Birse, J. Phys. **A 32** (1999) 3397; J. V. Steele and R. J. Furnstahl, Nucl. Phys. **A 637** (1998) 46.
- [60] G. P. Lepage, CLNS-89-971, Jun. 1989 (TASI'89 Summer School Proc.) and *nucl-th/9706029*.
- [61] U. van Kolck, Prog. Part. Nucl. Phys. **43** (1999) 337.
- [62] N. Kaiser, S. Gerstendorfer, W. Weise, Nucl. Phys. **A 637** (1998) 395.
- [63] D. B. Kaplan, M. J. Savage and M. B. Wise, Nucl. Phys. **B 478** (1996) 629.
- [64] D. B. Kaplan, M. J. Savage and M. B. Wise, Phys. Lett. **B 424**, 390 (1998).

- [65] S. Fleming, T. Mehen and I. W. Stewart, Nucl. Phys. **A 677**, 313 (2000); Phys. Rev. **C 61** (2000) 044005.
- [66] J. Gegelia, *nucl-th/9806028*; T. Mehen and I. W. Stewart, Phys. Lett. **B 445** (1999) 378; D. B. Kaplan and J. V. Steele, Phys. Rev. **C 60** (1999) 064002.
- [67] T. Frederico, V. S. Timóteo and L. Tomio, Nucl. Phys. **A 653** (1999) 209.
- [68] S. R. Beane, P. F. Bedaque, M. J. Savage and U. van Kolck, Nucl. Phys. **A 700** (2002) 377.
- [69] S. D. Glazek and K. G. Wilson, *hep-th/0203088*.
- [70] H. E. Camblong et al., Phys. Rev. Lett. **85** (2000) 1590; Annals Phys. **287** (2001) 14 and 57.
- [71] N. Brambilla, A. Pineda, J. Soto and A. Vairo, Phys. Lett. **B 470** (1999) 215.
- [72] N. Brambilla, A. Pineda, J. Soto and A. Vairo, Phys. Rev. **D 60** (1999) 091502.
- [73] S. R. Beane et al., Phys. Rev. **A 64** (2001) 042103; D. W. L. Sprung et al., Phys. Rev. **C 49** (1994) 2942.
- [74] E. Epelbaum, W. Glöckle, Ulf-G. Meißner, Nucl. Phys. **A 671** (2000) 295; Nucl. Phys. **A 637** (1998) 107.
- [75] A. Pineda and J. Soto, Nucl. Phys. **B (Proc. Suppl.) 64** (1998) 428.
- [76] G. T. Bodwin, E. Braaten and G. P. Lepage, Phys. Rev. **D 46** (1992) R1914.
- [77] G. T. Bodwin, E. Braaten and G. P. Lepage, Phys. Rev. **D 51**, (1995) 1125; E-ibid. **D 55** (1997) 5853.
- [78] R. Barbieri, R. Gatto and E. Remiddi, Phys. Lett. **B 61** (1976) 465; R. Barbieri, M. Caffo and E. Remiddi, Nucl. Phys. **B 162** (1980) 220; R. Barbieri, M. Caffo, R. Gatto and E. Remiddi, Phys. Lett. **B 95** (1980) 93; Nucl. Phys. **B 192** (1981) 61.
- [79] N. Brambilla, D. Eiras, A. Pineda, J. Soto and A. Vairo, *in preparation*.
- [80] A. Petrelli, M. Cacciari, M. Greco, F. Maltoni and M. L. Mangano, Nucl. Phys. **B 514** (1998) 245; F. Maltoni, PhD thesis (Univ. of Pisa, 1999) [<http://web.hep.uiuc.edu/home/maltoni/thesis.ps>].

- [81] D. E. Groom et al., Eur. Phys. Jour. **C 15** (2000) 1.
- [82] M. Ambrogiani et al., Phys. Rev. **D 62** (2000) 052002.
- [83] R. Mussa, private communication; see also the talk at *Charmonium spectroscopy: past and future*, Genoa, 7–8 June 2001 [<http://www.ge.infn.it/charm2001/>].
- [84] G. T. Bodwin and Y. Chen, Phys. Rev. **D 60** (1999) 054008 and Phys. Rev. **D 64** (2001) 114008; E. Braaten and Y. Chen, Phys. Rev. **D 57** (1998) 4236.
- [85] F. Maltoni, *hep-ph/0007003*.
- [86] G. T. Bodwin, D. K. Sinclair and S. Kim, Int. J. Mod. Phys. **A 12** (1997) 4019.
- [87] G. T. Bodwin, D. K. Sinclair and S. Kim, Phys. Rev. **D 65** (2002) 054504.
- [88] M. Pentic, *hep-ph/0001279*.
- [89] L. Rosselet et al., Phys. Rev. **D 15** (1977) 574; M. M. Nagels et al., Nucl. Phys. **B 147** (1979) 189.
- [90] M. Luke and A. V. Manohar, Phys. Lett. **B 286** (1992) 348.
- [91] R. Sundrum, Phys. Rev. **D 57** (1998) 331; M. Finkemeier, H. Georgi and M. McIrvin, Phys. Rev. **D 55** (1997) 6933; C. L. Lee, *hep-ph/9709238*.
- [92] H. Georgi, Nucl. Phys. **B 361** (1991) 339; M. Luke and A. V. Manohar, Phys. Lett. **B 286** 348; W. Kilian and T. Ohl, Phys. Rev. **D 50** (1994) 4649; C. Balzereit and T. Ohl, Phys. Lett. **B 386** (1996) 335; C. Balzereit, *hep-ph/9809226*; ; S. Scherer and H. W. Fearing, Phys. Rev. **D 52** (1995) 6445; G. Ecker and M. Mojzis, Phys. Lett. **B 410** (1997) 266 and Erratum-ibid. **B 438** (1998) 446.